DOT-TST-75-140

MEASUREMENT OF ROADWAY ROUGHNESS AND AUTOMOBILE RIDE ACCELERATION SPECTRA

ANTHONY J. HEALEY
RONALD O. STEARMAN

RESEARCH REPORT 13

JULY 1974

COUNCIL FOR ADVANCED TRANSPORTATION STUDIES

THE UNIVERSITY OF TEXAS AT AUSTIN

RESEARCH REPORTS PUBLISHED BY THE COUNCIL FOR ADVANCED TRANSPORTATION STUDIES

1 *An Integrated Methodology for Estimating Demand for Essential Services with an Application to Hospital Care.* Ronald Briggs, Wayne T. Enders, James Fitzsimmons, and Paul Jensen, April 1974 (DOT-TST-75-81).

2 *Transportation Impact Studies: A Review with Emphasis on Rural Areas.* Lidvard Skorpa, Richard Dodge, C. Michael Walton, and John Huddleston, October 1974 (DOT-TST-75-59).

3 *Land Value Modeling in Rural Communities.* Lidvard Skorpa, Richard Dodge, and C. Michael Walton, June 1974 (Draft Report).

4 *Inventory of Freight Transportation in the Southwest/Part I: Major Users of Transportation in the Dallas-Fort Worth Area.* Eugene Robinson, December 1973 (DOT-TST-75-29).

5 *Inventory of Freight Transportation in the Southwest/Part II: Motor Common Carrier Service in the Dallas-Fort Worth Area.* J. Bryan Adair and James S. Wilson, December 1973 (DOT-TST-75-30).

6 *Inventory of Freight Transportation in the Southwest/Part III: Air Freight Service in the Dallas-Fort Worth Area.* J. Bryan Adair, June 1974 (DOT-TST-75-31).

7 *Political Decision Processes, Transportation Investment and Changes in Urban Land Use: A Selective Bibliography with Particular Reference to Airports and Highways.* William D. Chipman, Harry P. Wolfe, and Pat Burnett, March 1974 (DOT-TST-75-28).

8 *A Preliminary Analysis of the Effects of the Dallas-Fort Worth Regional Airport on Surface Transportation and Land Use.* Harry P. Wolfe, April 1974 (Draft Report).

9 *Dissemination of Information to Increase Use of Austin Mass Transit: A Preliminary Study.* Gene Burd, October 1973.

10 *The University of Texas at Austin: A Campus Transportation Survey.* Sandra Rosenbloom, Jane Sentilles Greig, and Lawrence Sullivan Ross, August 1973.

11 *Carpool and Bus Matching Programs for The University of Texas at Austin.* Sandra Rosenbloom and Nancy Shelton Bauer, September 1974.

12 *A Pavement Design and Management System for Forest Service Roads: A Conceptual Study.* W. R. Hudson and Thomas G. McGarragh, July 1974.

13 *Measurement of Roadway Roughness and Motion Spectra for the Automobile Highway System.* Randall Bolding, Anthony Healey, and Ronald Stearman, December 1974 (DOT-TST-75-140).

MEASUREMENT OF ROADWAY ROUGHNESS AND AUTOMOBILE RIDE ACCELERATION SPECTRA

Anthony J. Healey
R. O. Stearman

July 1974

RESEARCH REPORT

Document is available to the public through the
National Technical Information Service,
Springfield, Virginia 22151

Prepared for

COUNCIL FOR ADVANCED TRANSPORTATION STUDIES
THE UNIVERSITY OF TEXAS AT AUSTIN
AUSTIN, TEXAS 78712

In cooperation with

DEPARTMENT OF TRANSPORTATION
OFFICE OF UNIVERSITY RESEARCH
WASHINGTON, D. C. 20590

Technical Report Documentation Page

1. Report No. DOT-TST-75-140

2. Government Accession No.

3. Recipient's Catalog No.

4. Title and Subtitle
Measurement of Roadway Roughness and Automobile Ride Acceleration Spectra

5. Report Date July, 1974

6. Performing Organization Code

7. Author(s)
A. J. Healey, R. O. Stearman

8. Performing Organization Report No. R R 13

9. Performing Organization Name and Address
Council for Advanced Transportation Studies
The University of Texas at Austin
Austin, Texas 78712

10. Work Unit No. (TRAIS) 00 3655 8

11. Contract or Grant No. DOT OS 30093

12. Sponsoring Agency Name and Address
Department of Transportation
Office of University Research
Washington, D. C. 20590

13. Type of Report and Period Covered Research Report

14. Sponsoring Agency Code

15. Supplementary Notes

16. Abstract

The present study is designed to support an overall program for the evaluation and establishment of ride quality criteria in transportation systems. This investigation, which is restricted to the automobile, outlines the procedures and equipment employed to measure, record, and analyze automotive vibrations and highway or roadway roughness. Detailed automobile vibration responses and corresponding roadway roughness have been measured and recorded here for 20 different roadway sections which are typical of those found in the Austin - Travis County, Texas, area. Our highway roughness models are also compared to some of the roughness models found in the literature.

17. Key Words
Ride Quality; Road Roughness; Automobile; Random Vibration; Power Spectral; Density

18. Distribution Statement
Document available to the public through the National Technical Information Service, Springfield, Virginia 22151.

19. Security Classif. (of this report)	20. Security Classif. (of this page)	21. No. of Pages	22. Price
Unclassified	Unclassified	99	

Executive Summary

INTRODUCTION

The broad aim of this work is to evaluate from a systems design and human factors viewpoint, criteria for assessing vibration levels in ground transportation systems. Excessive levels can lead to unsafe operation as well as uncomfortable rides.

Interest in the Department of Transportation in high speed ground transports using tracked air-cushion or magnetically levitated vehicles as well as in slower speed rapid transit and slow speed personal rapid transit (PRT) systems, has led to the discovery of a complete lack of acceptable specifications for random vibration levels imposed on passengers. Modelling techniques for guideway roughness, vehicle dynamics and acceptance criteria are essential to the design of innovative systems.

The work reported here is based on the automobile highway system and describes the measurement and data processing of measurements of both roughness of roadways and vibration response of an intermediate sedan.

RESULTS ACHIEVED

The results have shown that roadway roughness does not follow the simple models available in the literature. The use of a converted instrumented Chevrolet truck to measure roadway profiles has led to a large volume of typical roadway profiles. Power spectral analysis is described herein and power spectral density functions for several specific roadway sections are given. It is shown that the cross correlation between riding tracks appears to exhibit statistical characteristics similar to the tracks themselves. Simple roughness models do not predict the measured characteristics.

Similar data analysis procedures were applied to measured acceleration responses (vertical and lateral) of a 1974 Buick Century Luxus model sedan. A complete set of acceleration power spectral density functions are given, corresponding to 50 mph rides over each of the roadway sections used. The acceleration response shows marked peaks at frequencies around 1 cycle per second, due primarily to the body bounce mode of vehicle response. Peaks in response are also found around 8 - 12 cycles per second, which appear to be caused by rear-axle and front wheel bounce modes.

The data illustrate spectral composition of typical ride vibrations in the intermediate sedan.

CONCLUSION

This report compiles power spectral density data for roadway roughness and automobile ride vibration response which are helpful in the understanding and evaluation of criteria for ride acceptance. Better roughness models are needed than are currently available.

UTILITY

The data herein will likely be useful to automotive, railway and aerospace industry design engineers, State highway departments, and others interested in random vibration analysis.

ABSTRACT

The present study is designed to support an overall program for the evaluation and establishment of ride quality criteria in transportation systems. This report, which is restricted to the automobile, outlines the procedures and equipment employed to measure, record, and analyze automotive vibrations and highway or roadway roughness. Detailed automobile vibration responses and corresponding roadway roughness have been measured and recorded here for 20 different roadway sections which are typical of those found in the Austin - Travis County, Texas, area. Our highway roughness models are also compared to some of the roughness models found in the literature.

ACKNOWLEDGMENTS

We gratefully acknowledge the support of DOT Contract No. DOT-OS-30093, administered through the Council for Advanced Transportation Studies at The University of Texas at Austin. In addition, the help of Mr. H. Scholl at NASA Langley Research Center, who loaned the 3-axis accelerometer package, Mr. H. Dalrymple of the Center for Highway Research at The University of Texas at Austin, and the State Department of Highways and Public Transportation has been indispensible.

TABLE OF CONTENTS

LIST OF FIGURES

CHAPTER 1

INTRODUCTION

Increasingly in recent years the importance of passenger comfort in public and private transportation has come to the attention of the vehicle designer. It has become such a significant factor in the automotive industry that many companies advertise the fine ride quality of their automobiles. Now, with fuel shortages imminent and congestion of the inner city growing, public transportation planners are seeking an economical system that will lure the individual away from his private automobile by providing an equivalent or better ride quality in a faster or more efficient vehicle. To date, however, there is insufficient design information to define ride quality in engineering terms useful to the designer.

In general, ride quality is a measure of the subjective response of an individual to his transportation environment. Numerous attempts have been made to correlate ride quality with some objective measure of the transportation environment, in particular, the vibration. One approach is to correlate a measure of subjective response with a controlled laboratory vibrational environment; the multidimensional and stochastic nature of vehicle environment and motion is, however, difficult to simulate. Another approach is to correlate subjective response with the measured ride vibrations of an automobile in the field.

This report concentrates on the latter approach. It is concerned with the equipment and techniques used in measuring and recording the vibrations of automobiles in the field, along with the roadway or highway roughness, the analog-to-digital conversion of these data, and the reduction of the data to meaningful engineering measures of automotive vibration.

CHAPTER 2

SYSTEM FOR MEASURING AND RECORDING AUTOMOTIVE VIBRATIONS

EQUIPMENT

One system for measuring and recording vibrations in automobiles consists of a portable triaxial accelerometer and amplifier set, a four channel FM data recorded, and an inverter to provide AC power for the recorder. The measuring system components are described in this section and the resulting power spectral density measured data on automotive vibrations in the field are presented.

Accelerometer and Amplifier Set

The portable accelerometer and amplifier set (Fig. 1) was developed and fabricated by NASA at the Langley Research Center[1] and is on loan to the CATS Ride Quality Group. Three linear transducers are used to measure accelerations on mutually perpendicular axes (Fig. 2). The transducers have a frequency range of 0 to 25 Hz and a linear acceleration amplitude range of 0.01 to 1.0 g. A battery pack in the unit supplies transducer and amplifier power. The transducers and other electronics are mounted on a thick aluminum base plate with spike-legs for penetrating carpets so that undamped vibrations can be measured. The cover is equipped with an outlet for each axis and a handle. The unit is very portable and weighs only 20.0 pounds (2.765 newtons).

Data Recorder

A Teac R200 DR/FM data recorder (Fig. 3) from The University of Texas at Austin Department of Mechanical Engineering was used to record the amplified output of the accelerometers. Data were recorded in the FM mode on three channels

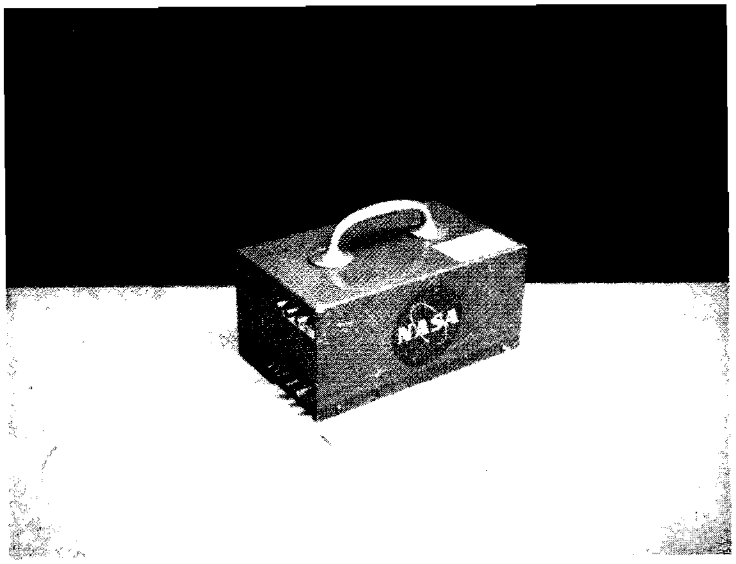

Figure 1. NASA Portable Accelerometer and Amplifier Set

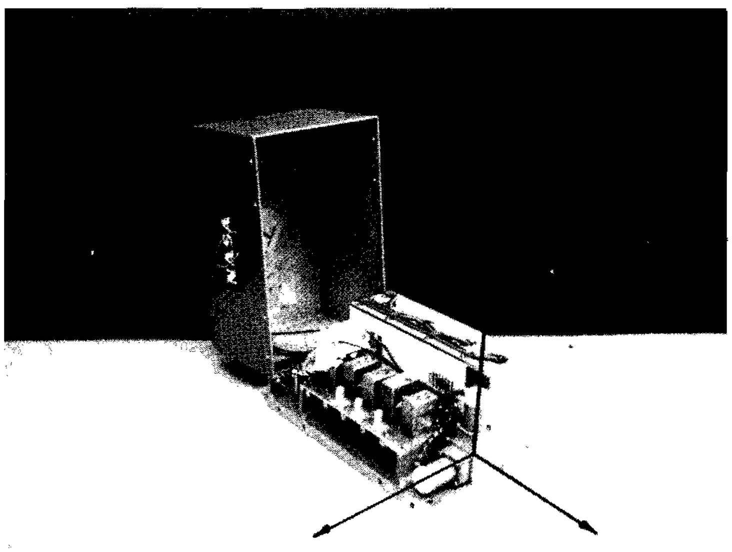

Figure 2. Transducers Mounted on Three Mutually Perpendicular Axes

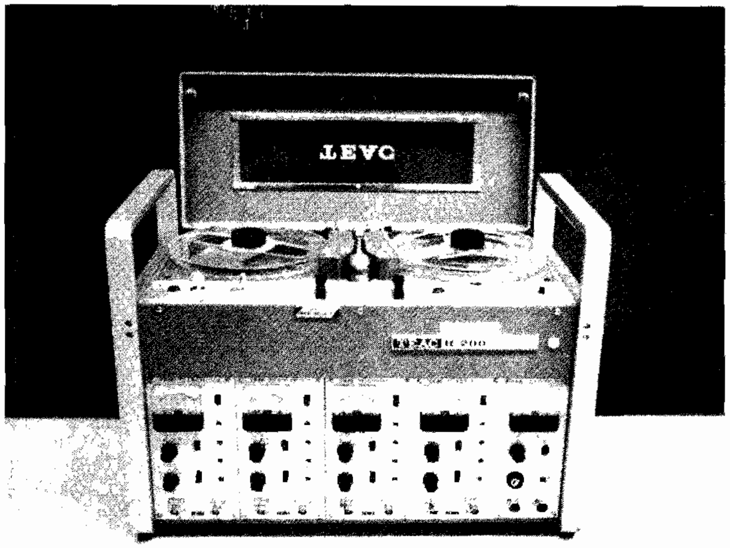

Figure 3. Teac R-200 DR/FM Data Recorder

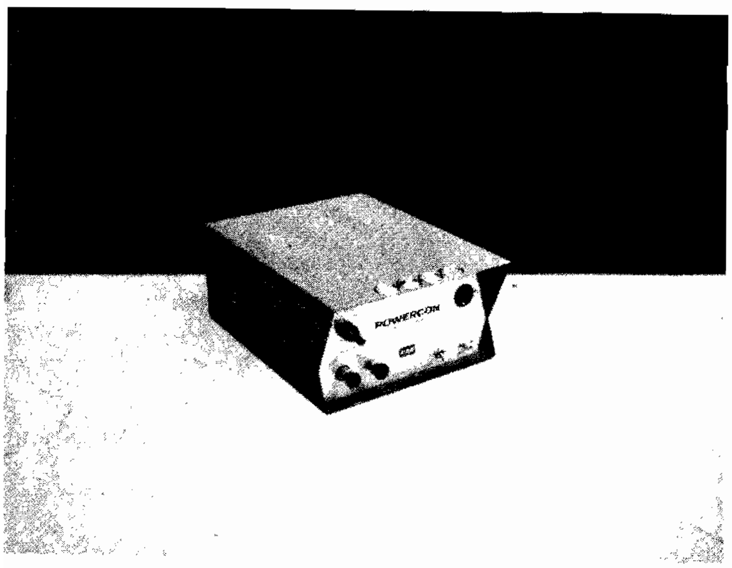

Figure 4. Powercon 12ESW25 Inverter

while commentary was recorded in the DR mode on the fourth. Each channel is equipped with a VU meter, input and output zeroing, and level controls; also provided are jacks for input and output. The tape deck required a 115 volt, 50-60 Hz power source.

Inverter

The Powercon 12ESW 25 inverter (Fig. 4) on loan from the Center for Highway Research (CFHR) at The University of Texas at Austin was wired into the vehicle electrical system to provide a mobile source of power for the data recorder. There was some question as to the effects of the inverter on the performance of the recorder. This was resolved by recording a 100 Hz sine wave on channel 1 while the recorder was powered by the inverter and then recording the same signal on channel 2 while the recorder was plugged into an ordinary wall outlet. The two outputs were then compared on a dual trace oscilloscope while the recorder was plugged into a wall outlet. No difference in the traces could be observed.

CALIBRATION AND MEASUREMENT PROCEDURE

Accelerometer - Recorder Calibration

Since the NASA accelerometer is sensitive down to 0 Hz., an output can be generated by the static gravitational field of the earth. However, this 1 g signal is "biased out" electronically in the vertical axis, and thus all axes give 0.0 v output from a 0.0 g dynamic acceleration. Static calibration curves are shown in Figures 5 and 6. The tape recorder was set up with one channel for each axis - vertical, transverse, and longitudinal - and the fourth for commentary. Throughout the testing, the channel-axis correspondence was maintained.

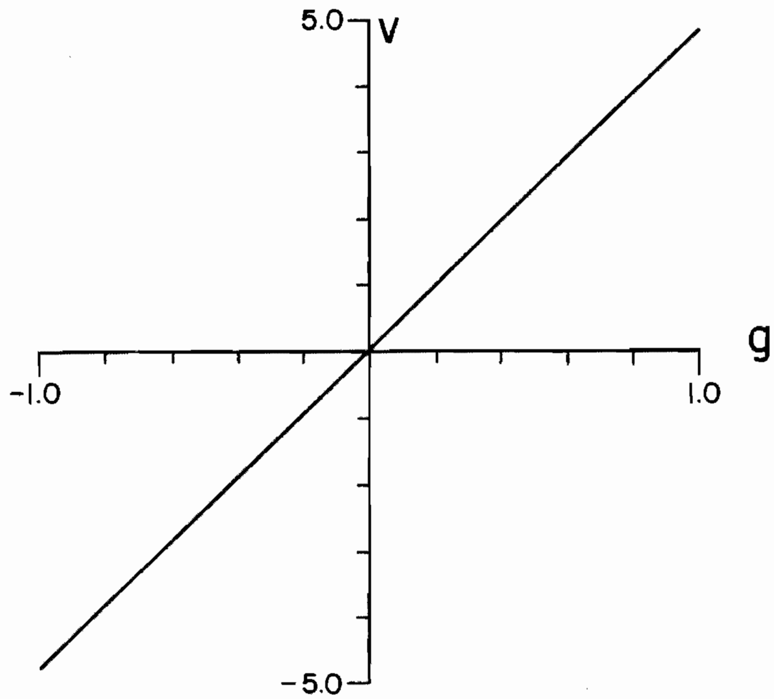

Figure 5. Static Calibration Curve for Transverse Axis

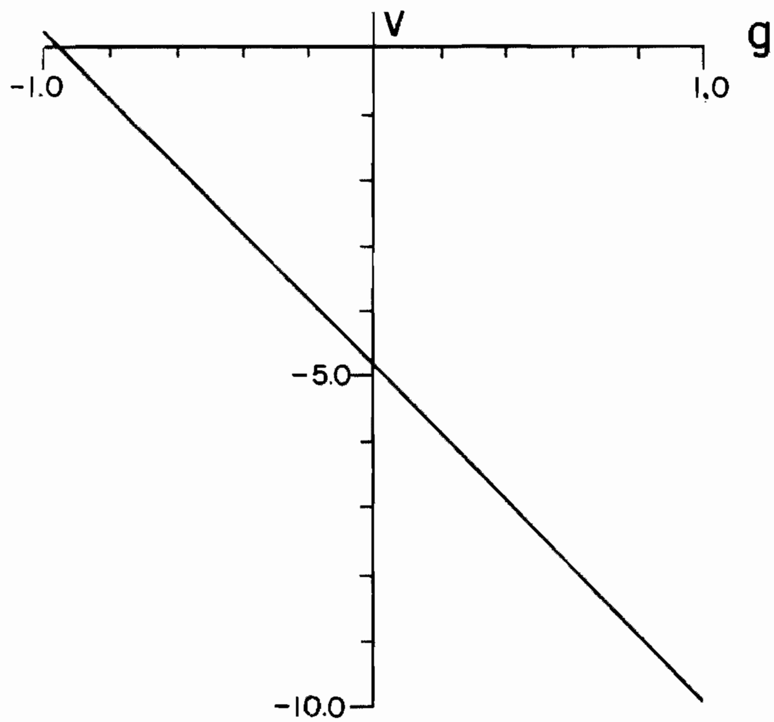

Figure 6. Static Calibration Curve for Vertical Axis (Bias On)

Calibration was begun by warming up the accelerometer set and the recorder in the record mode. The accelerometer was set on a level surface in such a way as to generate an output for a 0.0 g static acceleration field, and the respective tape inputs were zeroed. The accelerometer was then rotated and set on a level surface in such a way as to generate an output for a 1 g static acceleration field. The respective input level controls were then adjusted to give a reading of 100% modulation. These signals were then recorded for approximately 25 reel revolutions prior to the recordings for a test section as a reference for the A-to-D converter and for output calibration.

The tape deck was placed in the "playback" mode and an unmodulated portion of tape was played back while the output levels were zeroed. Then as the pre-recorded 1.0 g signals were played the levels were adjusted to give an output of 1 volt, as measured with a digital volt meter, which corresponds to approximately 90% modulation.

Although accelerations as high as 1.0 g were not expected in testing, the above procedure assures that the tape record/playback amplifiers will not be overloaded and clip and that the tape will not saturate and distort the recorded signal.

Installation

A 1965 Ford Galaxy 500 2-door hardtop provided by The University of Texas College of Engineering Industrial Associates was the vehicle used for preliminary tests (Fig. 7). The front suspension is conventional A-frame/coil/spring with antiroll bar and the rear suspension is trailing arms with coil

Figure 7. Council for Advanced Transportation Studies Ride Quality Test Vehicle

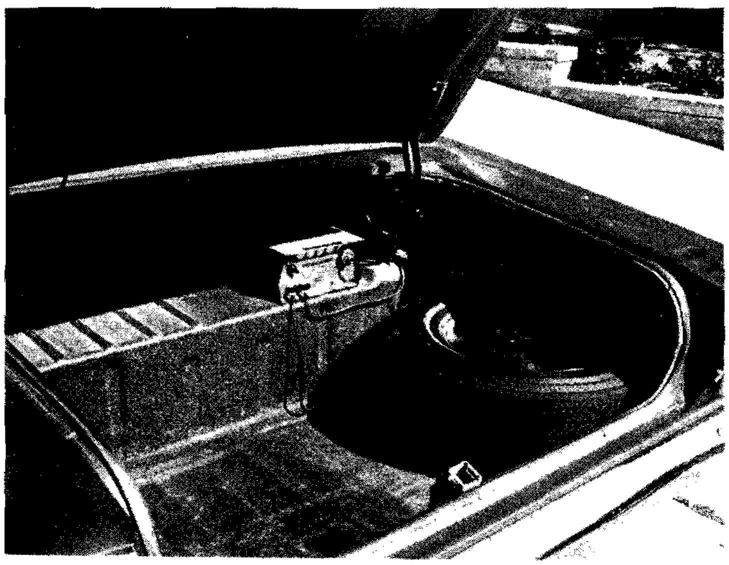

Figure 8. Installation of Powercon Inverter

springs and a locating arm to the live axle. The vehicle is equipped with radial tires. Its electrical system has a 12-volt, negative grounded battery and alternator with an external electromechanical voltage regulator.

Later tests were conducted in a 1974 Buick Century Luxus, a heavier 4-door sedan equipped with automatic transmission, air conditioner, and non-radial belted tires. The instrumentation installation was similar to that illustrated for the Ford and is not shown.

The Powercon inverter was installed in the trunk of the test vehicle (Fig. 8) so that vibration noise would not distract raters. It was connected to the vehicle electrical system via a cable attached to the "hot" side of the battery and another cable was grounded to the chassis. Because of possible damage to the battery the inverter was turned on only when the engine was running. The AC output was connected via an extension cord running under the back seat to the tape recorder.

The Teac data recorder was installed on a leveling board on the left side of the rear seat (Fig. 9), leaving room for two passengers in the rear and one in the front seat.

The NASA accelerometer set was installed on the front floor directly in front of the passenger seat (Fig. 10). The set was equipped with threaded spike feet which penetrated the carpet and padding and permitted leveling. Outputs from the accelerometers of interest were connected via coaxial cable under the front seat to appropriate channels in the recorder.

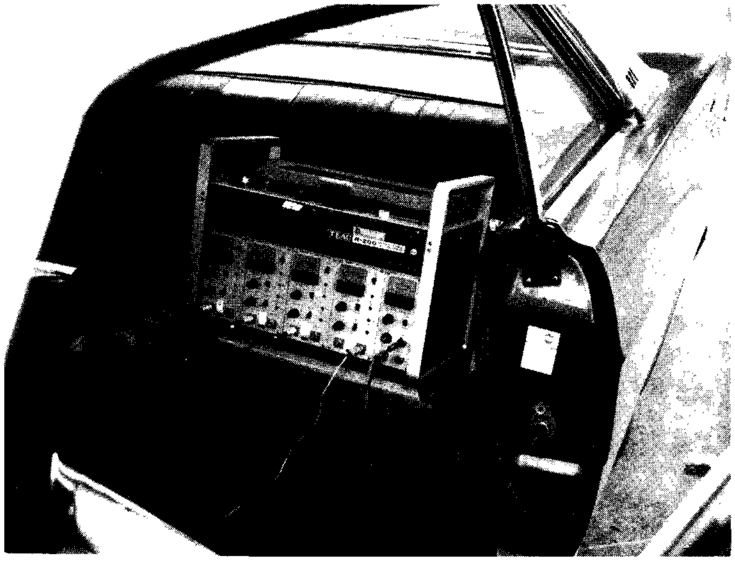

Figure 9. Installation of Teac Data Recorder

Figure 10. Installation of NASA Accelerometer Set

Data Acquisition

The Center for Highway Research (CFHR) has 28 test sections in the Travis County area (Fig. 11) each approximately 1200 feet in length. The CFHR has measured the profiles of these roads and these are available on digital tapes; these sections have also been surveyed with a Mays Road meter and serviceability indices have been computed for each section (2,3). The measuring technique employed here is described in Chapter 3 of this report.

The test vehicle was prepared and taken to one of the above test sites (Fig. 12 shows test section 2). The starting and ending points of each section had been previously marked by CFHR and these were noted prior to making a test run. The vehicle was returned to a point approximately 1/2 mile before the starting point of the test section and accelerated to 50 mph. The speed was held constant over the test section while the vehicle accelerations were recorded in analog form during the test run. This procedure was repeated for as many tests as required, with the driver attempting to traverse the section in as near the original wheel tracks as possible. Frequent checks on the repeatability of the measurements were made by rerunning a test after a few days interval. A total of twenty different test sites, which were known to represent the range of highway or roadway conditions, were studied.

Data Reduction

The analog data from the test runs had to be reduced to digital form for use with the CFHR Power-4 program, which computes power spectral density (PSD) and other vibration information. This was accomplished via a system at the Texas Highway Department made available through the CFHR. This system consisted of a

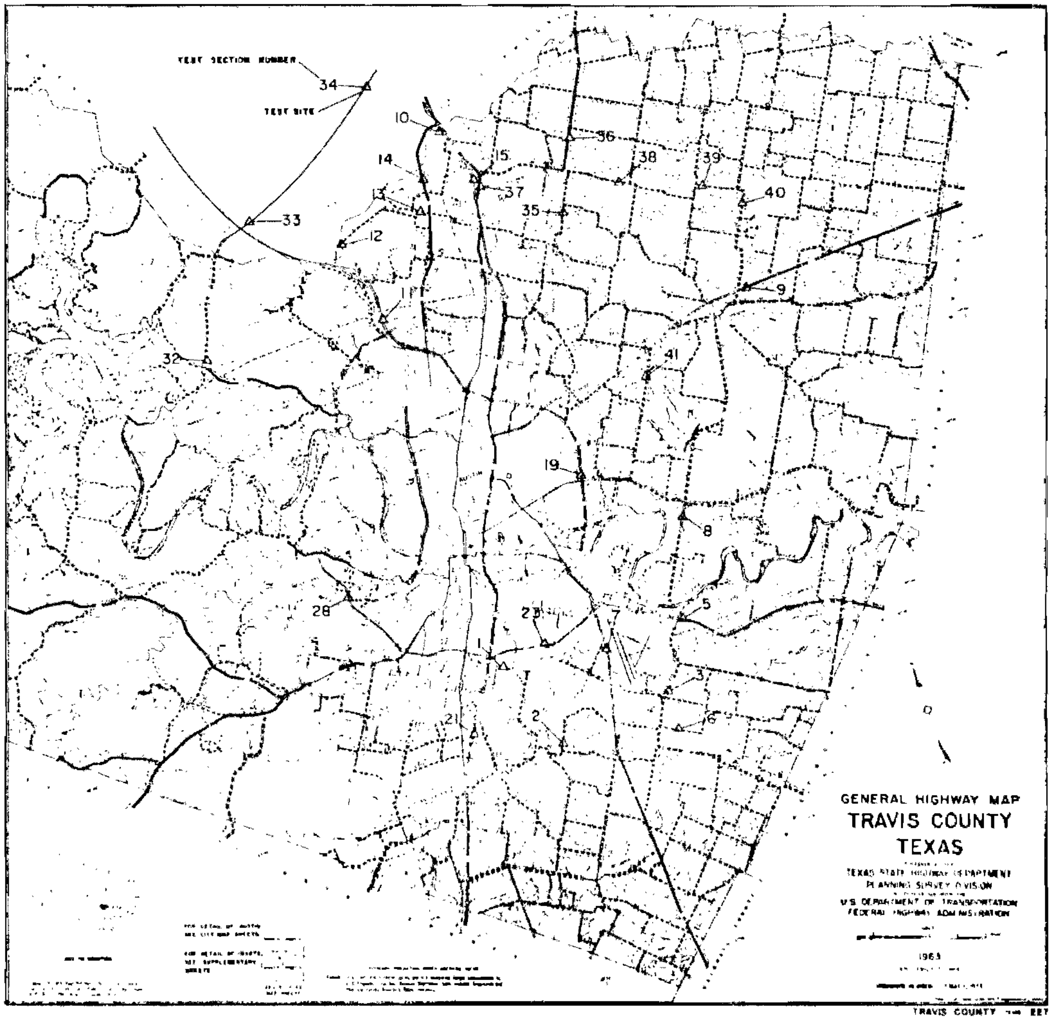

Figure 11. Center for Highway Research Test Sites

Figure 12. Typical Test Section

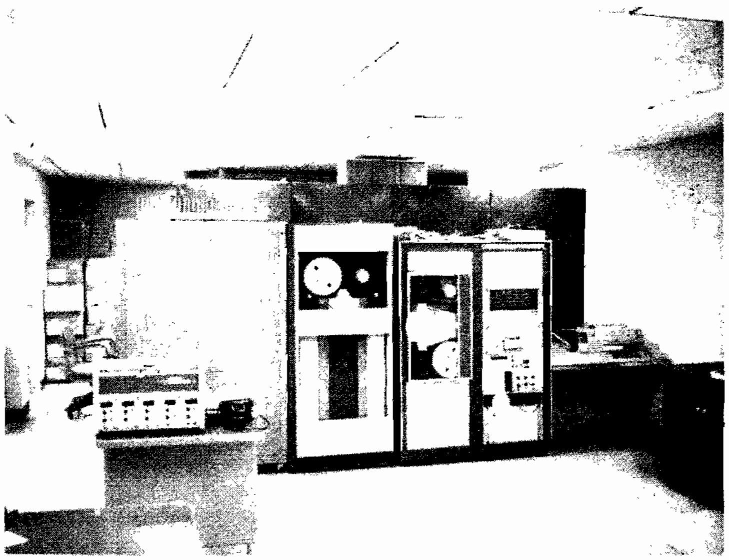

Figure 13. Analog - to - Digital Data Conversion System

Hewlett-Packard 2115 Central Processing Unit, 8,192 words of core memory, two direct memory access channels, an H-P 8003 pulse generator, a Raytheon multiverter, a high-speed tape reader, an ASR 35 teletypewriter, a Positive Logic Duplex Register for Special purpose interface, two tape units, and an Interface and Patch Logic Module (Fig. 13).

The analog data were digitized with the H-P 502 analog-to-digital program and the digital data were made compatible with the UT computer system through the H-P 500 program.[5] With some minor modifications by the user these data were ready for use with the CFHR Power-4 Program. PSD's from these data could be compared with predicted data and with data from other test sections to verify predictions, repeatability, and in general to test the feasibility of the system. Typical PSD's from test roads are shown in Figures 14, 15, and 16. The repeatability of the data was found to be within plotting accuracy for two test runs made over the same section of highway on different days. A discussion of the analytical procedure for calculating PSD's from measured and recorded data is presented in Chapter 3. Computed PSD information and vehicle vibration RMS responses measured over the twenty test sites are presented in Appendix A. Only vertical and lateral vibration data are presented since no significant longitudinal accelerations occurred during the test conditions.

DISCUSSION

Since these techniques evolved during the developmental stages, some problems had to be solved. Analysis of PSD plots indicated that the accelerometer package should be secured to the floor of the vehicle. However, this had to be accomplished

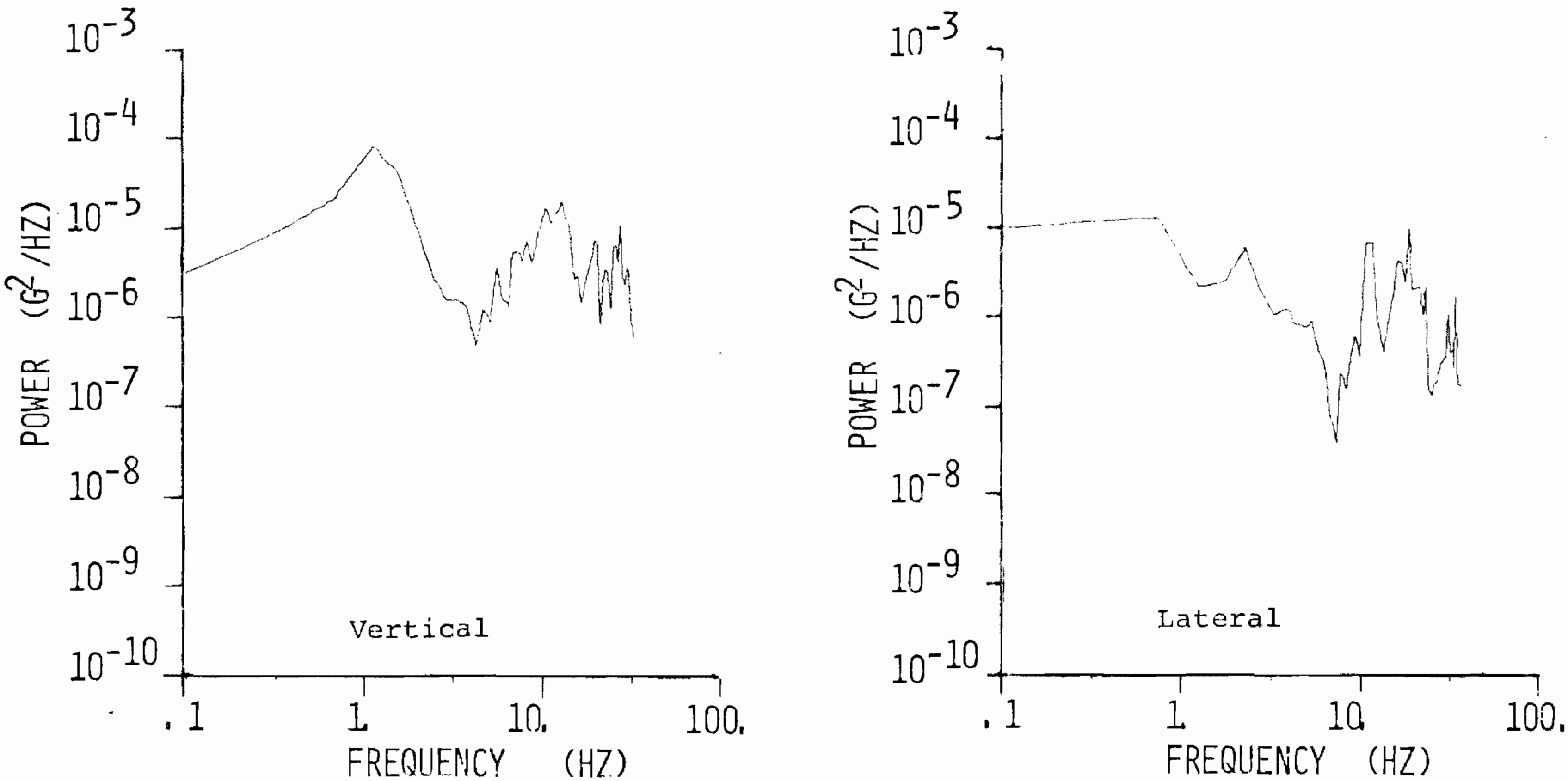

Figure 14. Vertical and Lateral PSD for CFHR Test Section 5

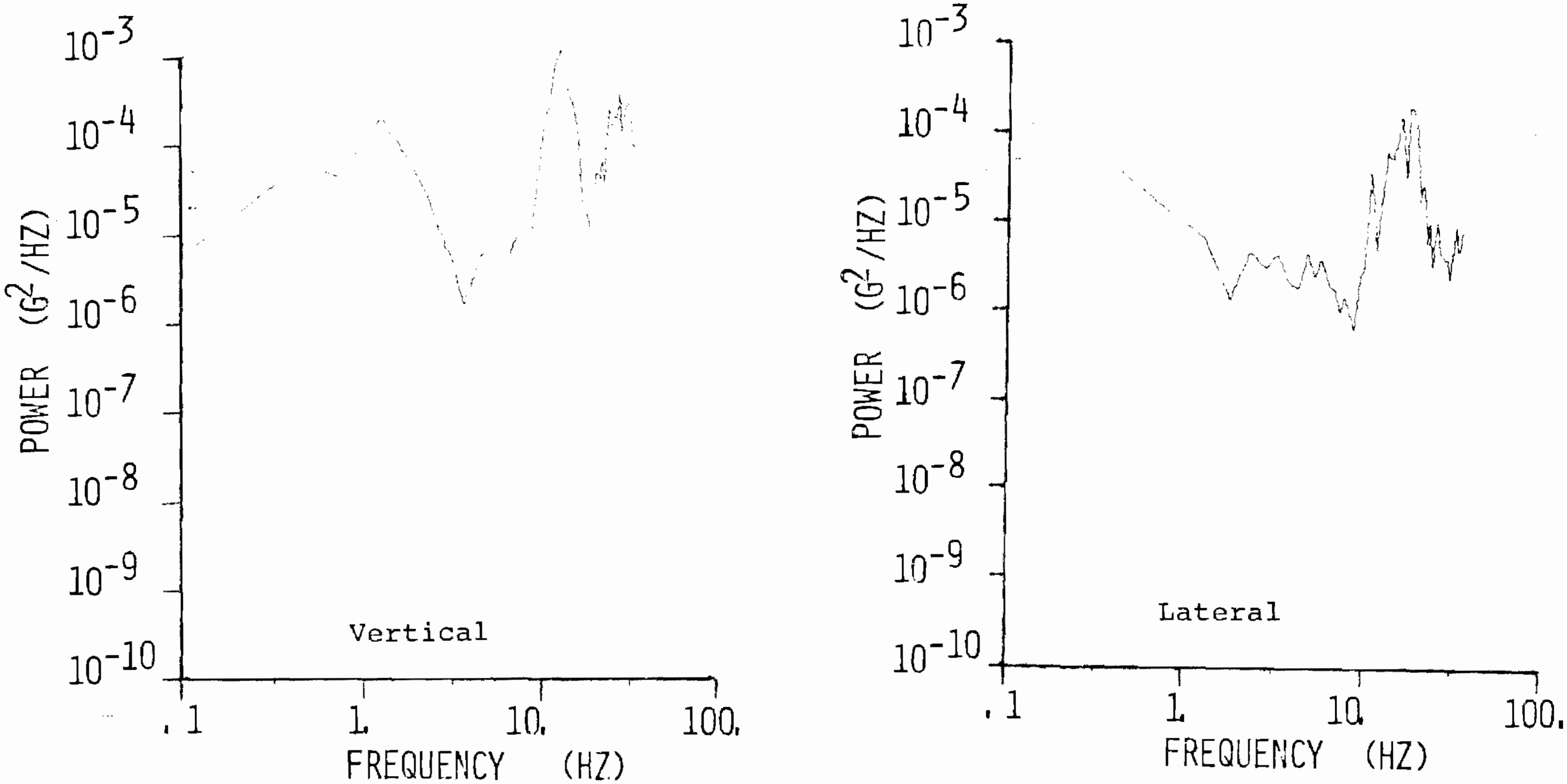

Figure 15. Vertical and Lateral PSD for CFHR Test Section 13

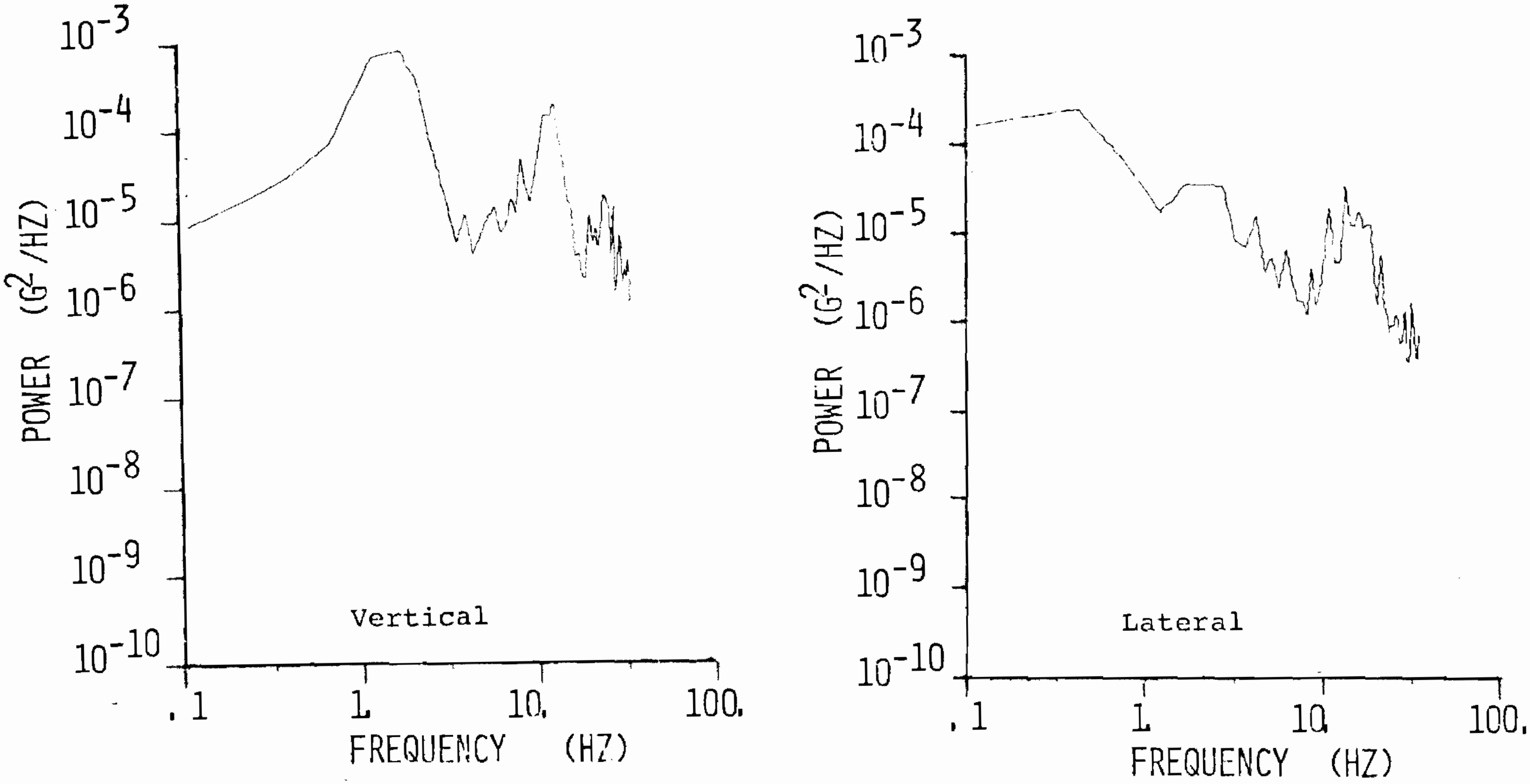

Figure 16. Vertical and Lateral PSD for CFHR Test Section 38

with no damage to the vehicle. Also, since the speed of the vehicle is manually controlled, it is not precisely constant over the test section. The H-P 8003 pulse generator produces a constant time-step pulse train, and thus data points may not correspond to equally spaced points on the roadway.

The first problem was solved by securing the accelerometer package under the driver's seat. The second problem was solved by skillful driving since speed variations could be kept to within 5% of the nominal 50 mph which was considered acceptable.

Test section beginning and end points are not exactly repeatable in the above technique and use of a photo cell trigger has been suggested to take care of this. However, it has been found that although the amplitudes of PSD's may vary slightly for runs over the same section, in general, repeatability was good. An examination of the complete set of data in Appendix A illustrates that the vertical and lateral acceleration components exhibit some similar tendencies at frequencies greater than 10 Hz but not at frequencies less than 2 Hz. This is not surprising in view of the high lateral compliance of pneumatic tires. The peaks around 1 Hz and 10 Hz in the vertical accelerations are certainly due to body bounce and wheel bounce modes of response respectively. Further discussion of this appears in Ref. 12. Lateral and vertical acceleration powers are noted to be of comparable magnitude.

To more completely define the automobile vibration characteristics measured in this program, roadway roughness measurements were obtained for each highway section on which vehicle vibrations were measured. A description of these measurements is presented in Chapter 3.

CHAPTER 3

DESCRIPTION OF MEASURING AND RECORDING SYSTEM FOR HIGHWAY ROUGHNESS MEASUREMENTS

While a large area of discrete roughness such as a rut can be considered as a deterministic reduction in roadway elevation, the dominant roughness occurs as a random variation of elevation. The mean elevation is not important but the random variations about the mean for any given section of roadway give rise to the need to treat the surface stochastically. Significant measures of the profiles are the variance and the power density spectrum.

Roughness profiles were measured with a Surface Dynamics Profilometer[6] (Fig.17). This is basically a Chevrolet carry-all truck with two sensing wheels - one in each wheel track - which are spring loaded to contact the roadway surface. This enables the system to be used at high speed (up to 60 mph). The instrumentation used consisted of an accelerometer located on the truck body immediately over each sensing wheel and a potentiometer to measure relative displacement between body and sensing wheel. The system block diagram is shown in Figure 18. The accelerometer signal is twice integrated, summed with the potentiometer signal to extract absolute motion of the sensor wheels, band-pass filtered, and recorded on analog tape. A pulse generator connected to the vehicle transmission provides a distance count to eliminate speed variation effects in the data. An automatic speed control is provided for driver convenience. The sensor wheels are made concentric with their shafts to within 0.005" and a natural rubber tire is molded to the wheel rim.

Figure 17. Surface Dynamics Profilometer

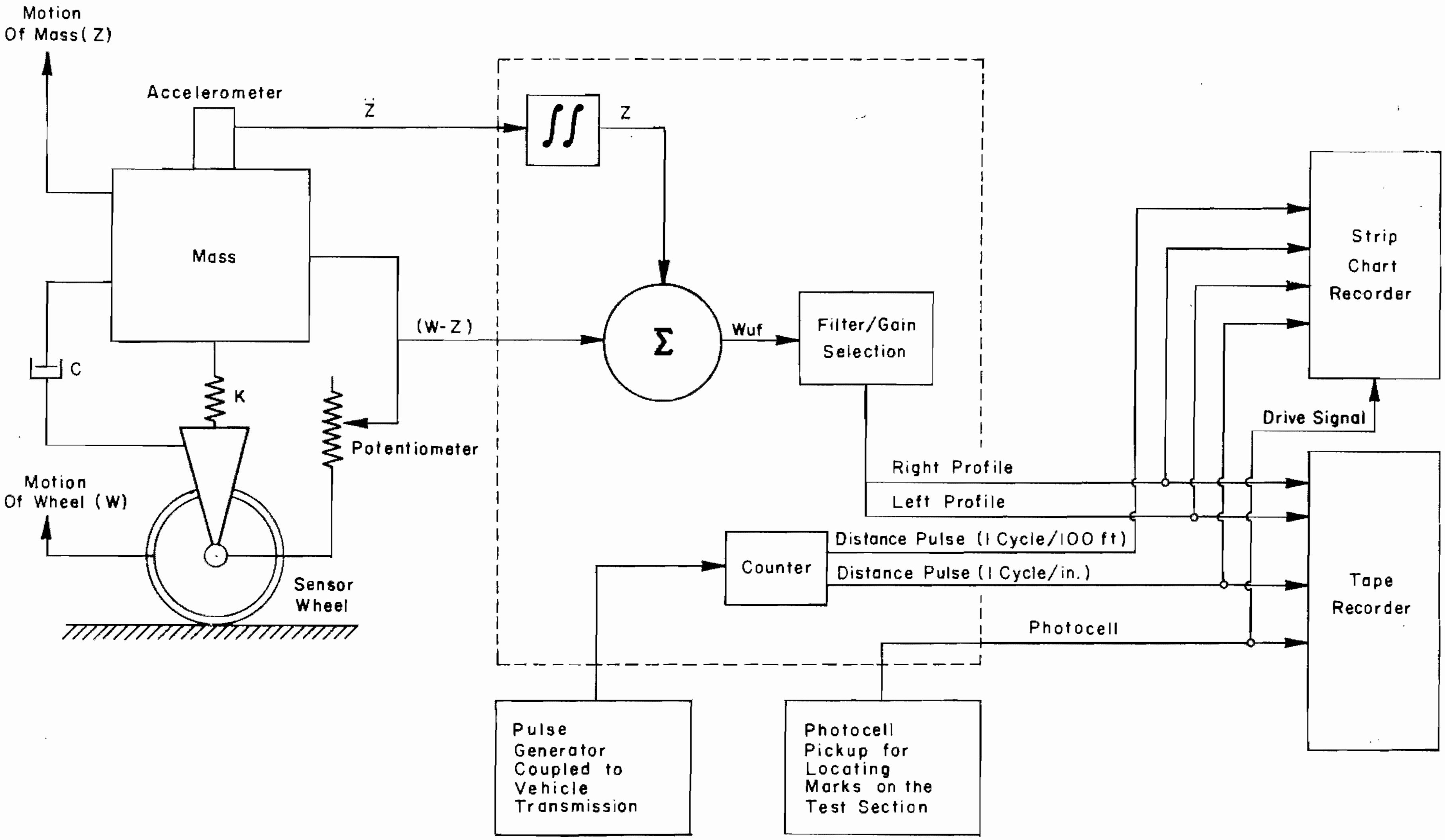

Figure 18. Profilometer Block Diagram

In making profile measurements, the short wavelength roughness is sensed primarily by the sensor wheel because of the isolation characteristic of the suspension system. The long wavelengths arising from hills and valleys are sensed primarily by the accelerometers. The double integration of the acceleration signal thus saturates the tape recorder unless adequate high-pass filtering is provided. Four filters can be selected, depending on wavelength range and vehicle speed. At a 20-mph measurement speed, for example, the filter used introduces a 3 db attenuation at 0.6 rad/sec, corresponding to a 306-ft. wavelength. High-frequency cut off occurs at 1000 rad/sec. Since the high-pass filter characteristic is known it may be compensated for in the data analysis.

The filtered profile, together with pulser output and photocell pulses to denote beginning and end of a test section, is recorded and subsequently digitized for analysis. The pulse generator output is fed to a counter which reduces the count to approximately 11.8 pulses per foot.

An H-P 2115A data processor is used for analog-to-digital conversion. Samples of right and left tracks are taken alternately, resulting in 5.9 samples per foot for each track. At the test speed of 20 mph, this is sufficient to prevent aliasing problems in the digitizing.

DATA ANALYSIS AND POWER SPECTRAL COMPUTATIONS

The H-P 2115A processor produces 12-bit words written on digital tape in 1500-word blocks at 556 ppi. Data analysis is carried out on a CDC 6600 machine and a transformation program converts the H-P 5101 tape into CDC 6600 compatible data (60-bit words) ending with a sequence of right and left wheel track elevation data:

$$x_0 , x_1 , x_2 - x_n$$

$$y_0 , y_1 , y_2 - y_n$$

For each test section approximately 4,096 samples were taken, corresponding to a 694-ft. total record length. A segment of a typical analog trace for both highway profiles, that is, for the right and left wheel traces, is shown in Figure 19.

Detrending

The roadway statistics and vehicle response are assumed to be random, stationary, and ergodic. Because of the form of many test sections, not only the mean, but also the linear trend, is extracted in computing deviations. Detrending is accomplished by the operation

$$x_k = x_{old} - \bar{x} - \beta(k - \bar{k})$$

where $\bar{x}$, the mean, $= \frac{1}{N} \sum_{k=D}^{N-1} x_k$

$$\bar{k} = \frac{1}{2} (N + 1)$$

and $\beta = \dfrac{\sum_{k=1}^{N} kx_{k-1} - \frac{1}{2} N(N + 1) \bar{x}}{\frac{1}{6} N(N + 1)(2N + 1) - \frac{1}{4} N(N + 1)^2}$

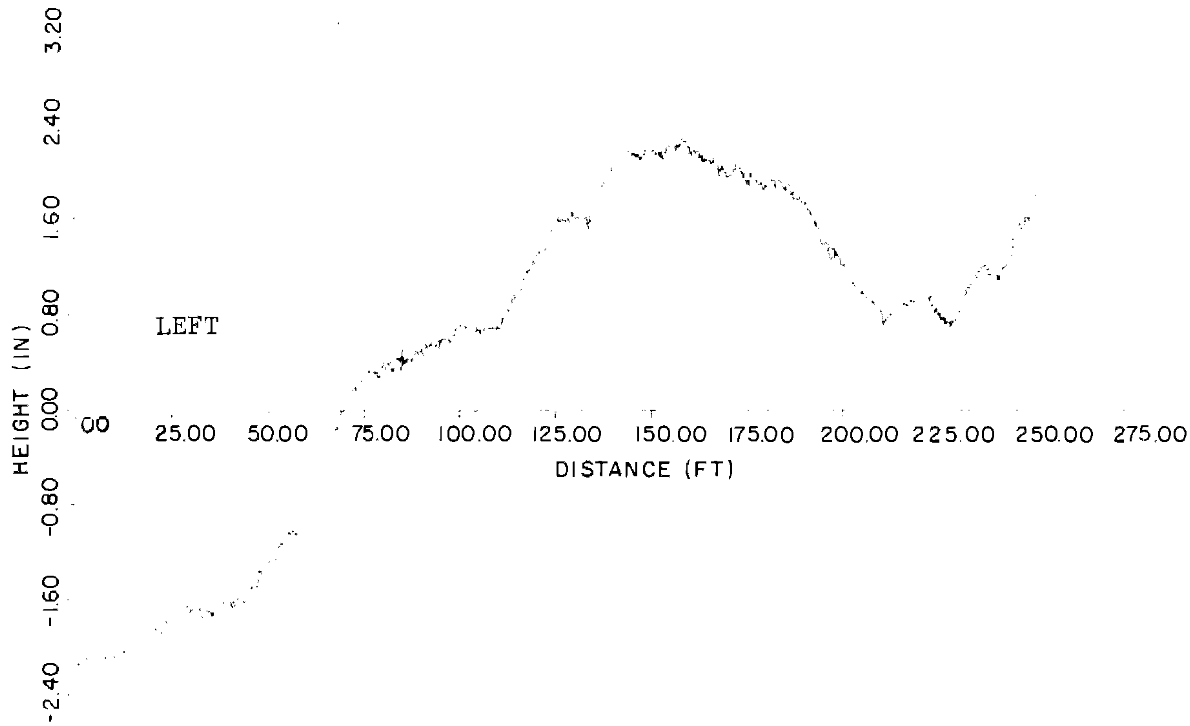

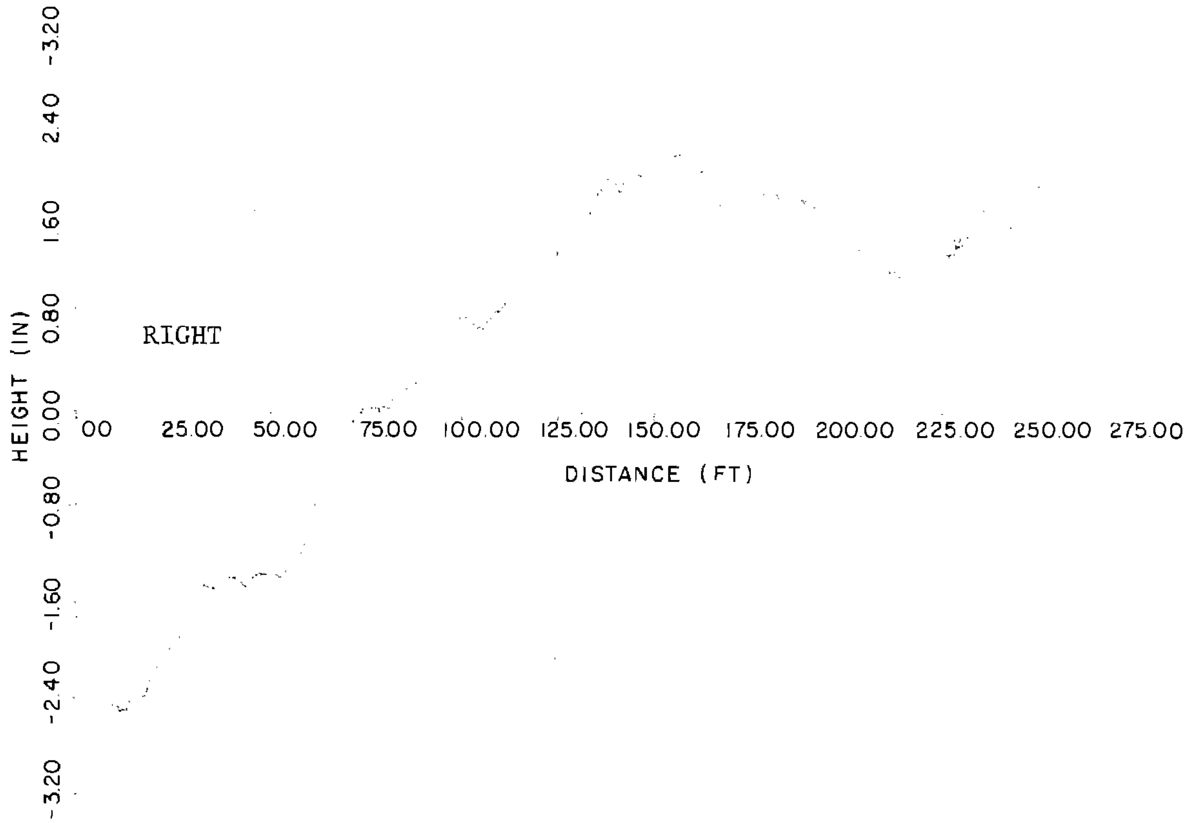

Figure 19. Roadway Elevation Profile for Section No. 2.

The resulting sequence

$$(x_0 \ldots x_k \ldots x_{N-1})$$

is analyzed for Hz power spectral composition. The auto covariance is obtained by

$$C(r) = \frac{1}{N} \sum_{k=0}^{N-1} x_k \cdot x_{k+r} \qquad (2)$$

<u>Power Spectrum Calculations</u>

The power spectral density is then given by the discrete Fourier transform of C(r):

$$P(k) = \frac{1}{N} \sum_{r=0}^{N-1} C(r)\ e^{-j2\pi rk/N} \qquad (3)$$

If the original sequence x_k is real, P(k) will be complex with a real and an imaginary part being symmetric and anti-symmetric, respectively, about the N/2 point.

Taking advantage of the Fast Fourier Transform Algorithm[7], it is better to compute the FFT of x_k. Using the property that the transform of a convoluted sequence is the product of the individual transforms with it, conjugate so that if

$$X(k) = \frac{1}{N} \sum_{r=0}^{N-1} x_r\ e^{-j2\pi rk/N} \qquad (4)$$

the power density is the magnitude of X(k), that is,

$$P(k) = (X_k\ X_k^*)\ L \qquad (5)$$

where L = total record length, which is included to reconstitute dimensional units in the power function (L = 694 ft).

The difficulties involved in reconstruction of finite data traces, which are inherently assumed to be periodic, are overcome by windowing. Here, a cosine taper window is employed, and then a sufficient number of zeros is added to the sequence to ensure that N is an integer power of two.

The window used was

$$X_k = X_{old} \cdot W_k$$

where

$$W_k = \begin{cases} 0.5\ [1 - \cos\ (\pi(k' - 1/2)/r] & 1 < k < r \\ 1.0 & r < k < N-r \\ 0.5\ [1 - \cos\ \{\pi(N - k + 1/2)/r\}] & N-r < k < N \end{cases} \tag{6}$$

r was chosen as N/10.

High-Pass Filter Correction on Roadway PSD Calculations

The transfer function of the high-pass filter used in the profilometer measurements to avoid saturation of the recording equipment is

$$G(S) = \frac{(\frac{S}{\omega_n})^3}{(\frac{S}{\omega_n})^3 + (1+2\zeta)(\frac{S}{\omega_n})^2 + (1+2\zeta)(\frac{S}{\omega_n}) + 1} \tag{7}$$

where $\zeta = 0.5$ for all filters and where ω_n can be chosen as 0.3, 0.6, or other values, depending upon the requirements of the particular roadway being measured. To correct the power density measurements for the high-pass filter effect, each power spectra density is multiplied by the square of the magnitude of the filter transfer function at the appropriate frequency:

$$p_k^{corrected} = p_k^{filtered} \div |G_f(j\omega_k)|^2 \qquad (8)$$

where

$$\omega_k = \frac{2\pi k\, V_m}{L}$$

V_m = velocity of profilometer during profile measurement,

L = test section length.

Data Averaging

Because of the finite length of the measured trace and the nonstationarity of actual profiles, data averaging is necessary.

The sampling frequency occurred at about 5.9 cycles per foot and the incremental discretion frequency was 0.00144 cpf. Averaging over d incremental bands yielding d degrees of freedom for each averaged power computation, the power spectral sequence

$$p_0 \text{ -- } p_k \text{ -- } p_n$$

converts to the data smoothed sequence

$$\hat{p}_d \text{ -- } \hat{p}_k \text{ -- } \hat{p}_{N-1-d}.$$

According to

$$\hat{p}_k = \frac{1}{(2d+1)} \sum_{k-d}^{k+d} p_k \; ; \; k = d \text{ to } N - 1 - d. \qquad (9)$$

The frequency associated with $\hat{p}_k$ still remains at k times the sampling frequency.

While equation (9) smooths the data, total power is not conserved in the smoothing process. The errors are introduced by the failure to include points from k = 0 to d and k(N-1-d) to k = (N-1). With typical spectra this error is small, that is,

$$\text{Total Power Error} = \frac{1}{(2d+1)} \sum_{\lambda=0}^{\lambda=2d} (2d-\lambda)\ (p_{\lambda} + p_{N-1-\lambda})$$

A typical result for the averaged power density of a section of highway is shown in Figure 20. The abscissa has been converted to Hz rather than cycles per foot in view of our interest in ride quality. The conversion is

$$\Omega \text{ cpf} = \frac{f\,(\text{Hz})}{V} \quad ;$$

where V = test vehicle speed ≃ ft/sec.

Appendix B shows data for individual tracks for several roads, including rough, medium, and smooth, while Figure 21 shows a typical plot of cross-power result:

$$\text{Cross Power} = L(X_k^{*}\ Y_k) \tag{10}$$

DISCUSSION OF THE ROAD PROFILE MEASUREMENTS

A review of the figures in Appendix B, which illustrate measured roadway power spectral density data, indicates significant variations between the primary and secondary highways within the Austin, Texas, area, as identified in Figure 11. An earlier roughness model which assumed the roadway random roughness to be proportional to $(\text{frequency})^{-2}$, that is[8],

$$\phi(\Omega) = A/\Omega^2$$

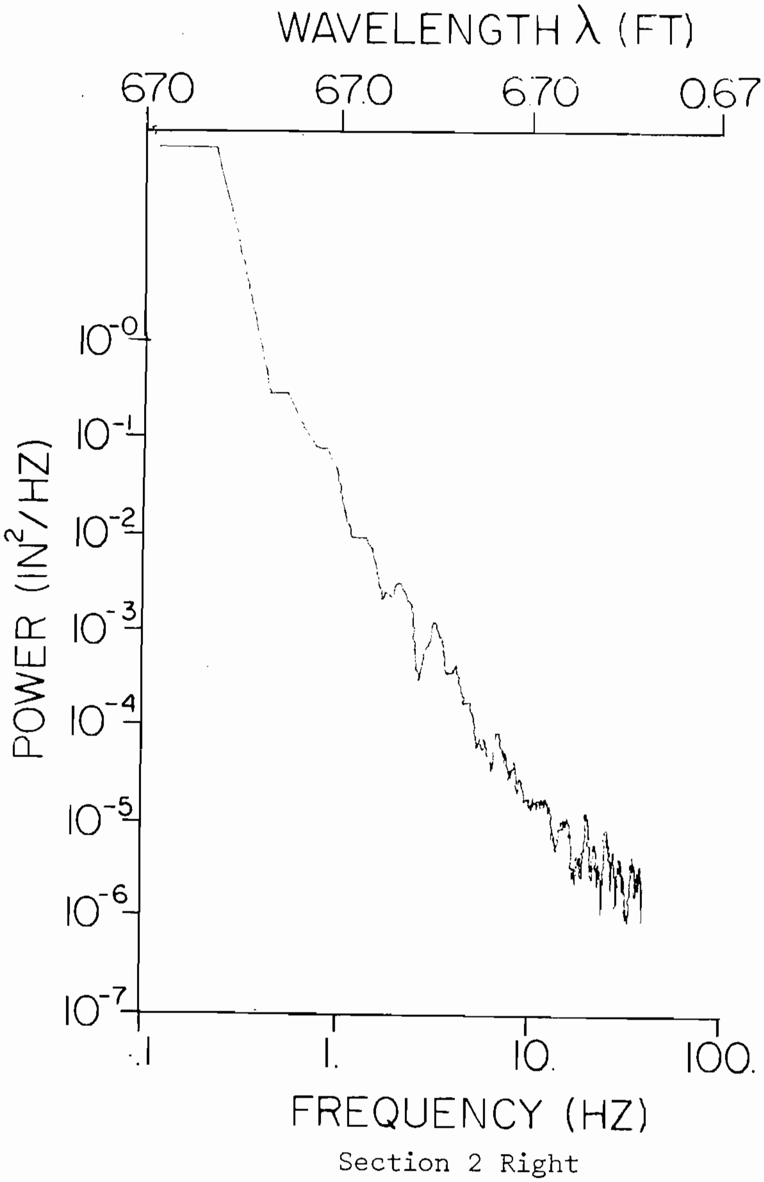

Figure 20. Roadway PSD Roughness Spectra Section 2 from Measured Data

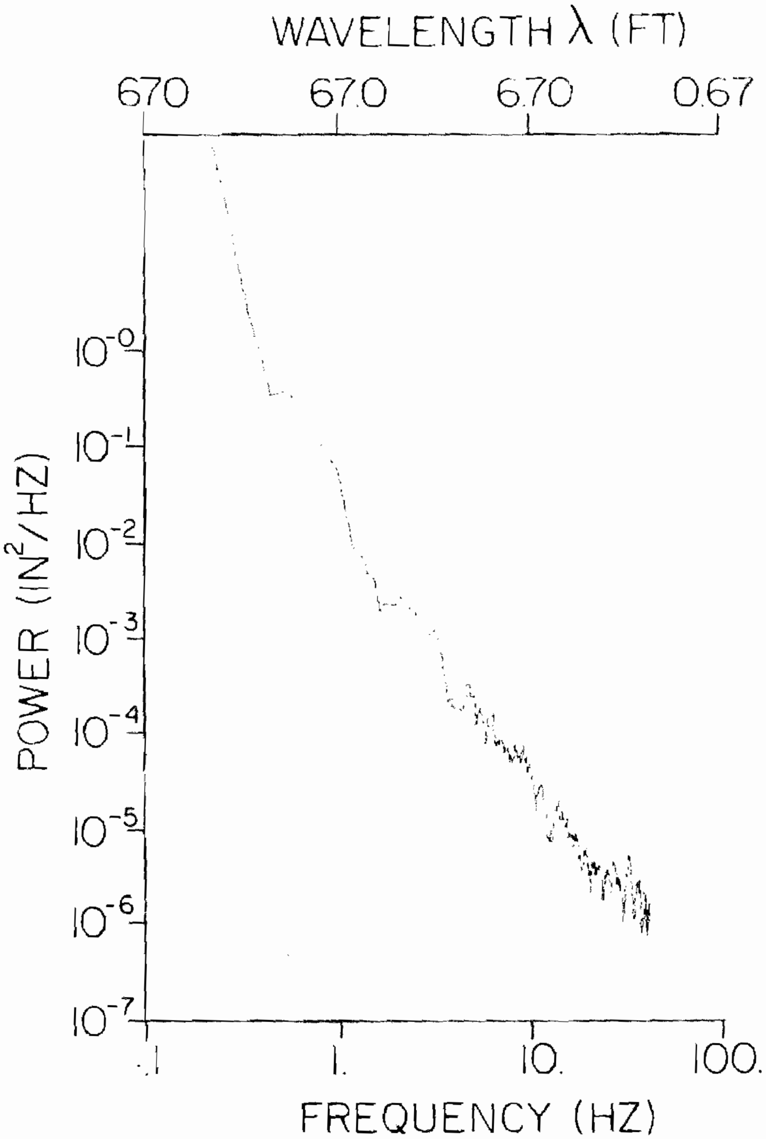

Section 2 Left

Figure 20. (continued)

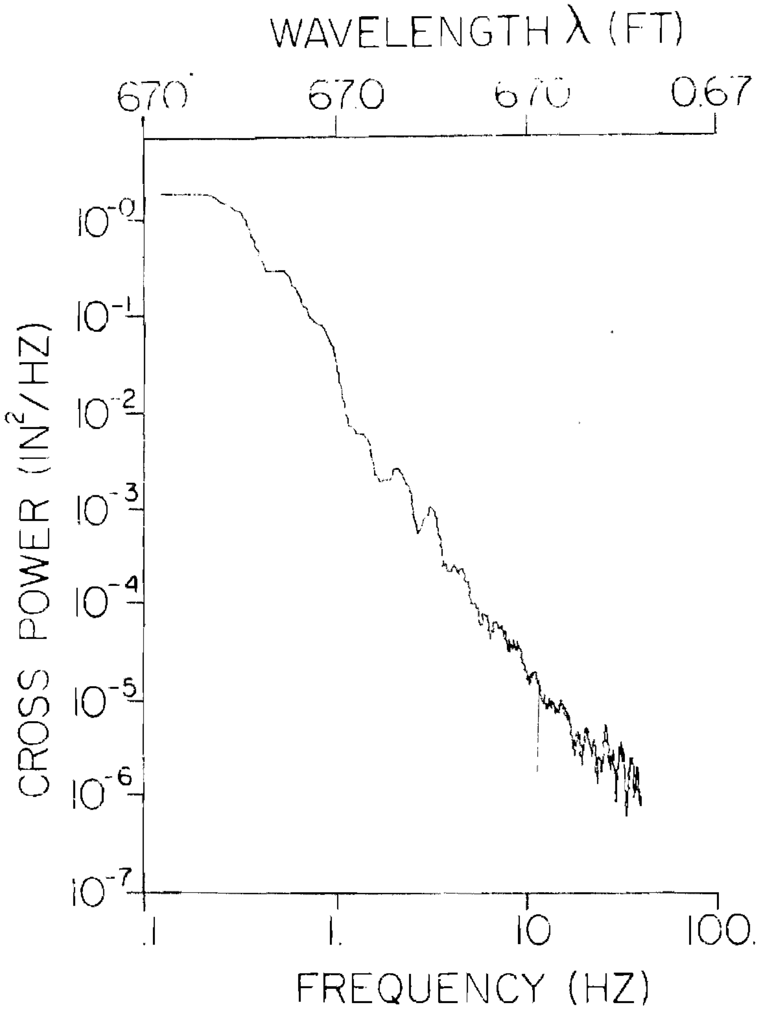

Section 2

Figure 21. Cross-Power Density

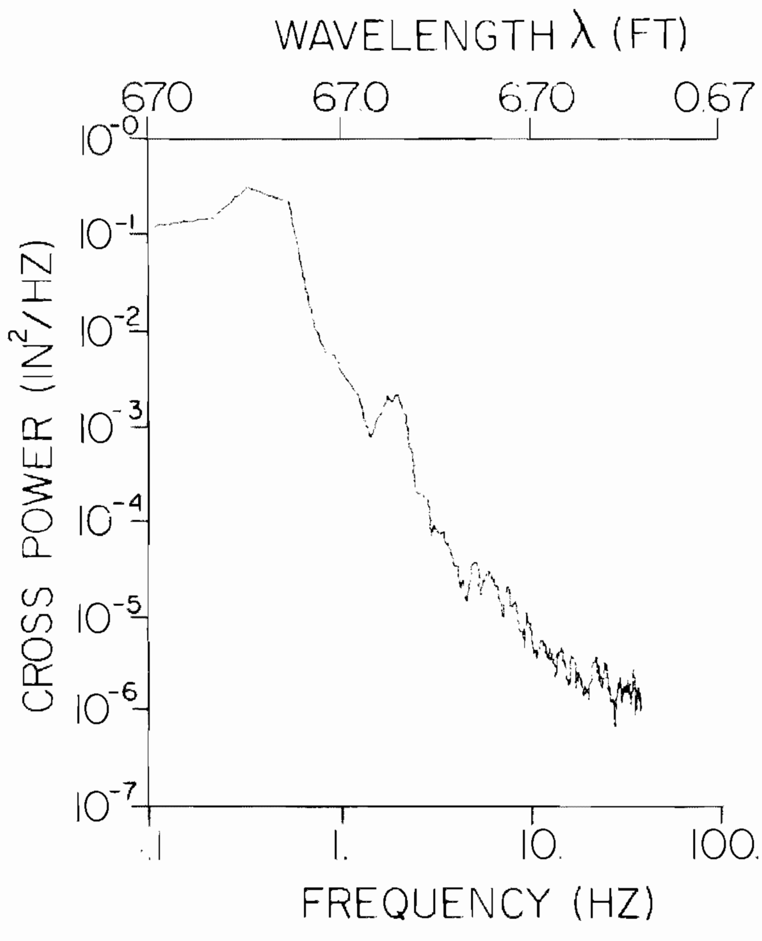

Section 3

Figure 21. (continued)

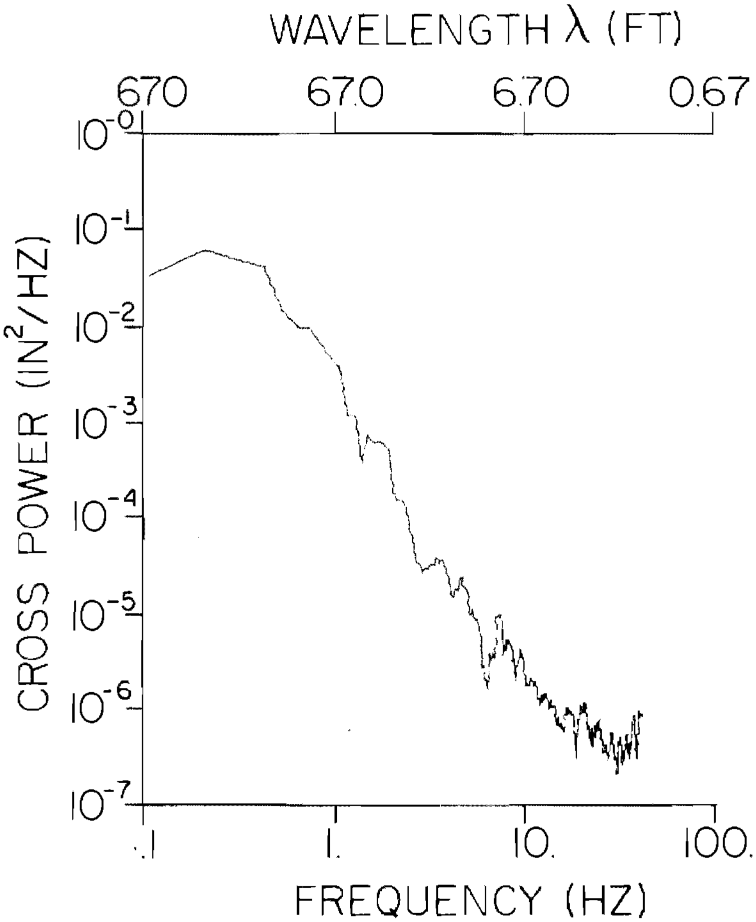

Section 5

Figure 21. (continued)

is simply not borne out by the data. A piecewise linear or polynomial fit would appear to be more nearly representative of even the smoother highways. Based on the data of La Barre et al[10], Dodds and Robson[9,11] have suggested a spectra representation of the form

$$\phi(\Omega) = \begin{cases} \phi(\Omega) \quad \left(\frac{\Omega}{\Omega_o}\right)^{-\omega_1} & \Omega \leq \Omega_o \\ \phi(\Omega) \quad \left(\frac{\Omega}{\Omega_o}\right)^{-\omega_2} & \Omega \geq \Omega_o \end{cases}$$

where $\phi(\Omega_o)$ is the "roughness coefficient" (value of the spectral density at the discontinuity frequency Ω_o). On the basis of the data presented in Appendix B the discontinuity between the two branches of the suggested form would be approximately a 20-ft. wavelength, as found in Reference 9. A classification of roads according to the constants $\phi(\Omega_o)$ and ω_1, ω_2 yields constants which are in some cases significantly different, however, from those presented in Table 1 of Reference 9, even for the same quality of road. This lack of roadway PSD generalization suggests that one may wish to work directly with the computer stored power spectra data as measured and not attempt to develop idealized models of PSD roadway roughness from a limited sample of data. The vehicle response calculations would then proceed directly on the computer. One additional observation was made with the present data audit which appears to deserve further study. It is concerned with the findings of Reference 9 about the stated isotropic character of the random roadway roughness. The present data indicate that although the power spectral densities taken from pairs of tracks for the different road surfaces are for all practical purposes roughly similar in character, a measurable RMS roughness difference of at least 10 does exist between each track in the majority of cases (Table B-1). Our initial examination of cross-power spectra of the roadways is illustrated in Figure 21. The general form of the cross spectra is similar to the longitudinal spectra, as can be seen by comparing Figure 21 with its counterparts in Appendix B. Further examinations of coherency are being conducted. It appears at first glance that the assumption of an isotropic random roughness field is a simplifying assumption and that is borne out by our data. Further study is needed in this area since to assess the relationship between two roadway tracks the phase relationship must also be studied. In view of these findings, it seems desirable at this stage to obtain a more complete catalogue or correlation of measured highway and/or roadway PSD data for obtaining a better classification and modeling of the roughness.

CHAPTER 4

CONCLUSION

The CATS Ride Quality Group has assembled and checked the equipment necessary for the acquisition, reduction, and analysis of ride vibrations of an automobile in the field and for the collection of highway roughness profile data. Techniques have been developed for the optimum utilization of this equipment and they give accurate and repeatable results. Detailed automobile vibration responses and corresponding roadway roughnesses have been measured for twenty different roadway sections which are typical of those found in the Austin - Travis county area. A review of our typical roadway roughness data and the roughness models presented in the literature indicates that further modeling efforts and data sampling are necessary before an adequate roadway roughness model can be developed. At the present time, the most representative vehicle vibration response calculations can best be obtained by storing the measured roughness data in numerical form in the computer and calculating the vehicle responses numerically from a representative mathematical model. The basic task of this study is to support a program to obtain objective measurements of an automotive transportation environment with which some measure of the subjective response of an individual can be correlated for the establishment of a ride quality criterion.

REFERENCES

1. Catherines, J. J., Clevenson, S. A., and Scholl, H. F., "A Method for the Measurement and Analysis of Ride Vibrations of Transportation Systems," NASA TN D-6785, Langley Research Center, May 1972.

2. Walker, R. S. and Hudson, W. R., "A Correlation Study of the Mays Road Meter with the Surface Dynamics Profilometer," Research Report 156-1, Center for Highway Research, The University of Texas at Austin, February 1973.

3. Roberts, F. L. and Hudson, W. R., "Pavement Serviceability Equations Using the Surface Dynamic Profilometer," Research Report 73-3, Center for Highway Research, The University of Texas at Austin, April 1970.

4. Nathman, E. T., "Evaluations of Automobile Ride Accelerations with Random Roadway Roughness," M.S. Thesis, The University of Texas at Austin, August 5, 1974.

5. Walker, R. S. and Hudson, W. R., "Analog-to-Digital System," Research Report 73-4, Center for Highway Research, The University of Texas at Austin, April 1970.

6. Spangler, E. B. and Kelly, W. J., "GMR Road Profilometer - A Method for Measuring Road Profiles," Research Report GMR-452, December 1964.

7. Brigham, E. O. and Morrow, R. E., "The Fast Fourier Transform," IEE Spectrum, page 63, December 1967.

8. Houboult, J. C., "Runway Roughness Studies in the Aeronautical Field," Transactions of ASCE, Vol. 127, Part 4, pp. 427-447.

9. Dodds, C. J. and Robson, J. D., "The Description of Road Surface Roughness," Journal of Sound and Vibration, Vol. 31(2), pp. 175-183, November 22, 1973.

10. LaBarre, R. P., et al, "The Measurement and Analysis of Road Surface Roughness," Motor Industry Research Association Report No. 1970/5, 1969.

11. Dodds, C. J., "Generalized Terrain Dynamic Inputs to Vehicles," BSI Document 72/34562 {ISO/TC/108/W69 (MEE/158/3/1)} , May 1972.

12. Healey, A. J., et al, "Research Report RR-14, Council for Advanced Transportation Studies, The University of Texas at Austin (1974).

APPENDIX A

Vehicle RMS and PSD Vibration Spectra From Measured Data

TABLE A-1

Measured RMS Vibration Response

Section	RMS Vertical	RMS Transverse	$\sqrt{(RMSV)^2 + (RMST)^2}$
1	.0419	.0218	.0472
7	.0252	.0259	.0361
2	.0634	.0273	.0690
6	.0604	.0262	.0658
3	.0461	.0214	.0508
5	.0269	.0141	.0304
37	.0638	.0245	.06834
38	.0634	.0281	.0693
39	.0545	.0320	.0632
40	.0399	.0169	.0433
41	.0558	.0226	.060221
8	.0425	.0160	.0454
11	.0371	.0154	.0402
12	.0592	.0228	.0634
13	.0712	.0300	.077
10	.0337	.0145	.0367
15	.0685	.0286	.07423
36	.0354	.0132	.0377

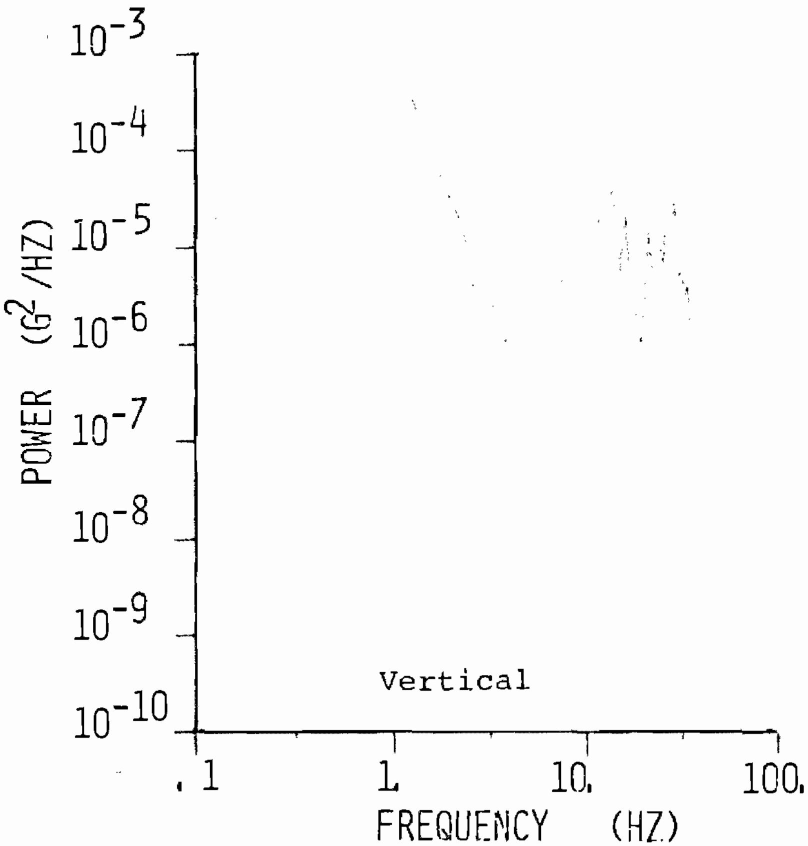

Section 1

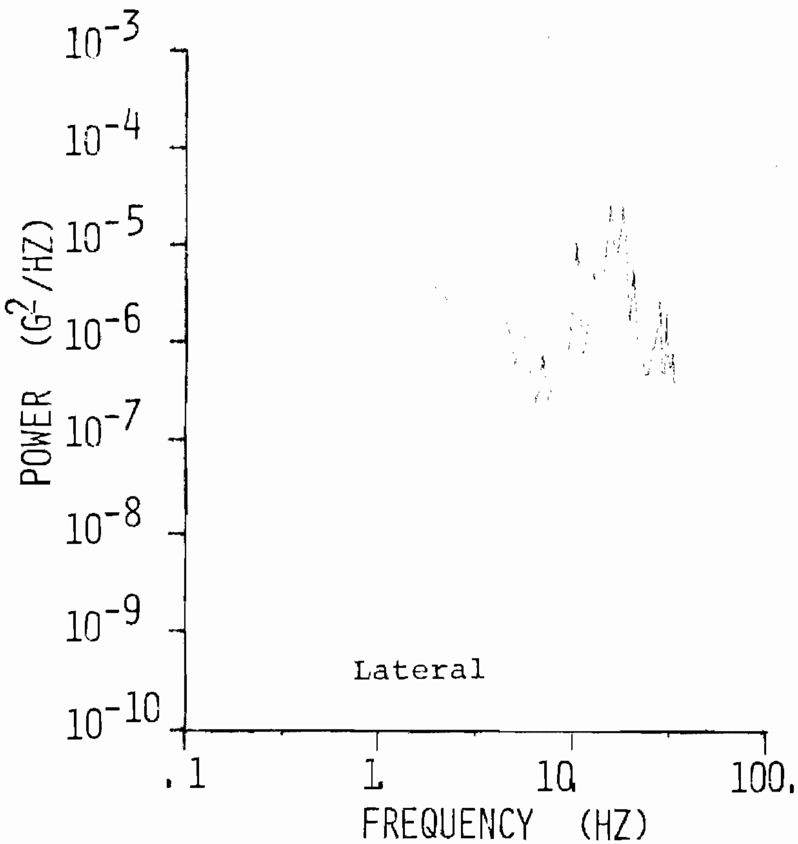

Section 1

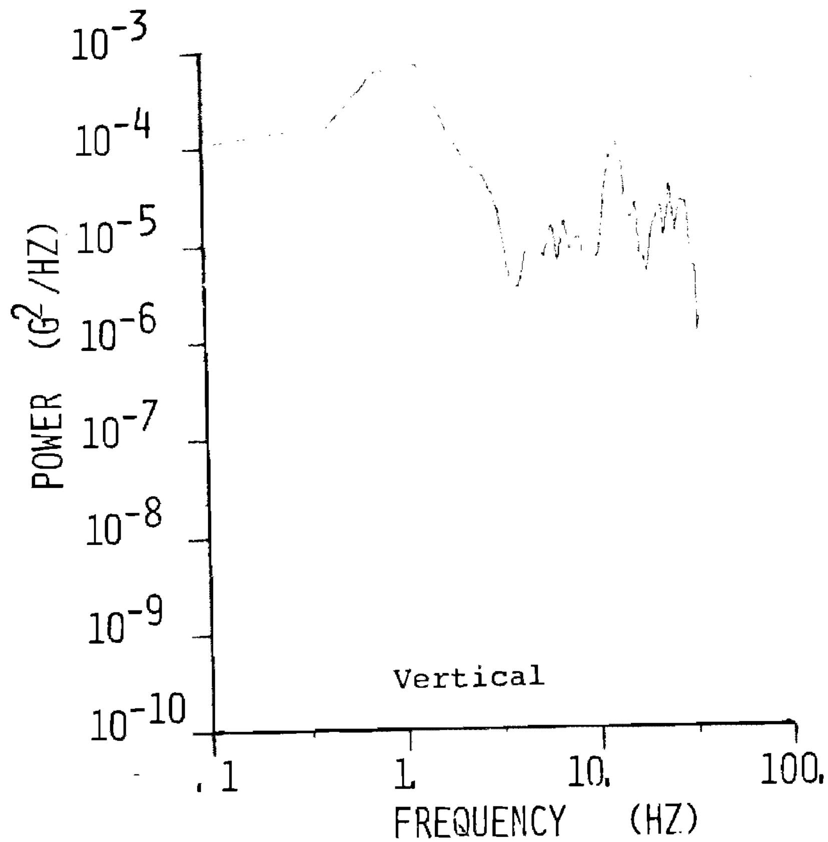

Section 2

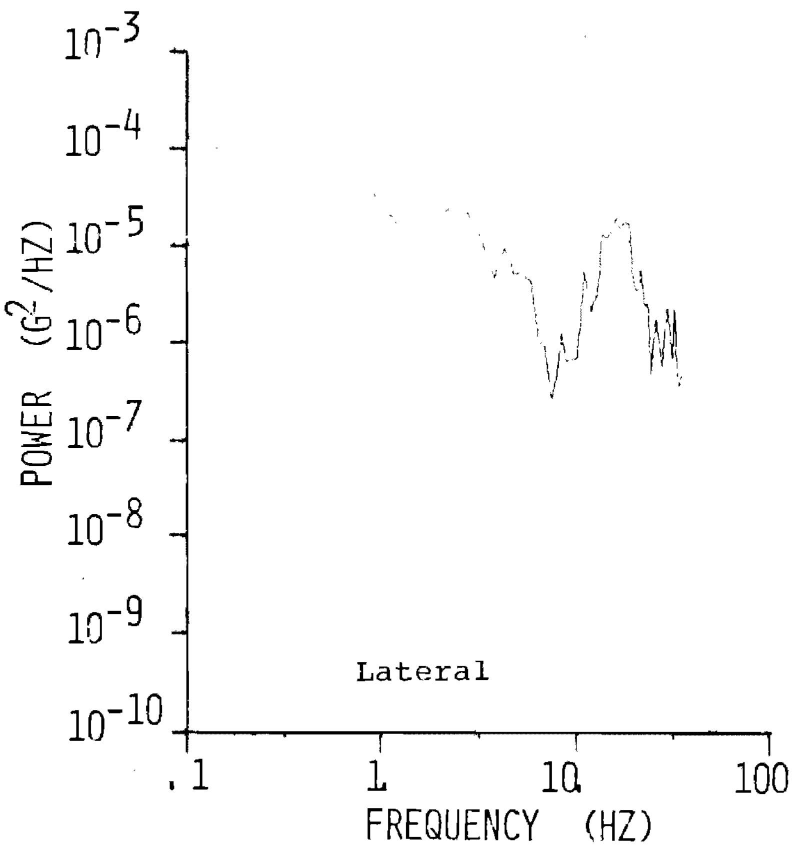

Section 2

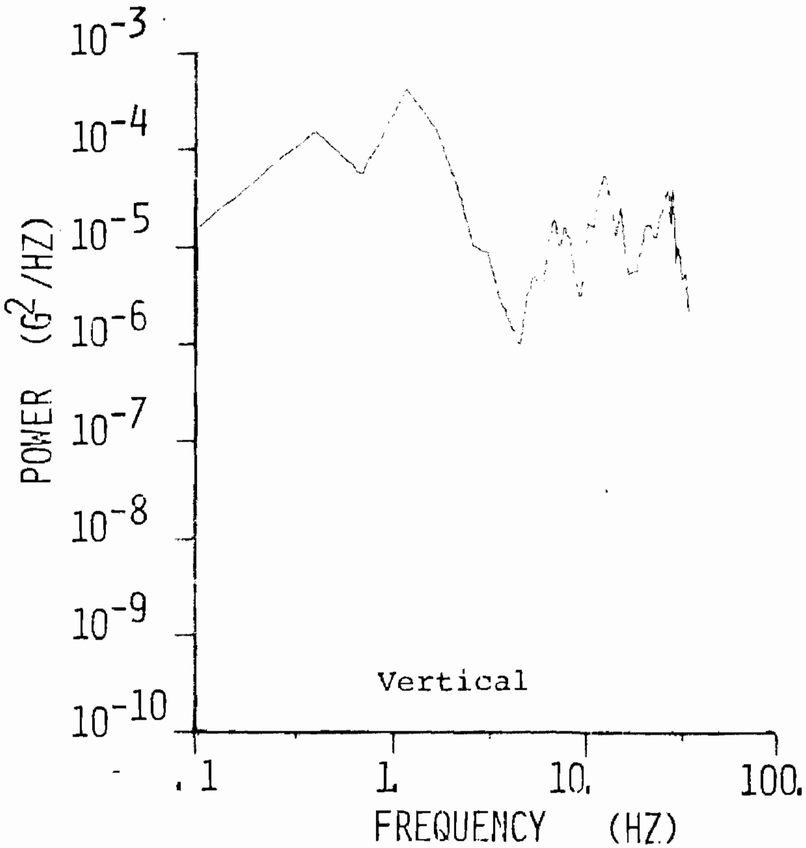

Section 3

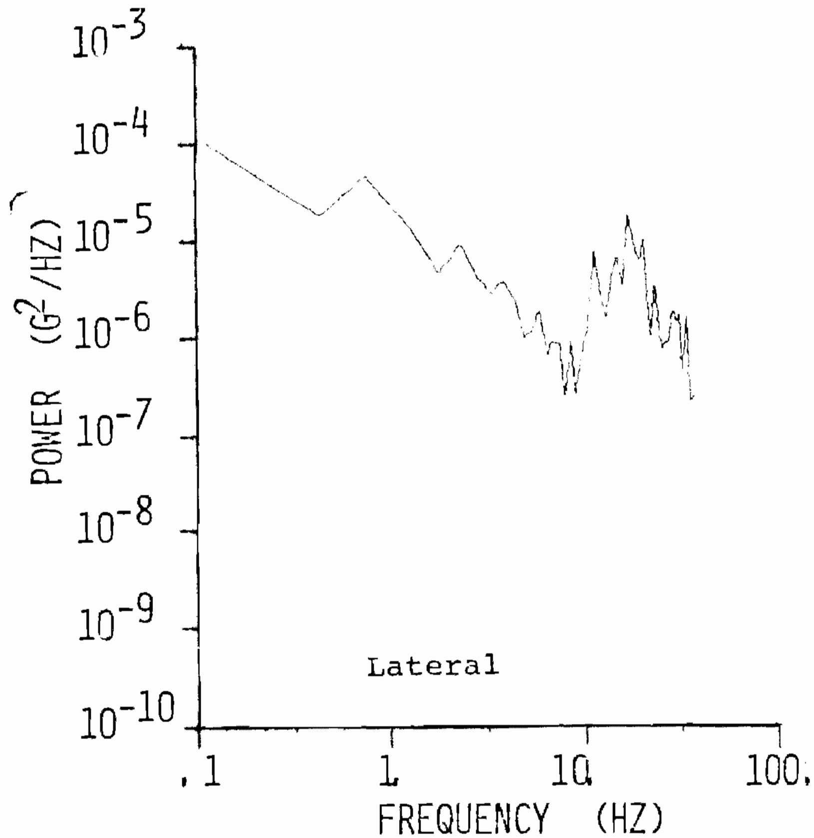

Section 3

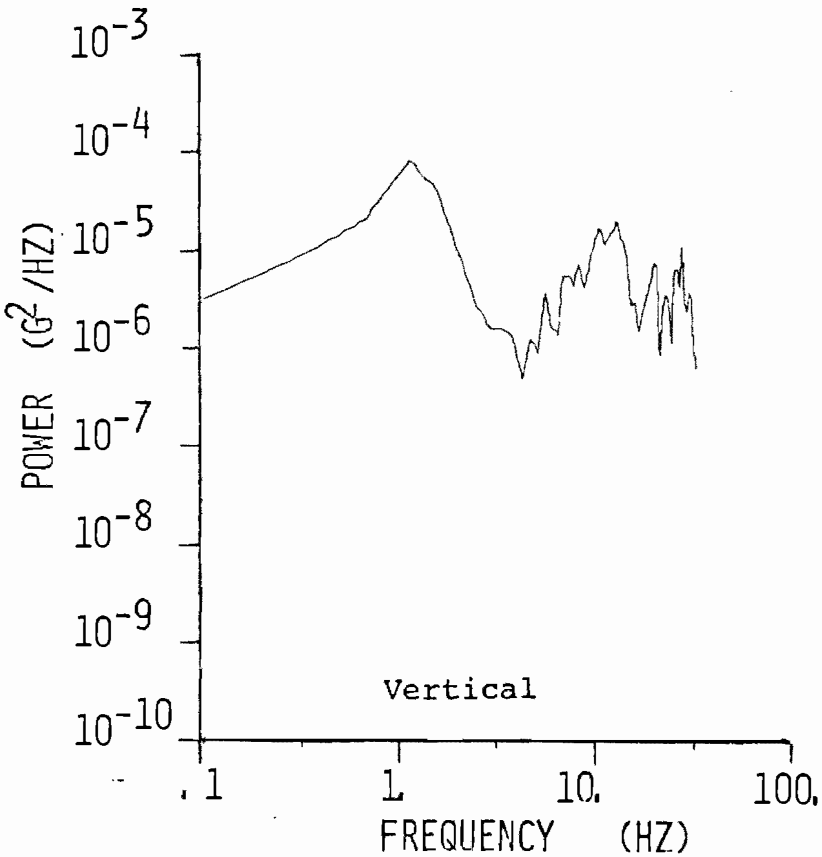

Section 5

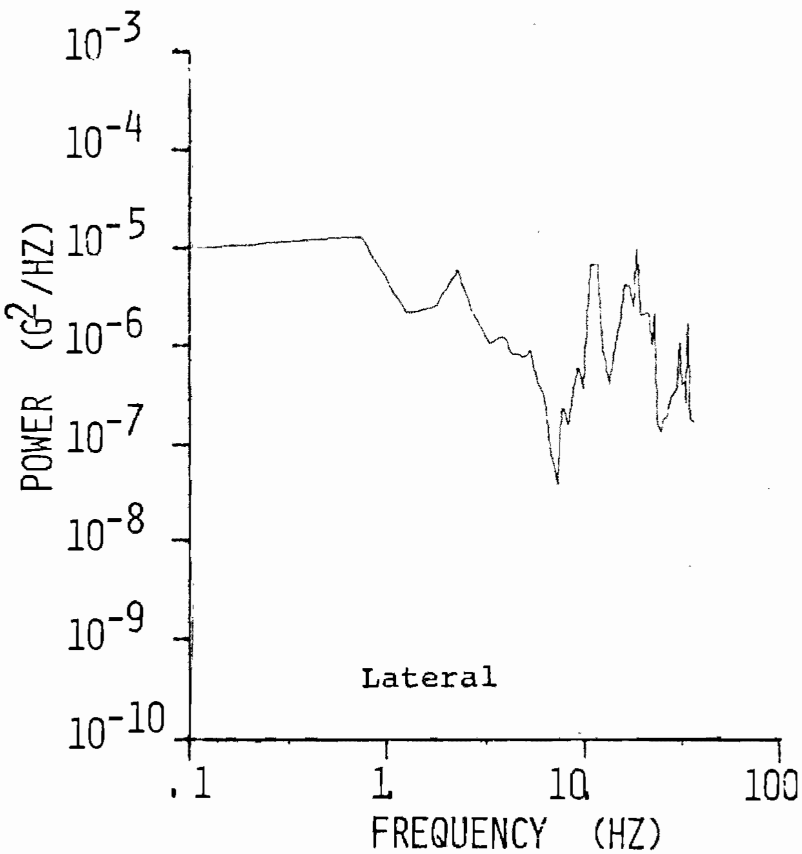

Section 5

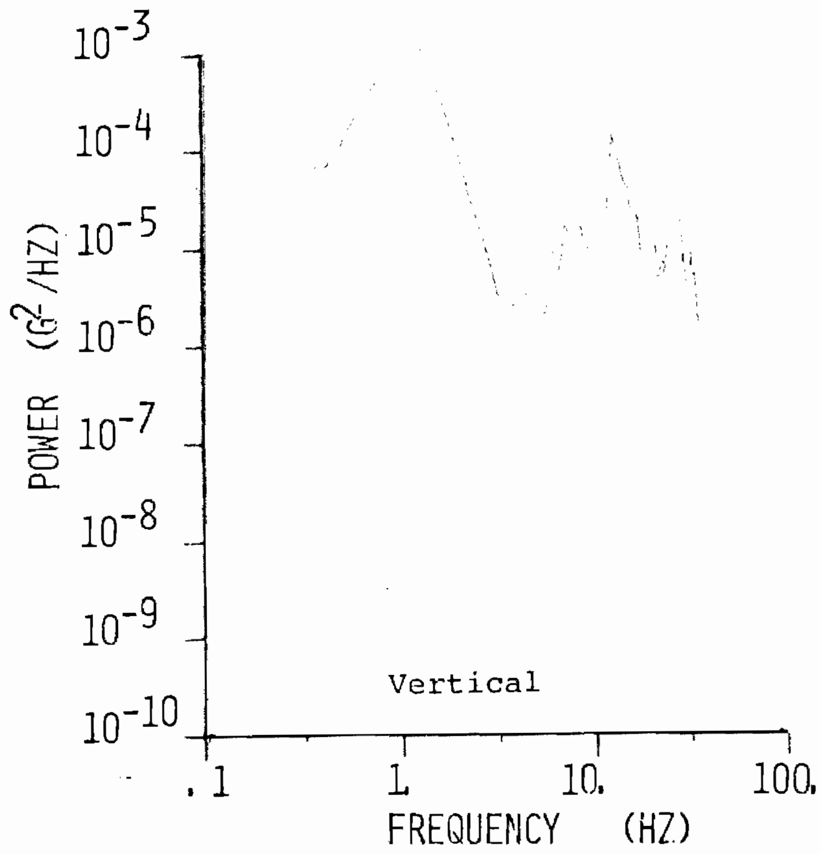

Section 6

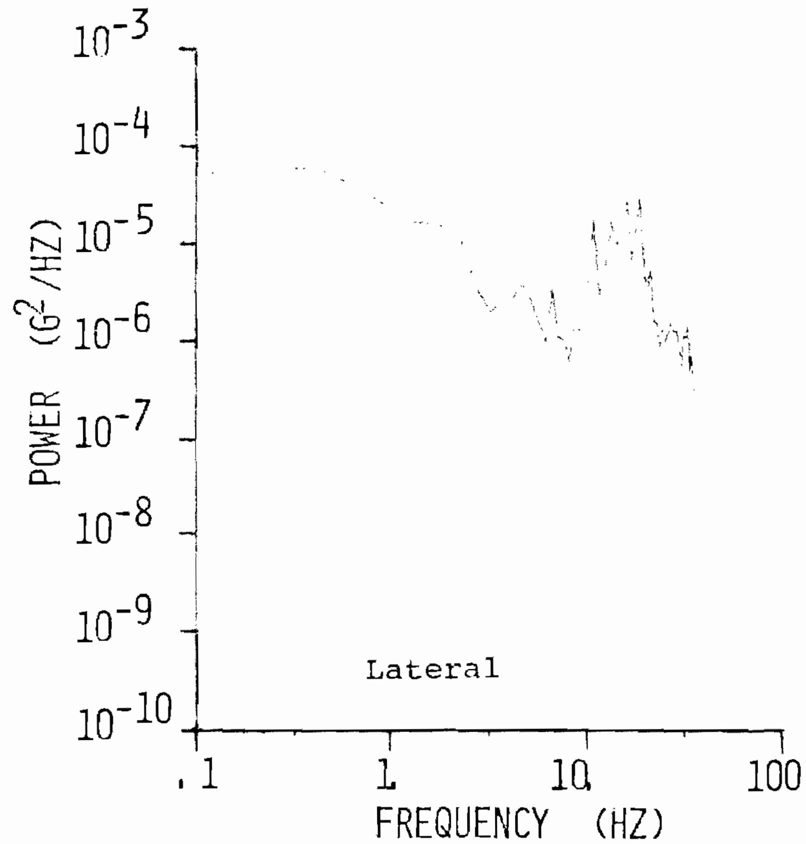

Section 6

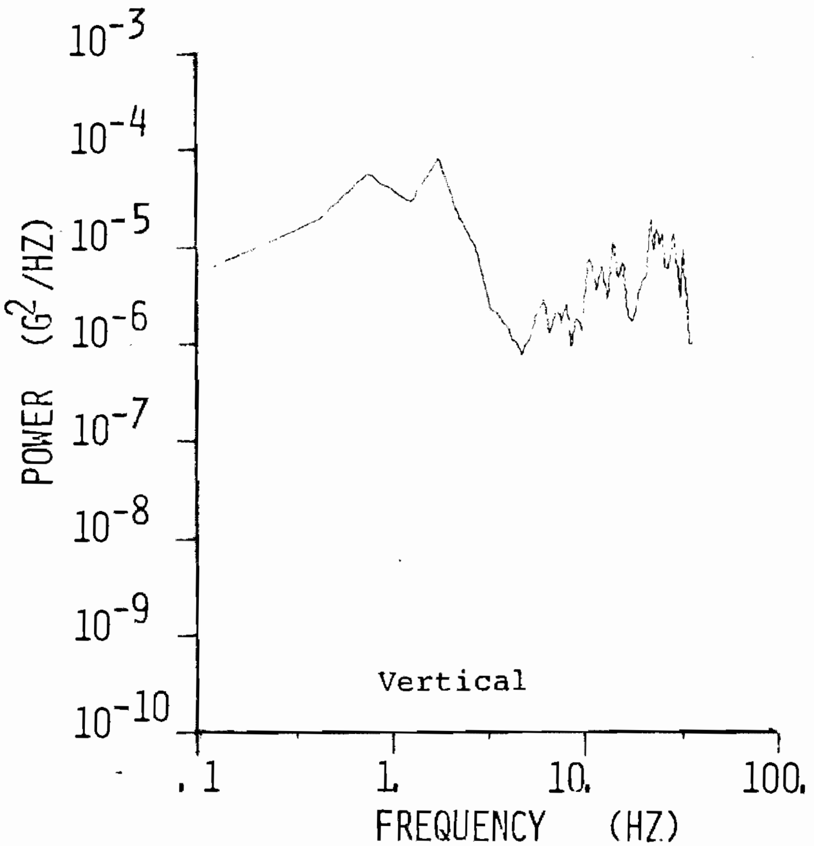

Section 7

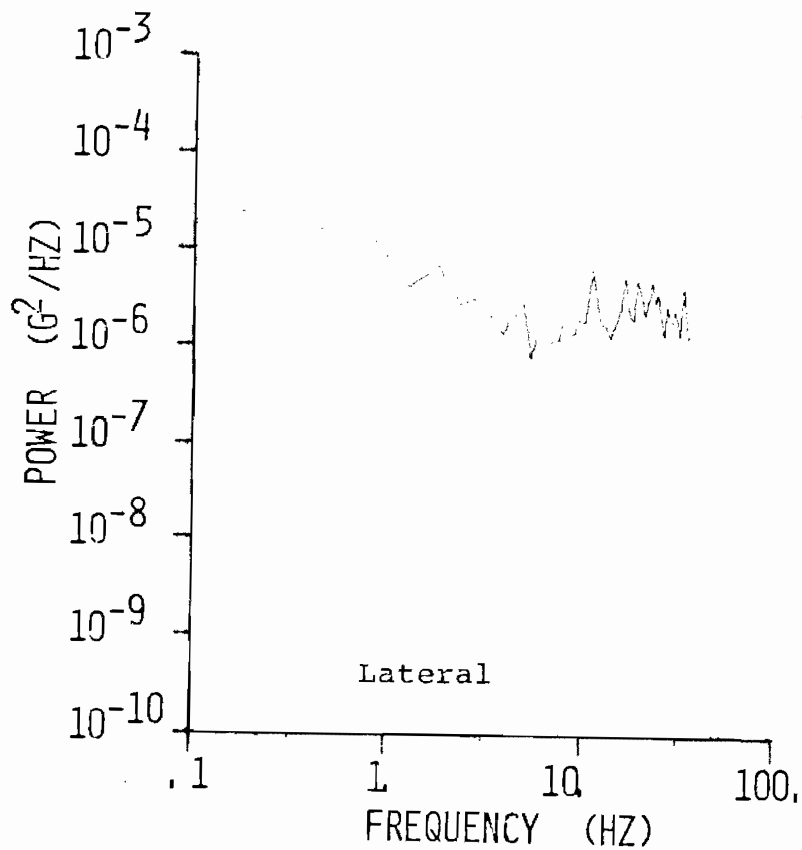

Section 7

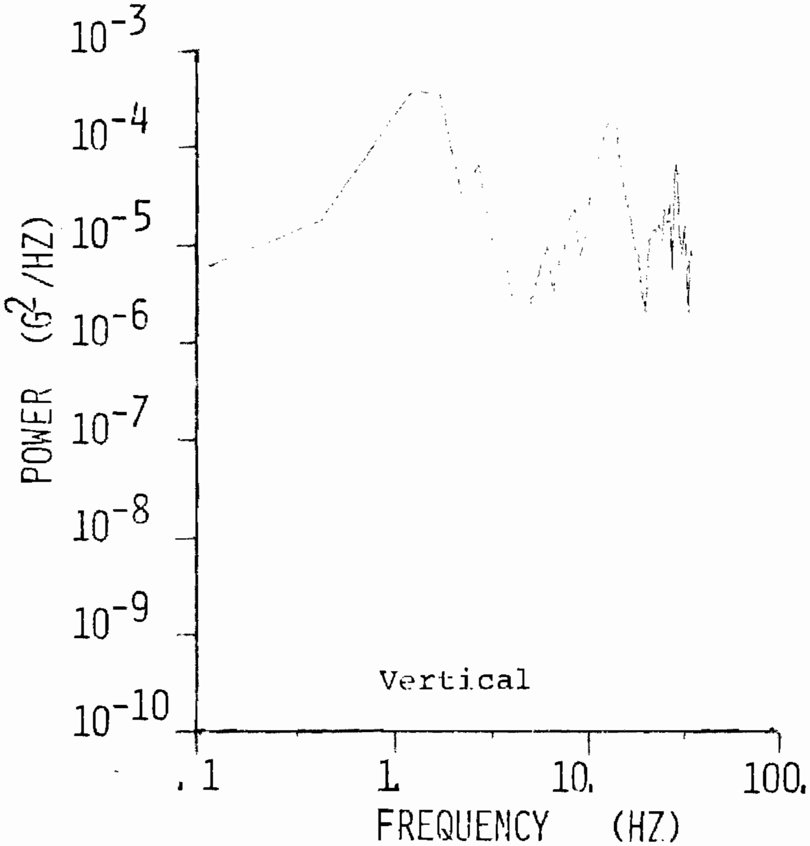

Section 8

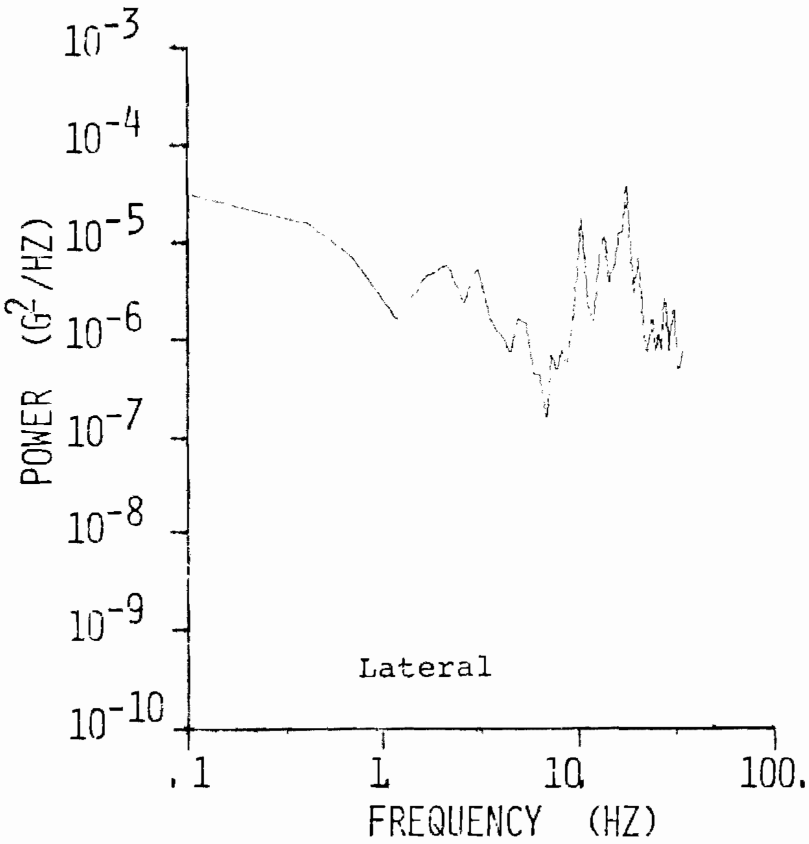

Section 8

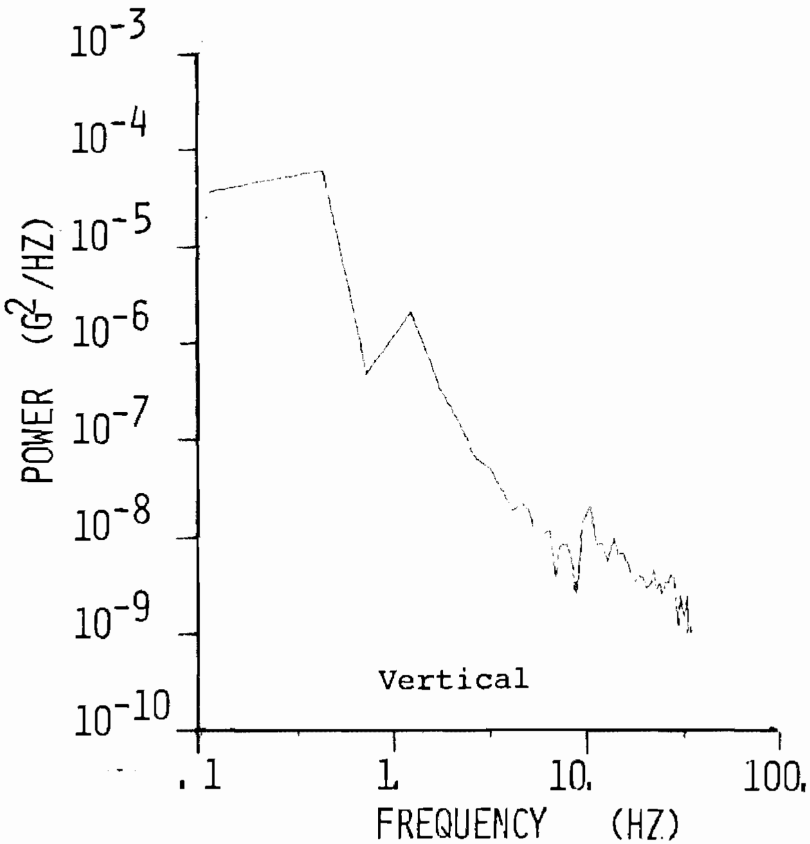

Section 9

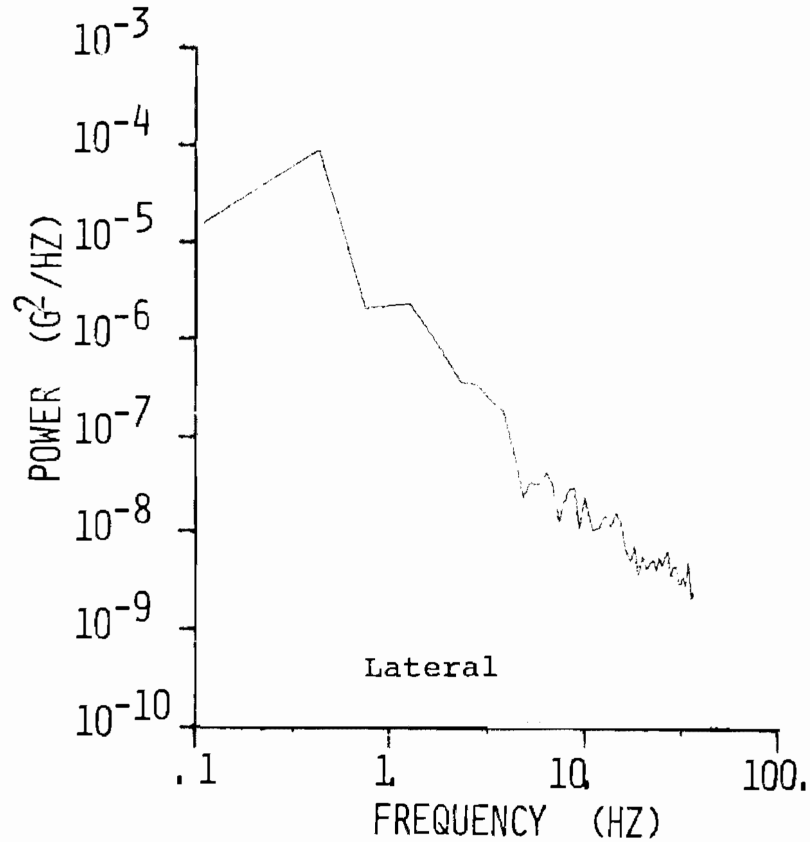

Section 9

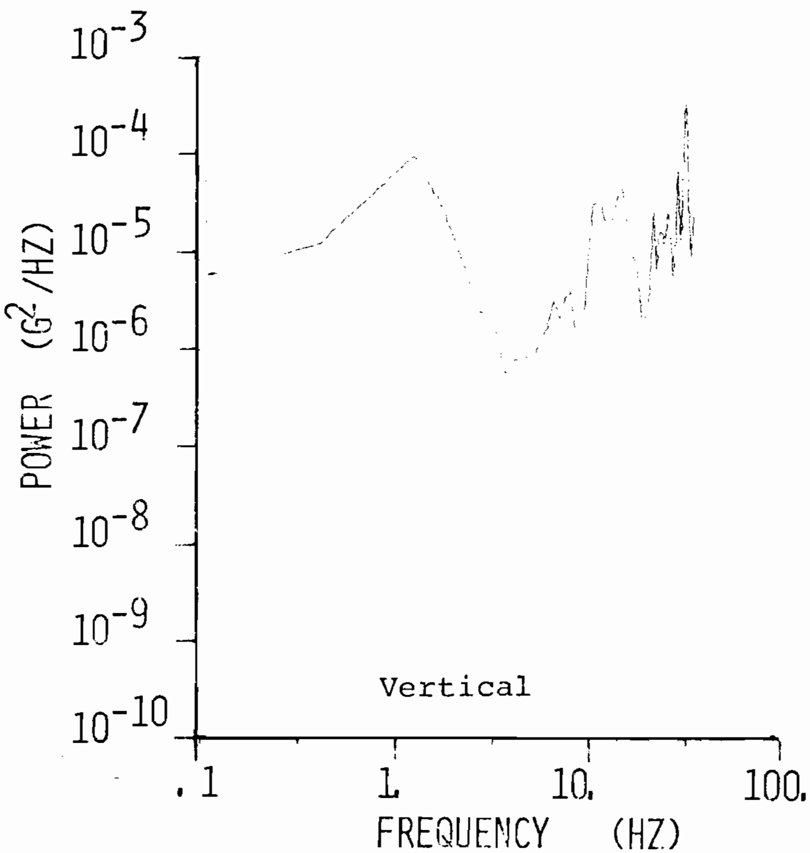

Section 10

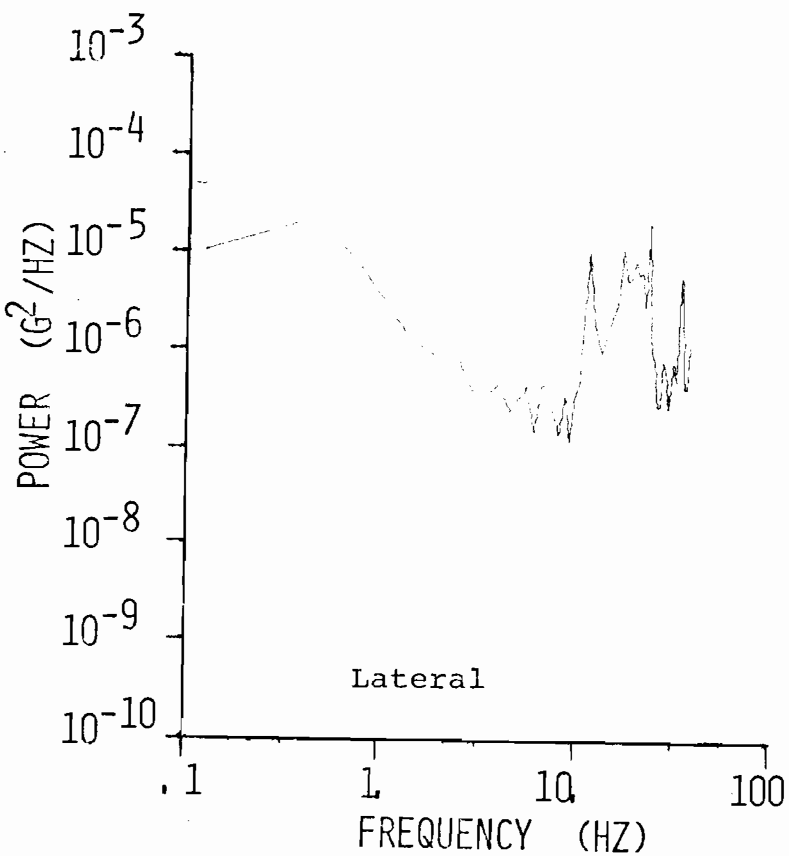

Section 10

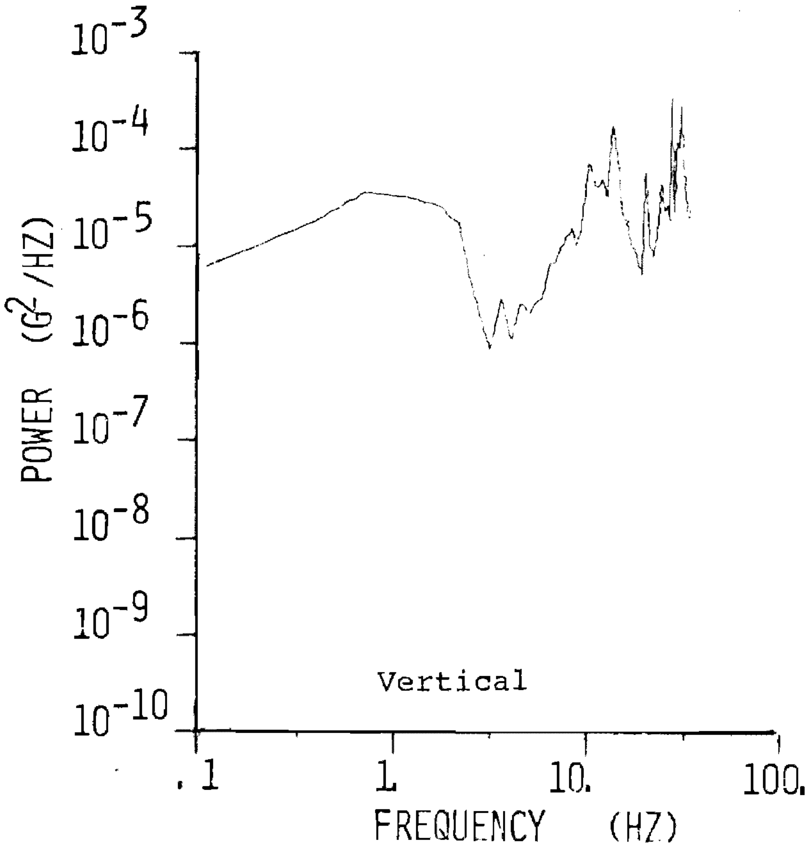

Section 11

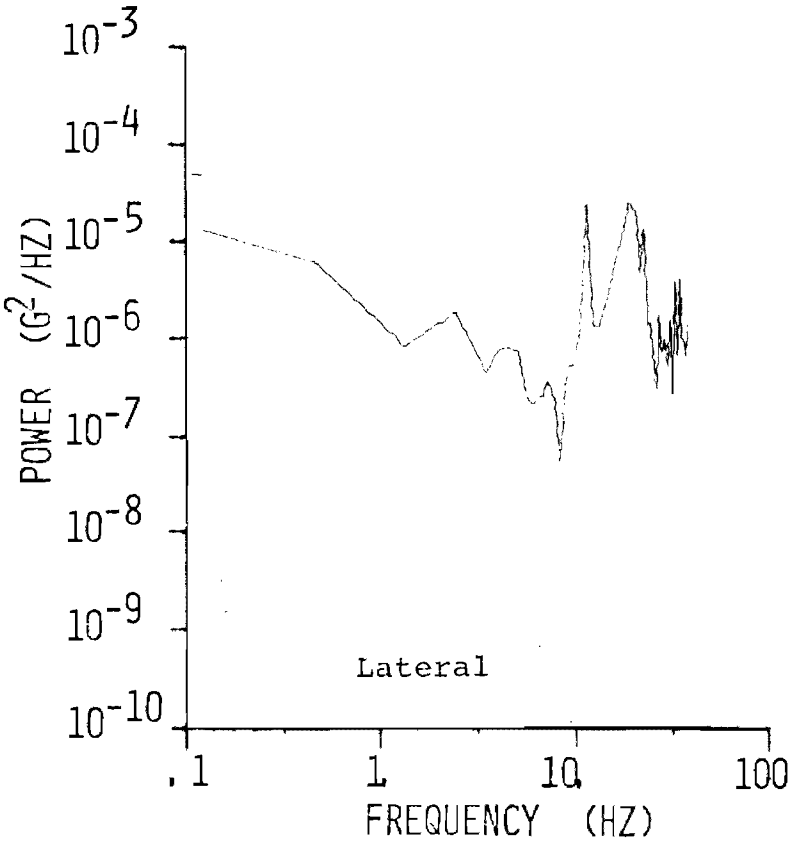

Section 11

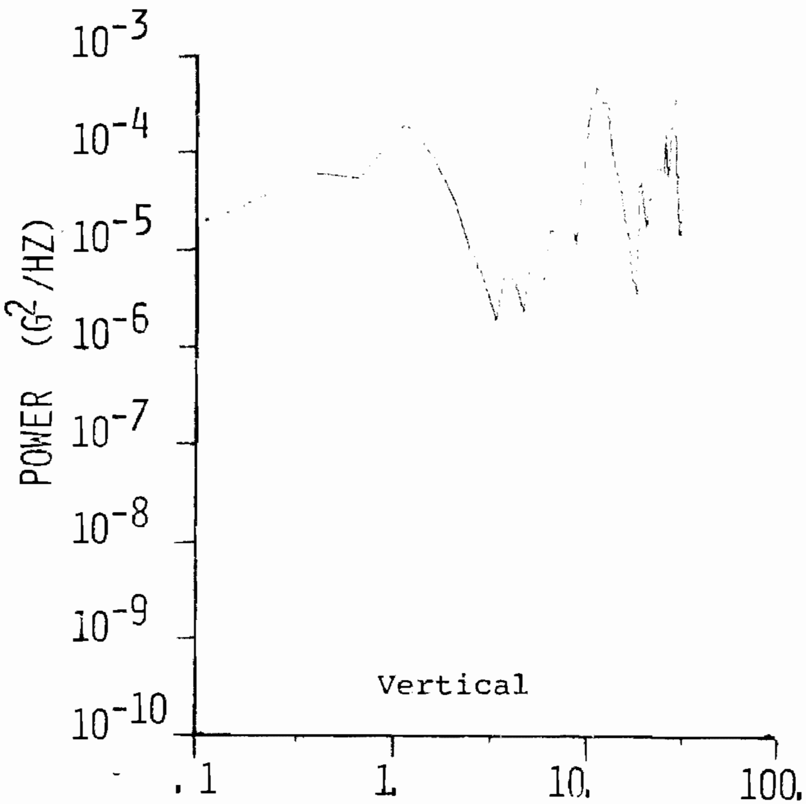

Section 12

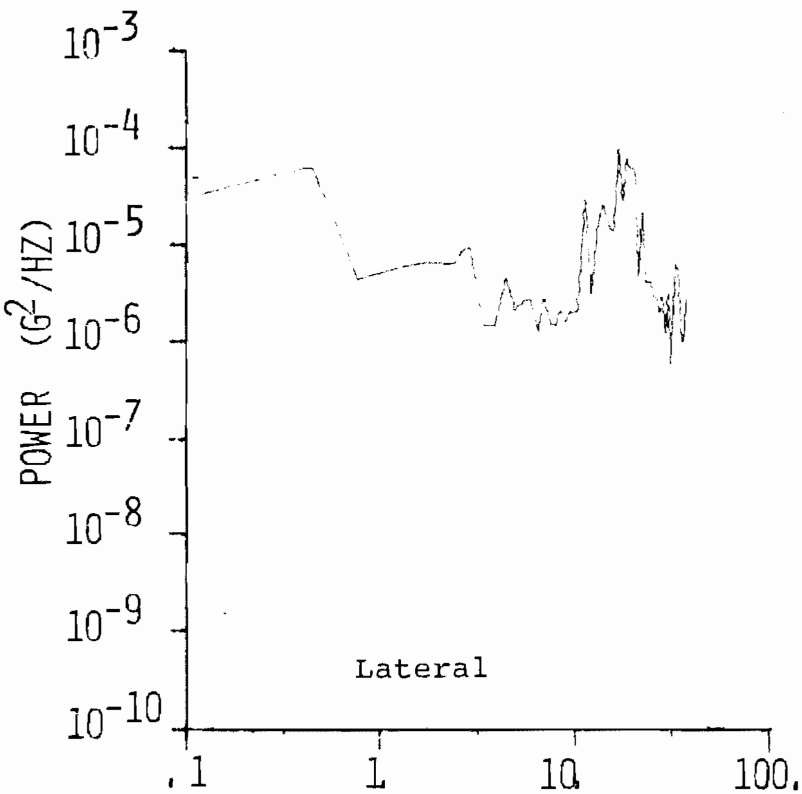

Section 12

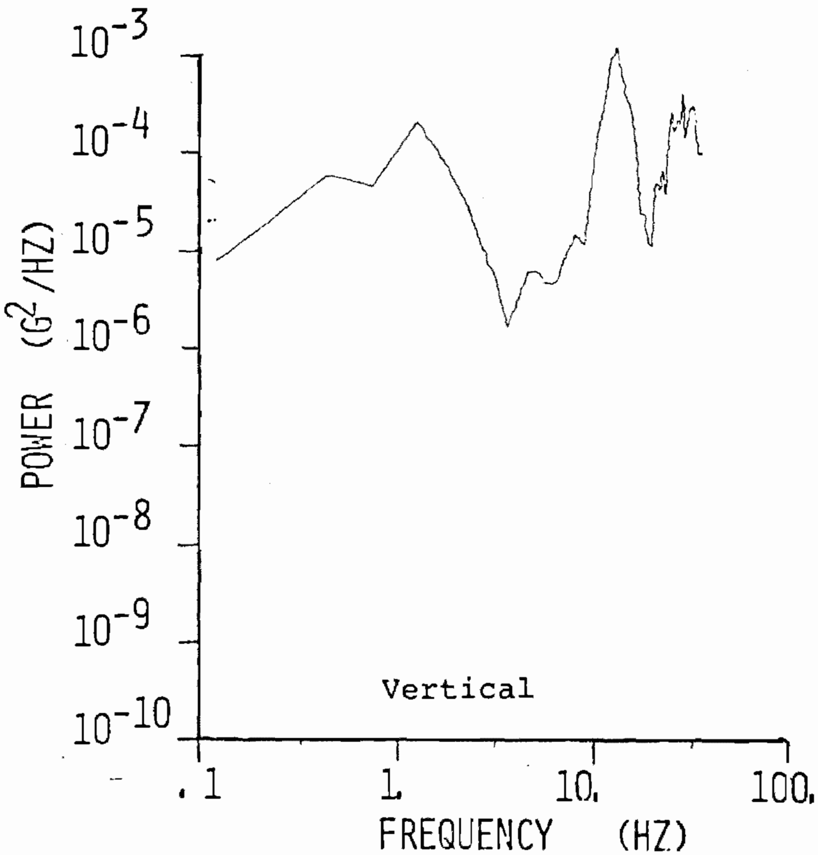

Section 13

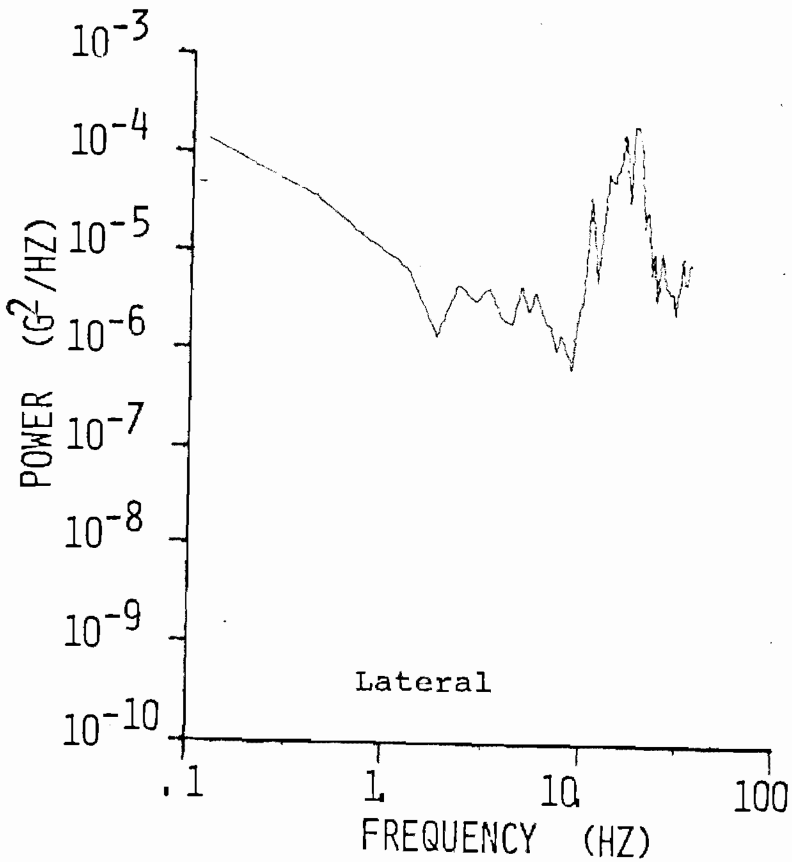

Section 13

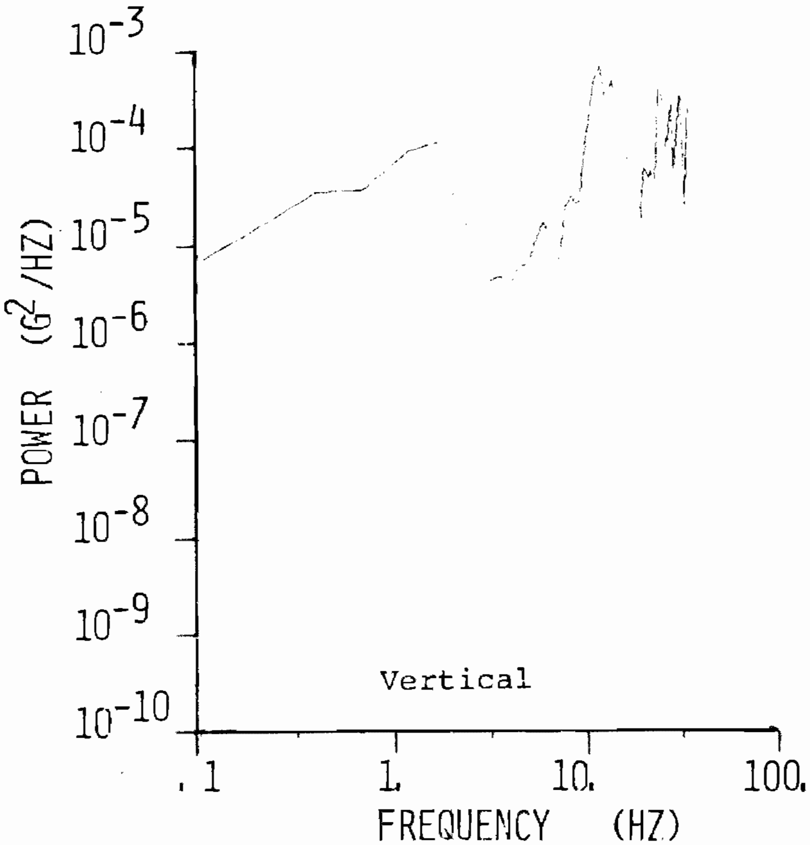

Section 15

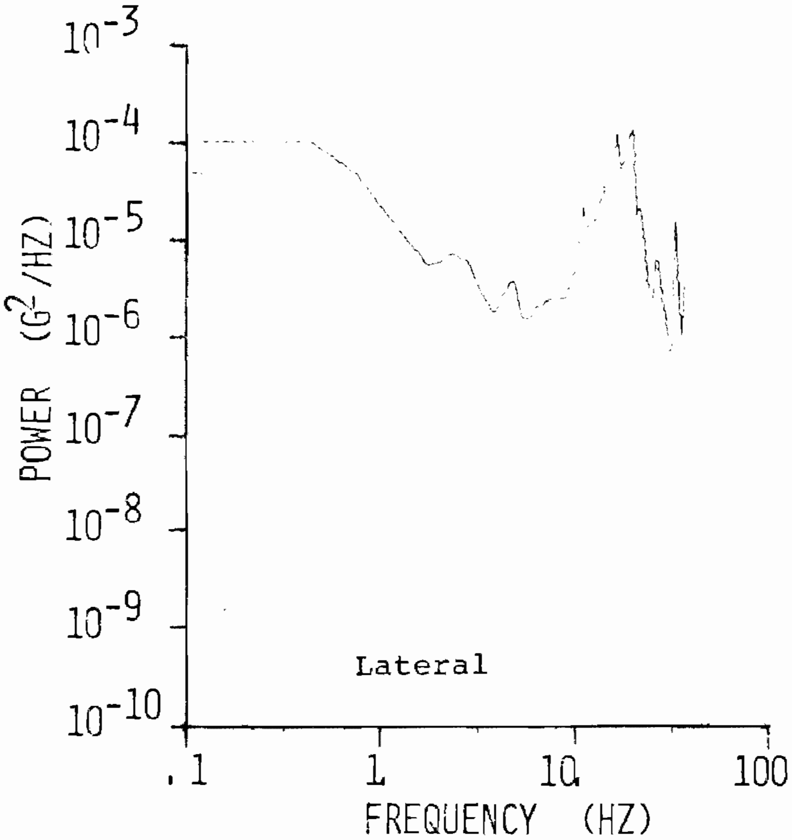

Section 15

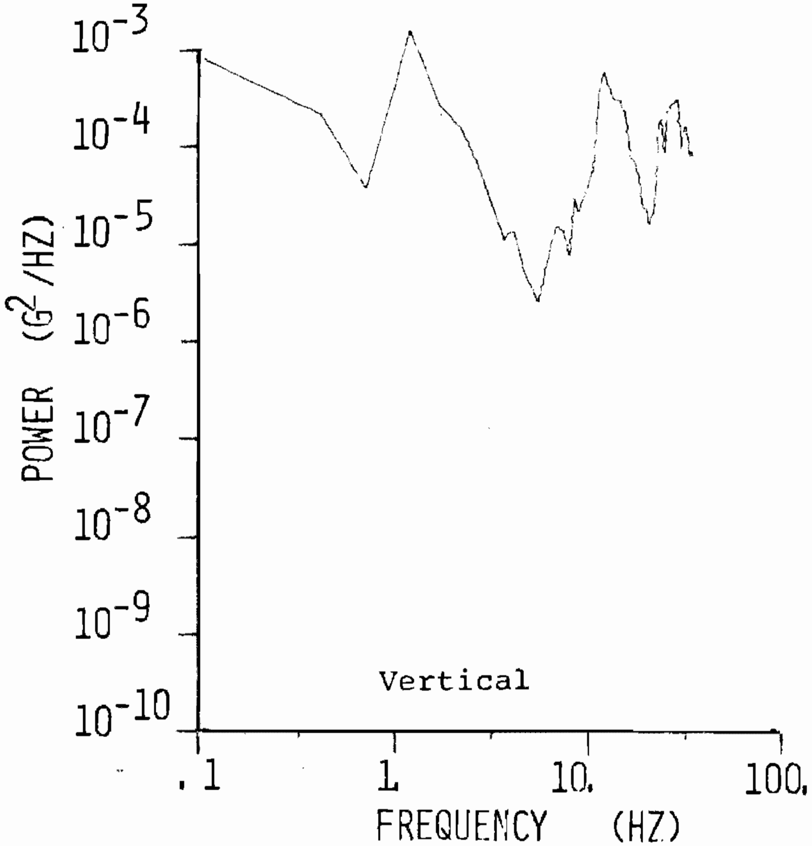

Section 35

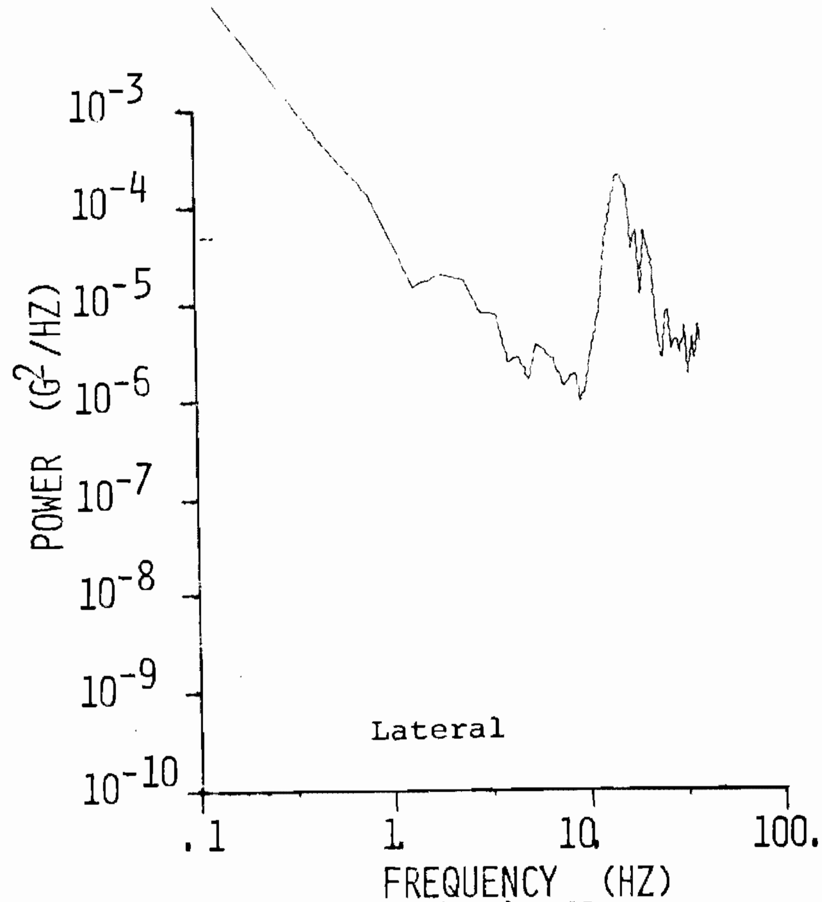

Section 35

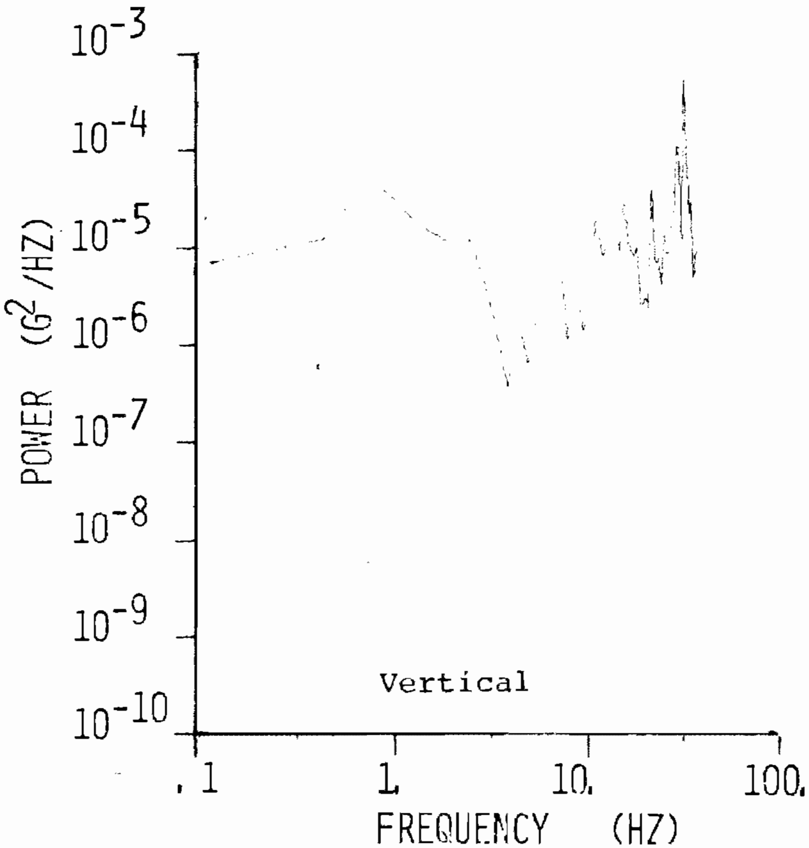

Section 36

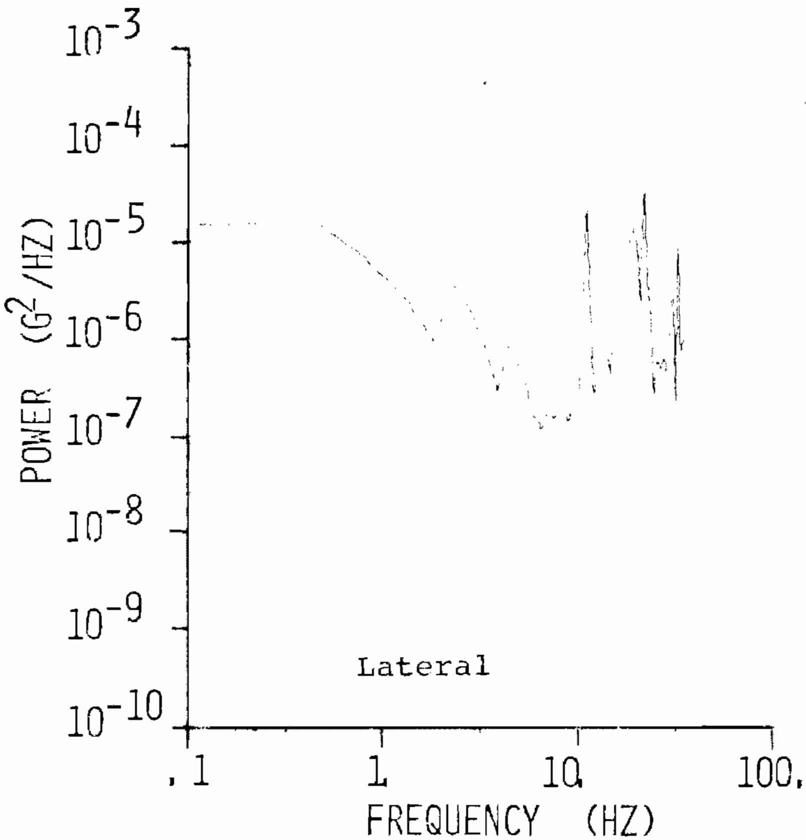

Section 36

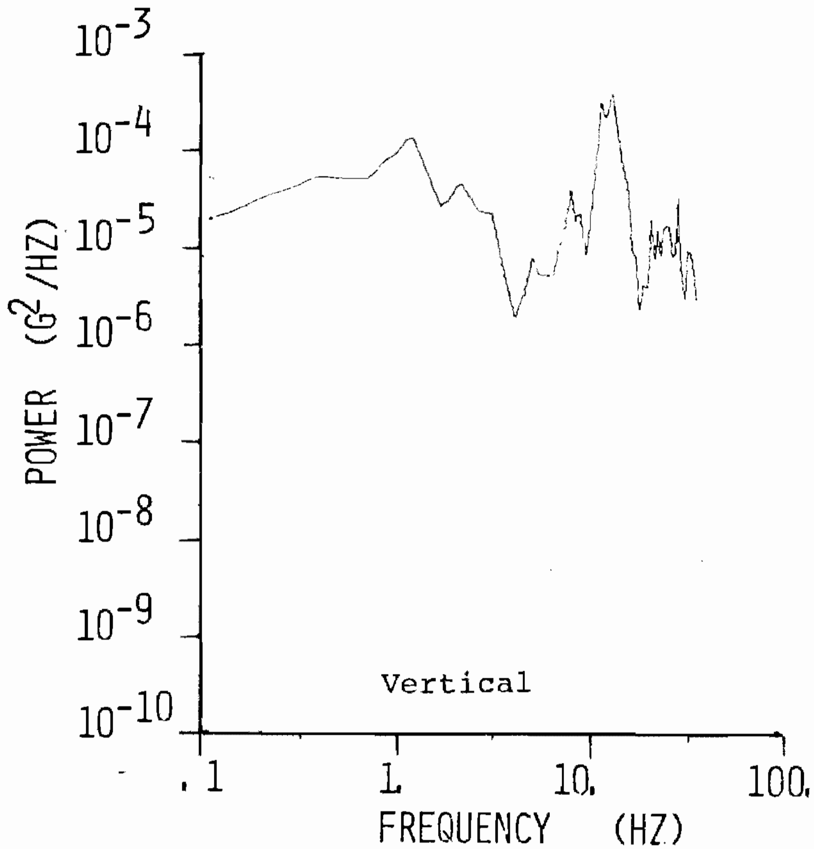

Section 37

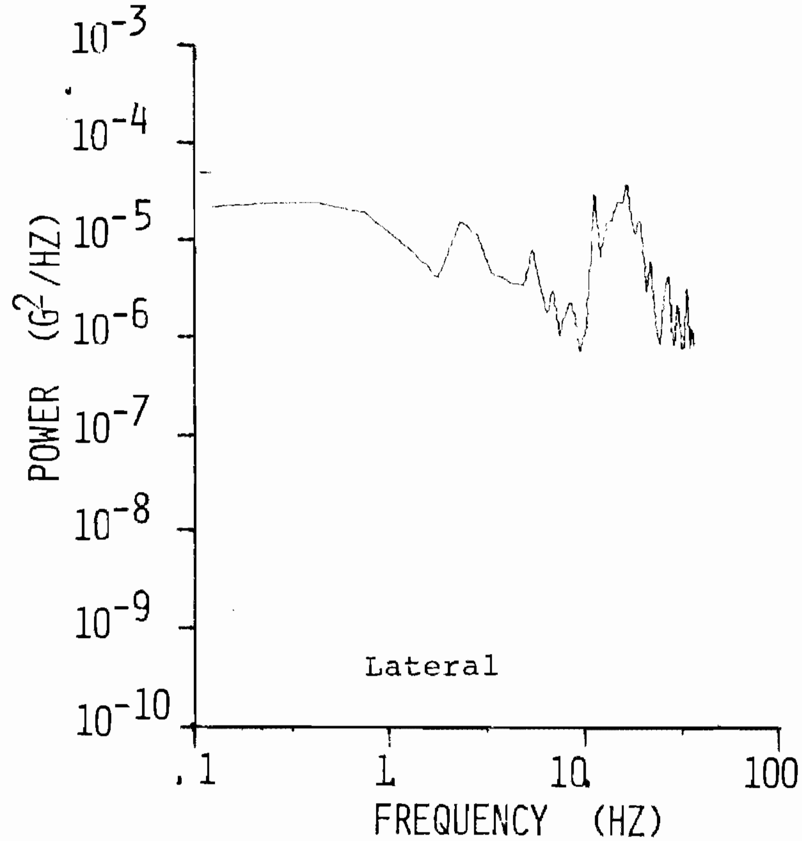

Section 37

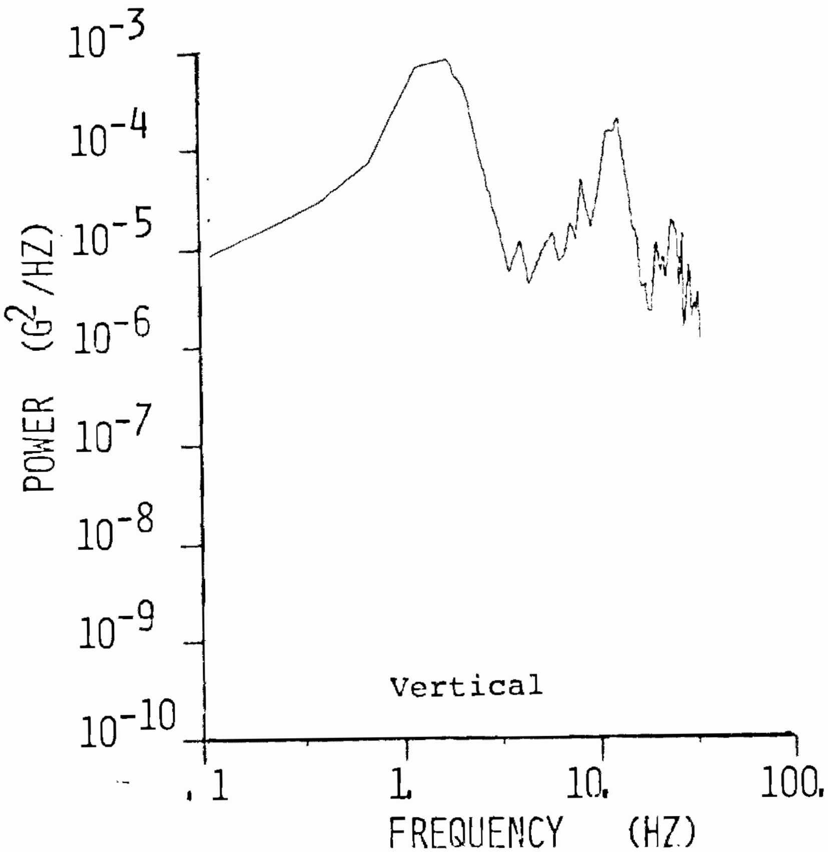

Section 38

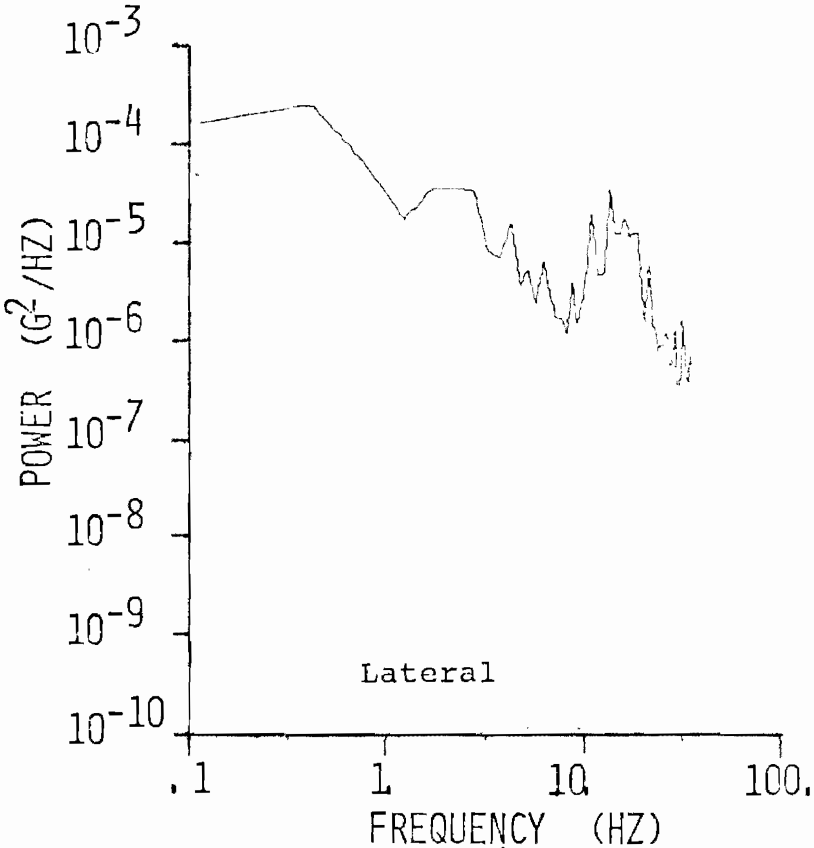

Section 38

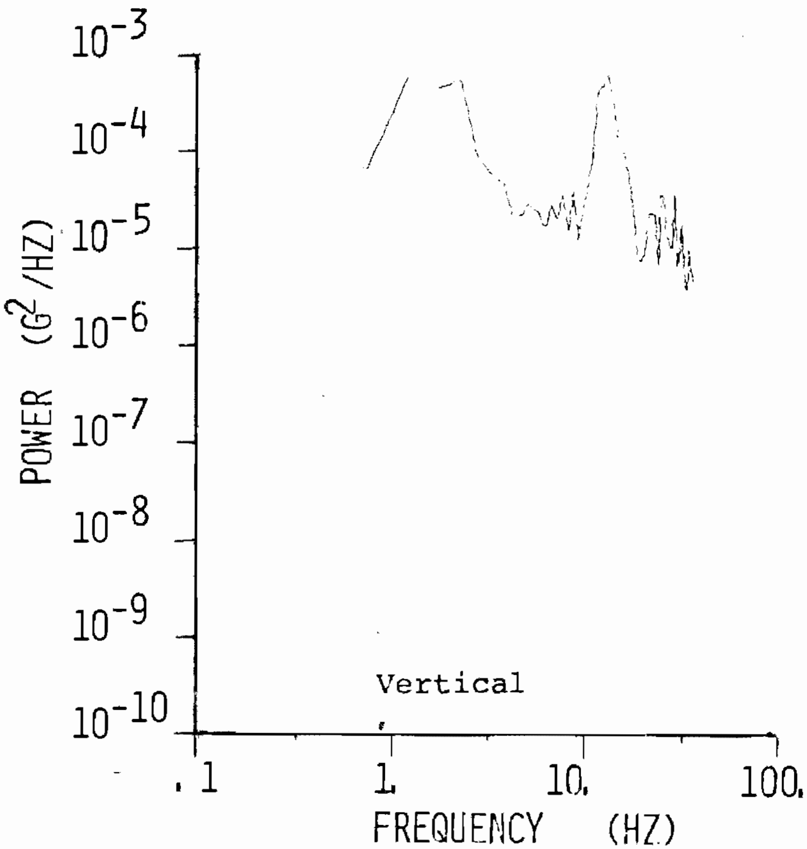

Section 39

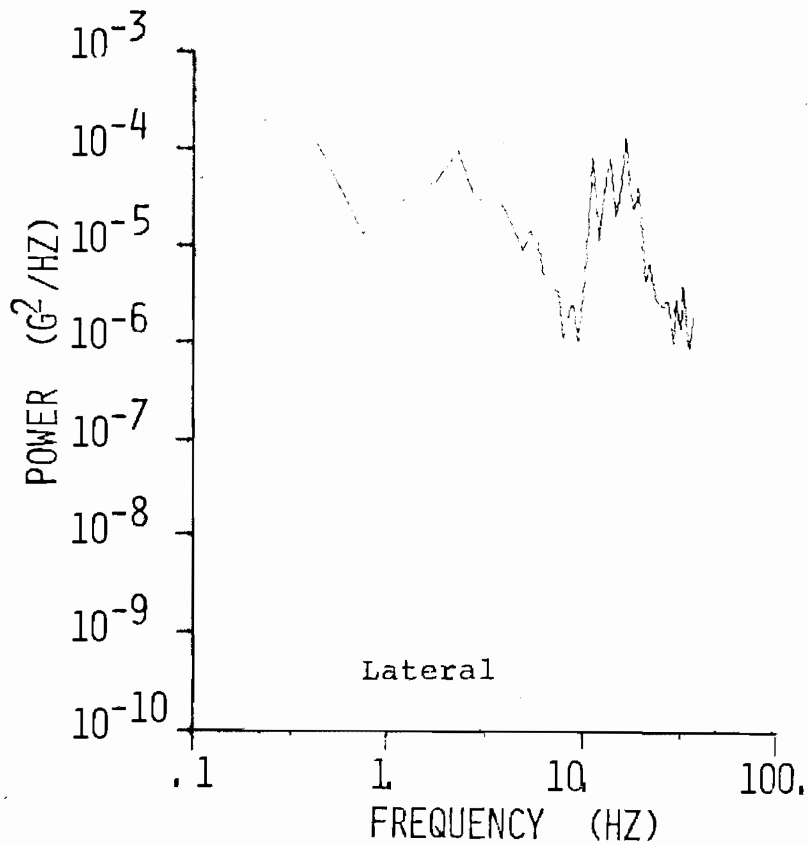

Section 39

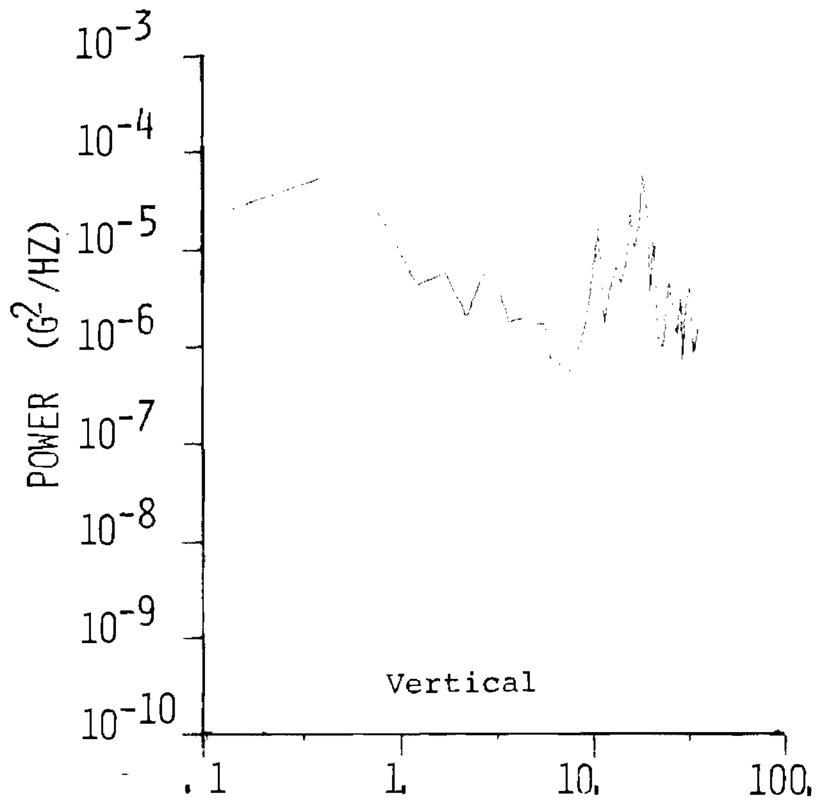

Section 40

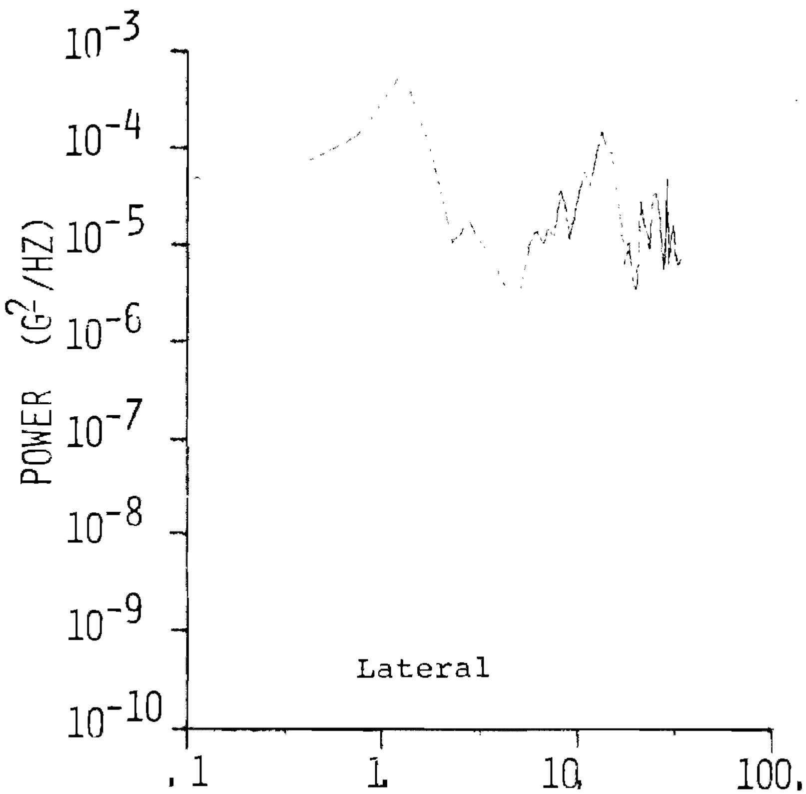

Section 40

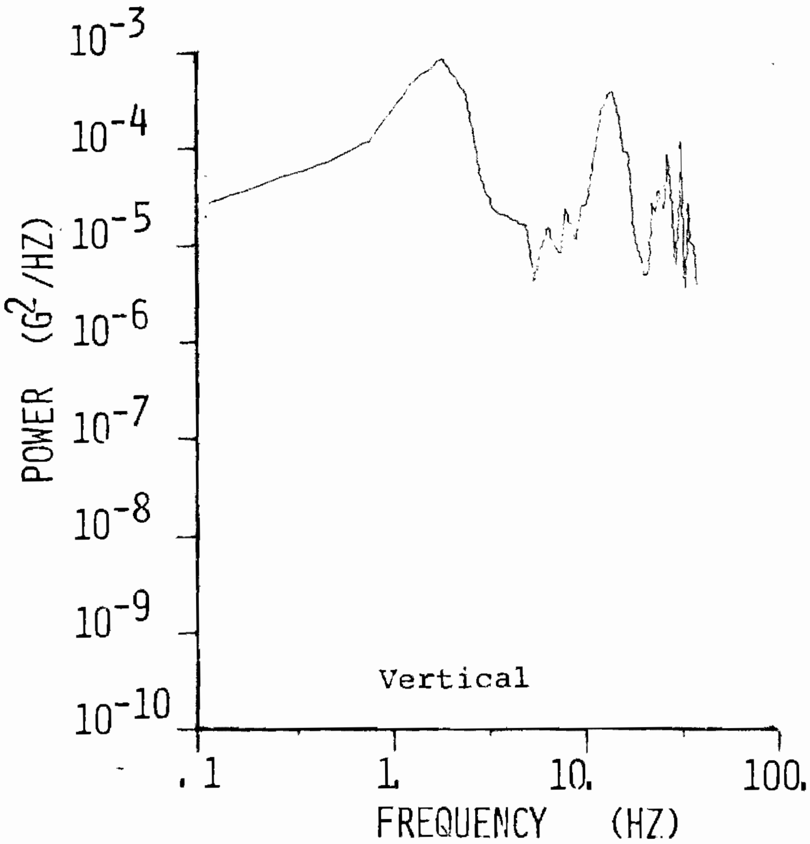

Section 41

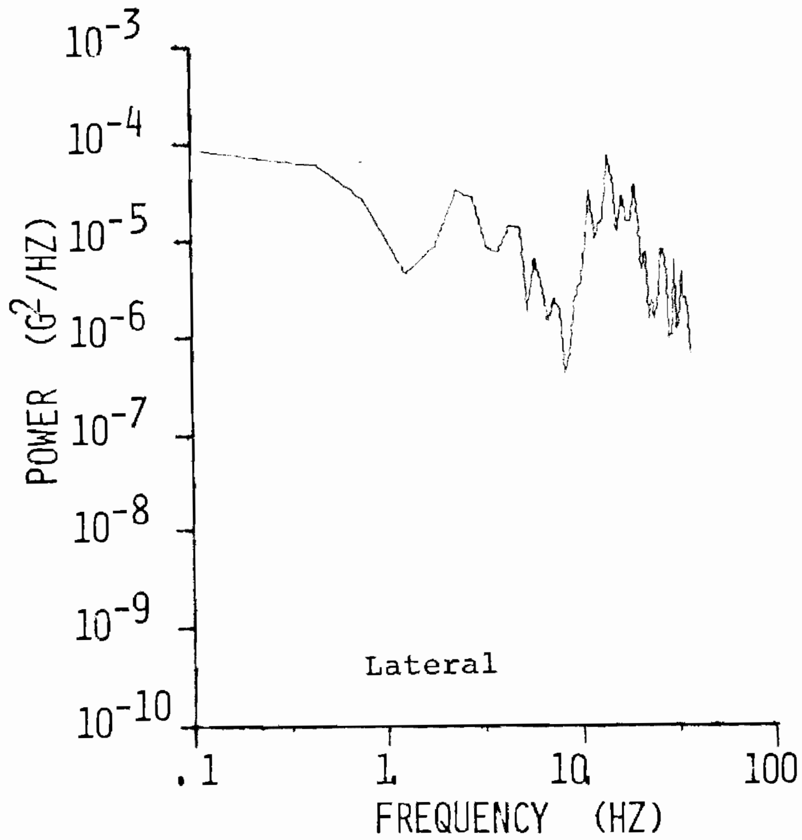

Section 41

APPENDIX B

Roadway RMS and PSD Roughness Spectra From Measured Data

TABLE B-1

Measured RMS Roadway Roughness

Section	RMS Values, Rt (in)*	RMS Values, Lft (in)
1	∞ → 2.54451 10 → 2.49708 40 → 2.49712	∞ → 2.20151 10 → 2.14582 40 → 2.14586
2	∞ → 5.03176 10 → 4.95042 40 → 4.95043	∞ → 5.93251 10 → 5.86254 40 → 5.86255
3	∞ → 1.29078 10 → 1.20435 40 → 1.20441	∞ → 9.31236×10^{-1} 10 → 8.51657×10^{-1} 40 → 8.51722×10^{-1}
5	∞ → .782912 10 → .766739 40 → .766755	∞ → .811449 10 → .795181 40 → .795199
6	∞ → .930339 10 → .815072 40 → .815170	∞ → 1.09136 10 → 1.01809 40 → 1.01817
7	∞ → .3162 10 → .267700 40 → .267746	∞ → .2973 10 → .23733 40 → .2374
8	∞ → .460479 10 → .409978 40 → .410034	∞ → .606358 10 → .536021 40 → .536126
9	∞ → .501549 10 → .459483 40 → .459509	∞ → .321946 10 → .256218 40 → .256272
10	∞ → 1.43430 10 → 1.399804 40 → 1.39805	∞ → 1.33532 10 → 1.30023 40 → 1.30025
11	∞ → .831835 10 → .814590 40 → .637745	∞ → .596537 10 → .572225 40 → .436809

*Integration Interval ∞ → 0-217 Hz
40 → 0-40 Hz
10 → 0-10 Hz

TABLE B-1 (continued)

Section	RMS Values, Rt (in)	RMS Values, Lft (in)
12	∞ → .683545 10 → .637709 40 → .637745	∞ → .518989 10 → .436765 40 → .436809
13	∞ → .690554 10 → .641715 40 → .642024	∞ → .938342 10 → .865738 40 → .865946
15	∞ → .685446 10 → .633457 40 → .633882	∞ → .683340 10 → .647062 40 → .647269
35	∞ → 2.82102 10 → 2.77033 40 → 2.77036	∞ → 3.09123 10 → 2.98745 40 → 2.98752
36	∞ → 1.52378 10 → 1.49759 40 → 1.49759	∞ → 1.39521 10 → 2.06604 40 → 1.37792
37	∞ → 2.54854 10 → 2.52389 40 → 2.52395	∞ → 3.25811 10 → 3.22824 40 → 3.22827
38	∞ → .663817 10 → .614568 40 → .614587	∞ → 1.08115 10 → 1.00338 40 → 1.00339
39	∞ → 1.28777 10 → 1.21211 40 → 1.21217	∞ → .586566 10 → .521300 40 → .521674
40	∞ → .824179 10 → .745830 40 → .745870	∞ → 1.48187 10 → 1.37419 40 → 1.37424
41	∞ → .455754 10 → .352876 40 → .353109	∞ → 1.22045 10 → 1.17878 40 → 1.87886

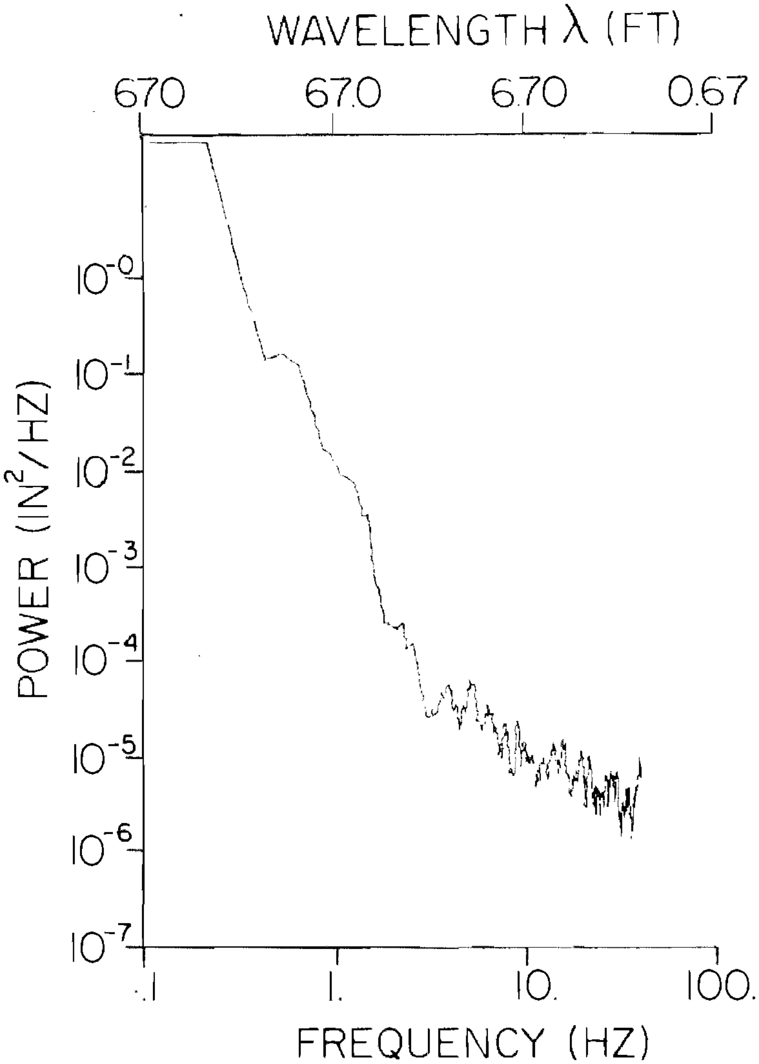

Section 1 Right

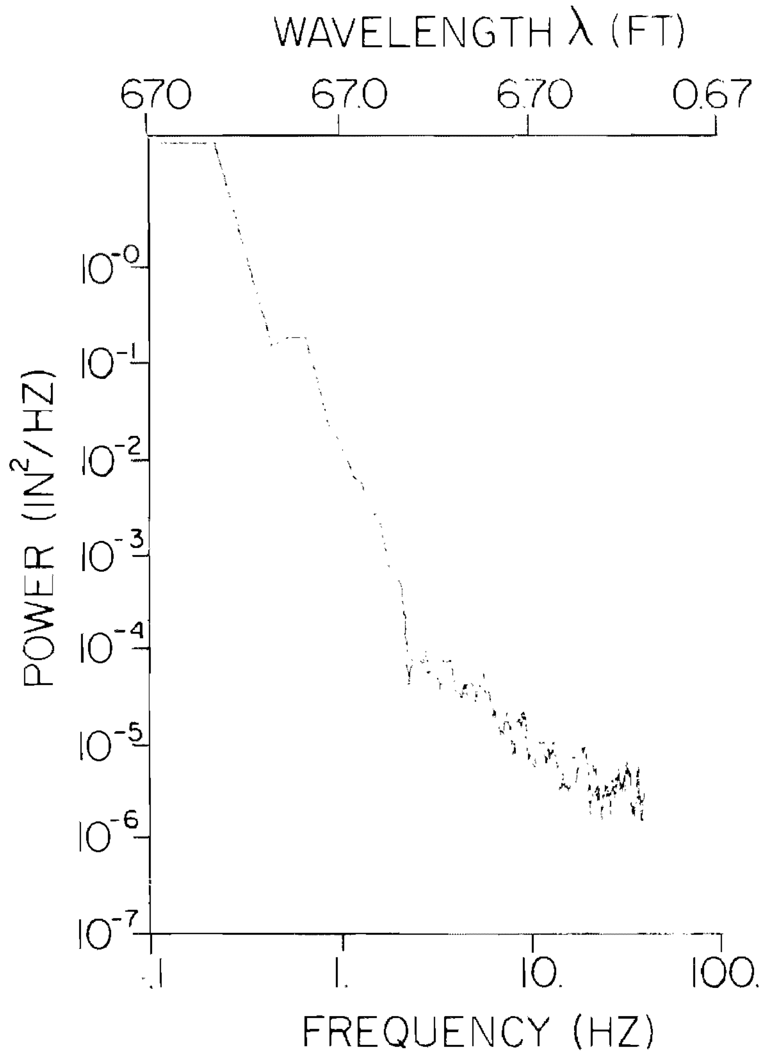

Section 1 Left

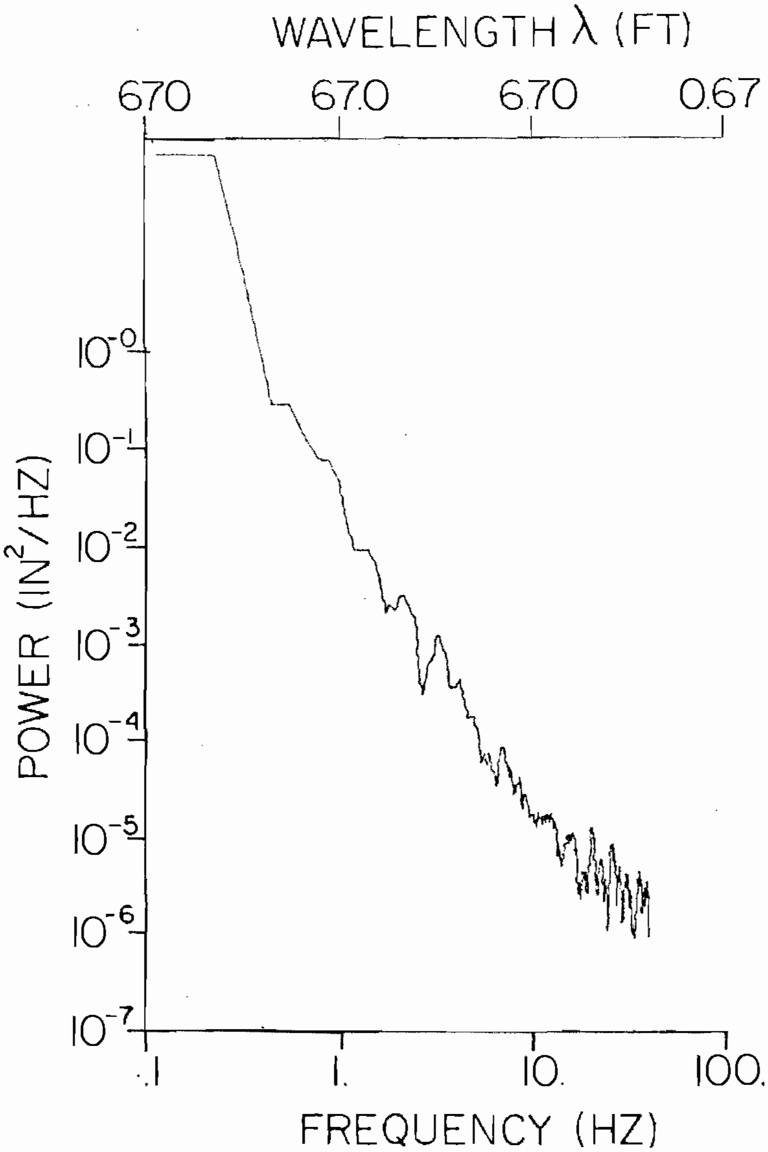

Section 2 Right

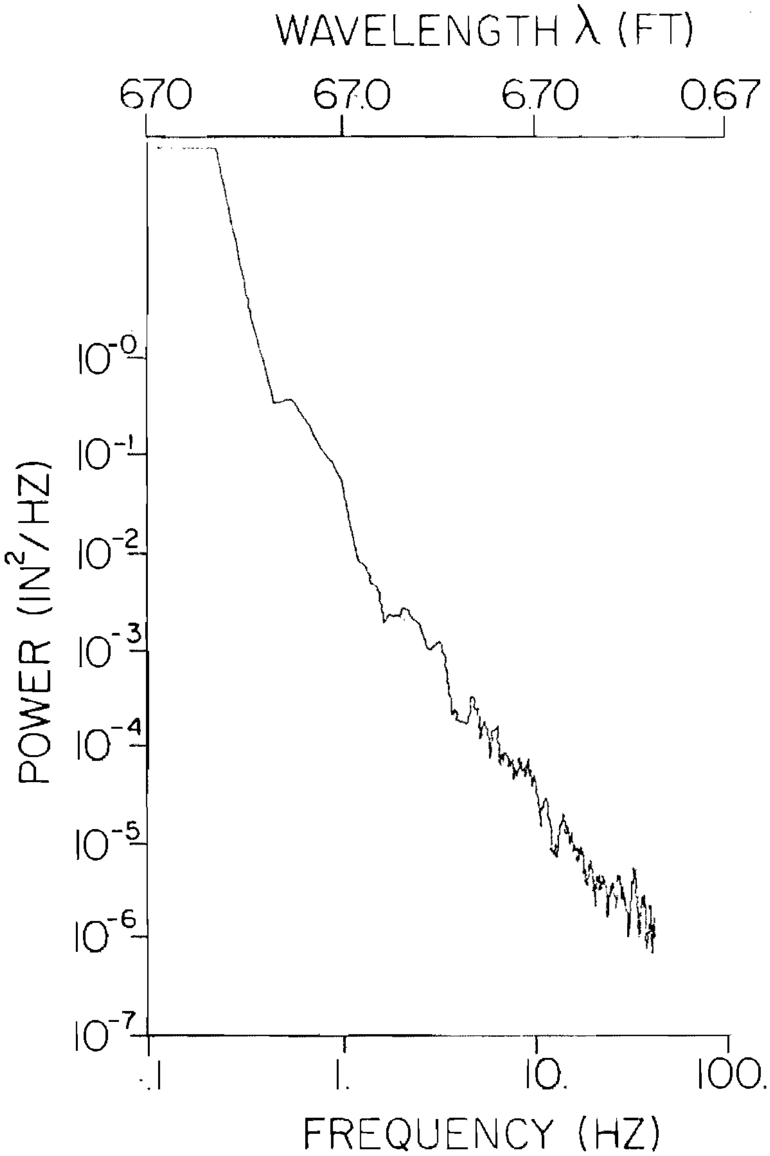

Section 2 Left

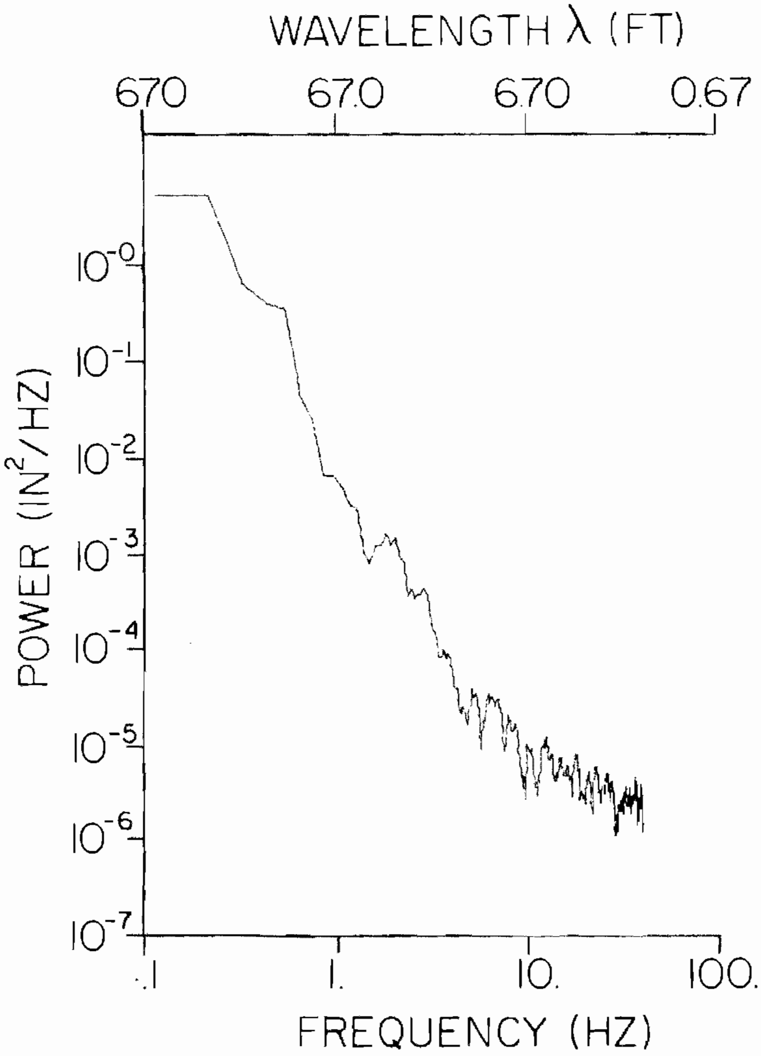

Section 3 Right

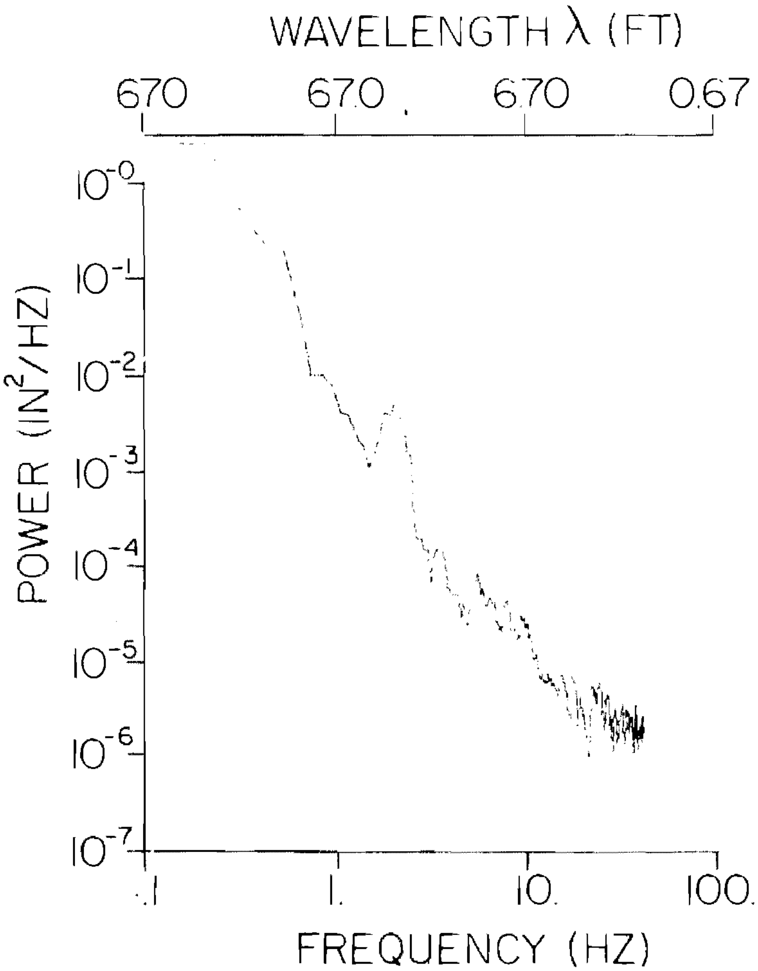

Section 3 Left

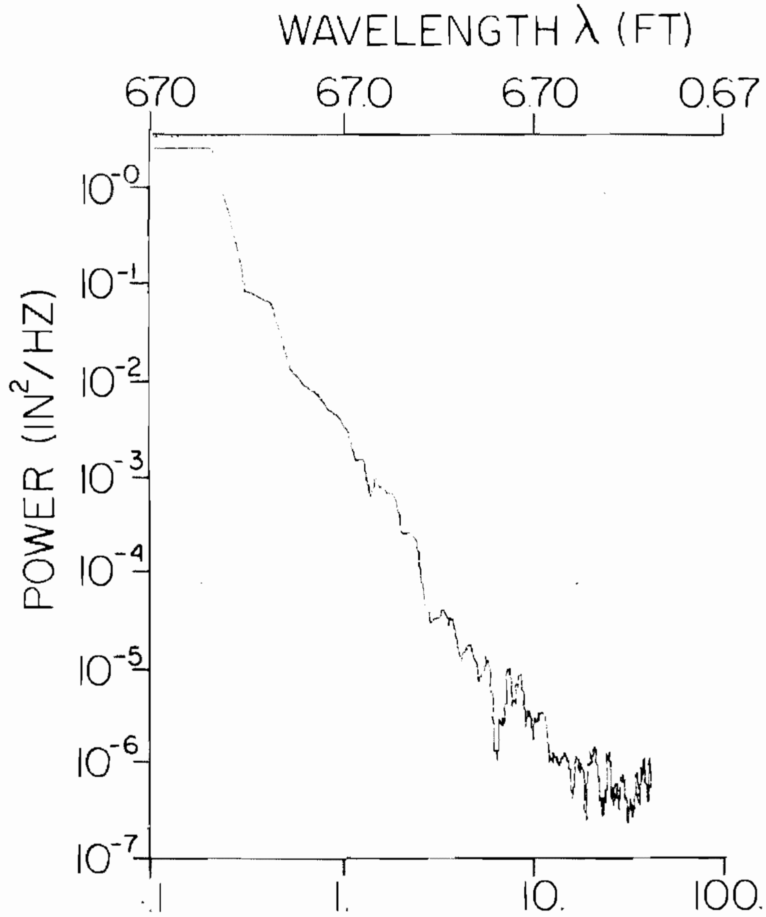

Section 5 Right

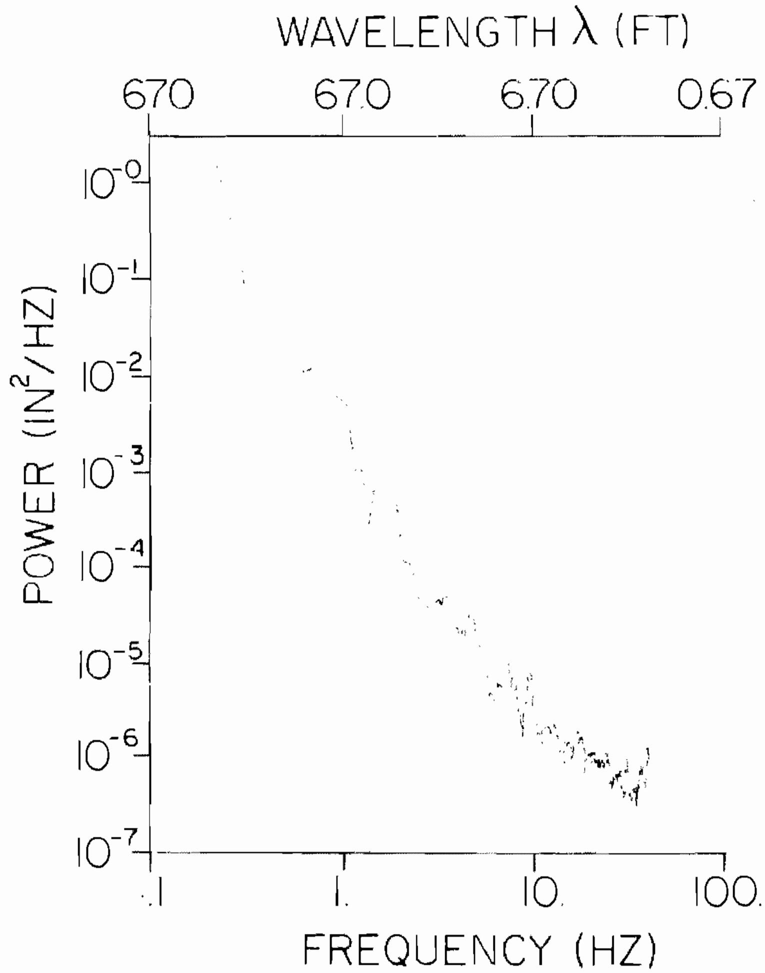

Section 5 Left

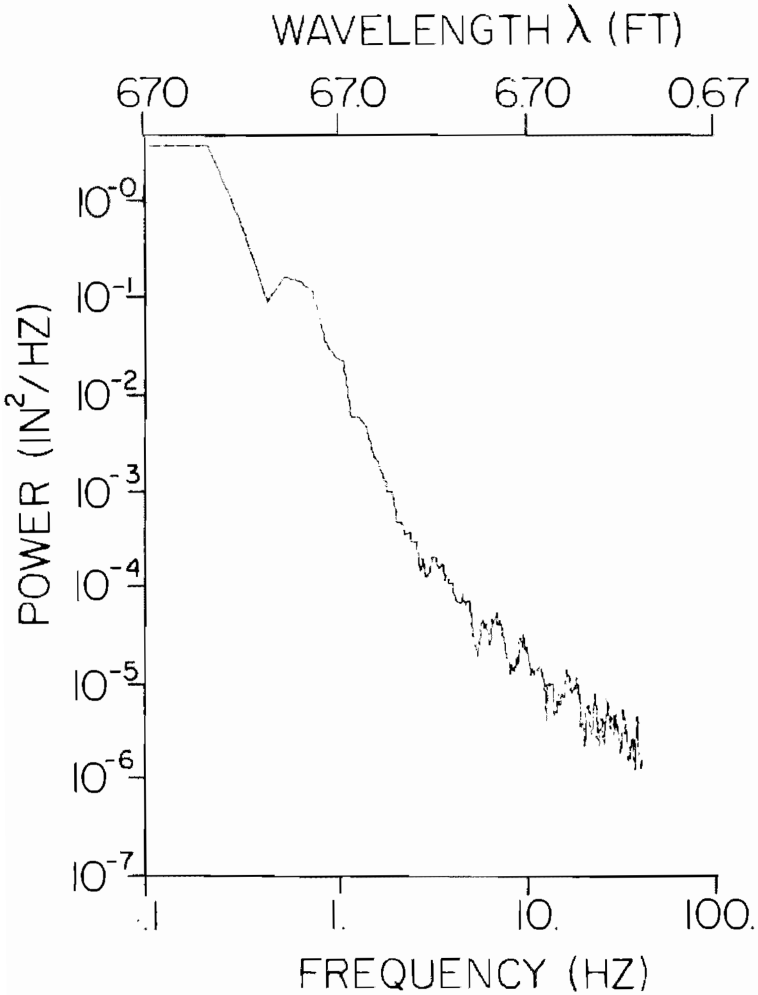

Section 6 Left

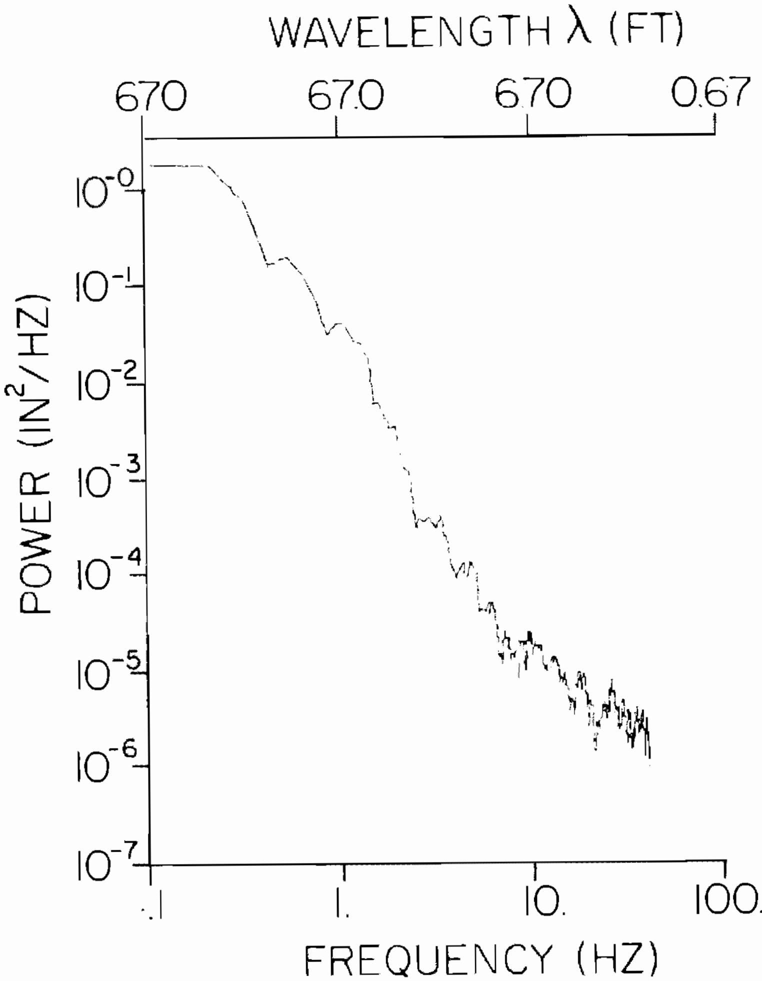

Section 6 Right

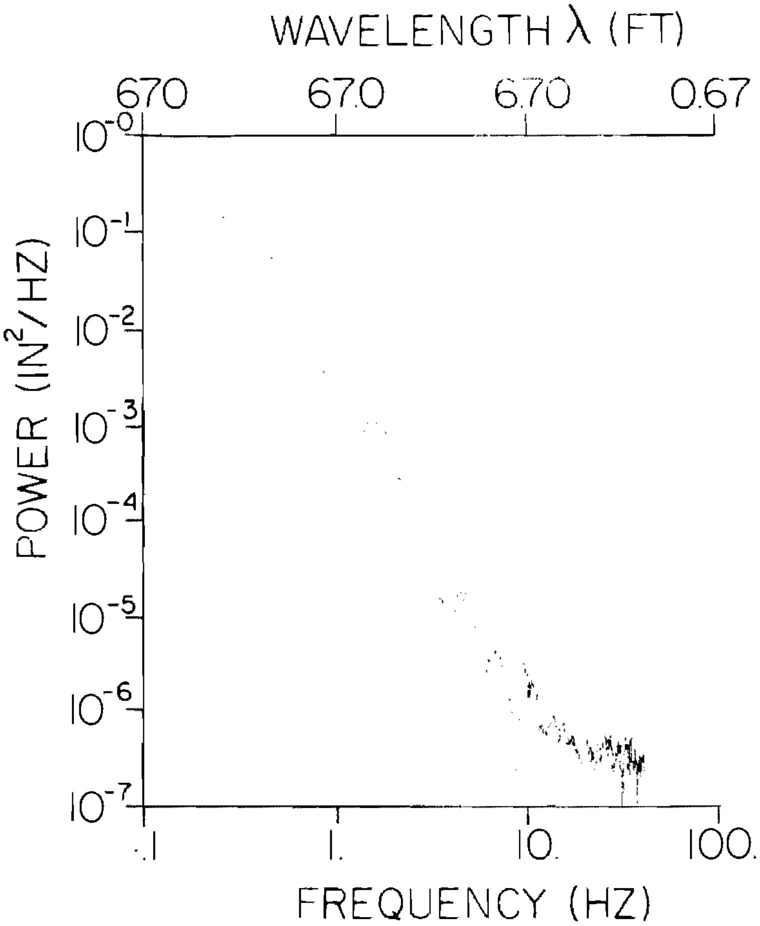

Section 7 Left

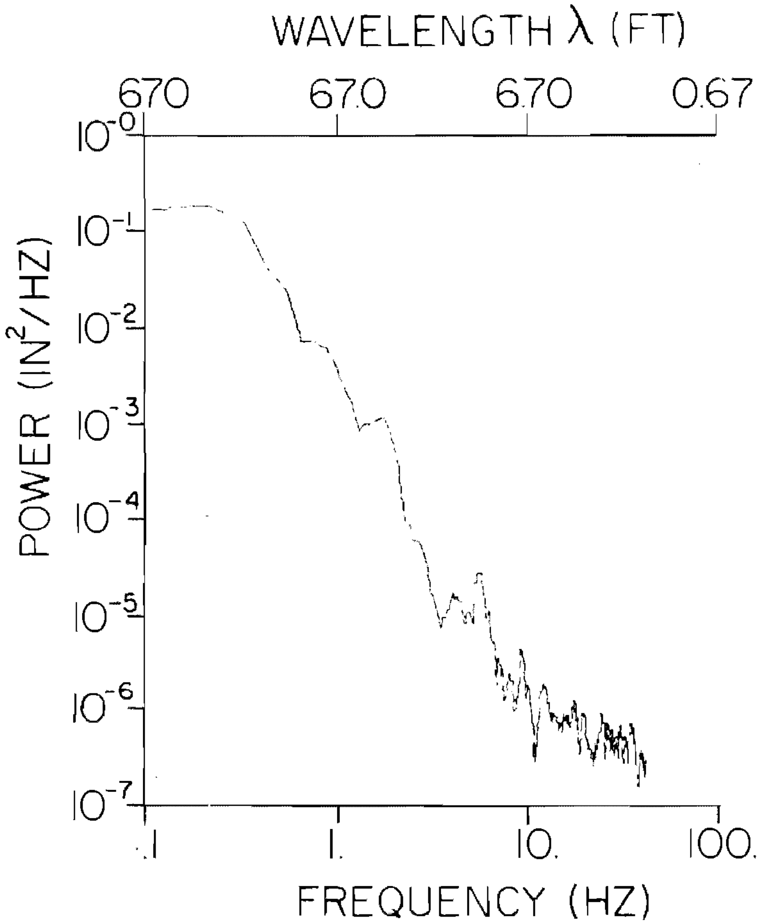

Section 7 Right

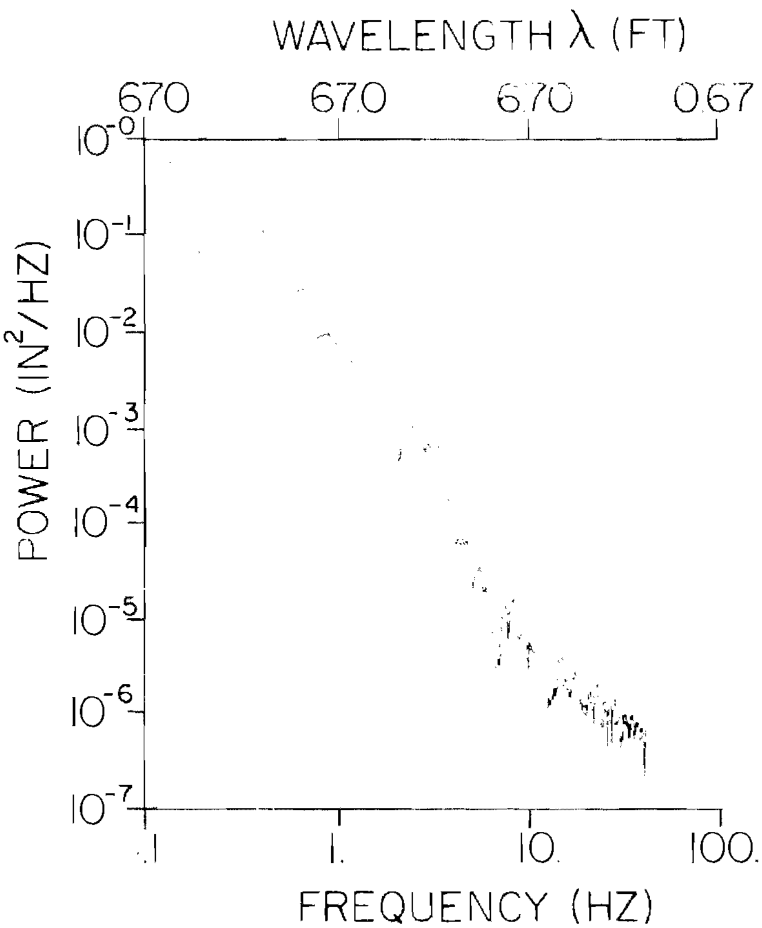

Section 8 Right

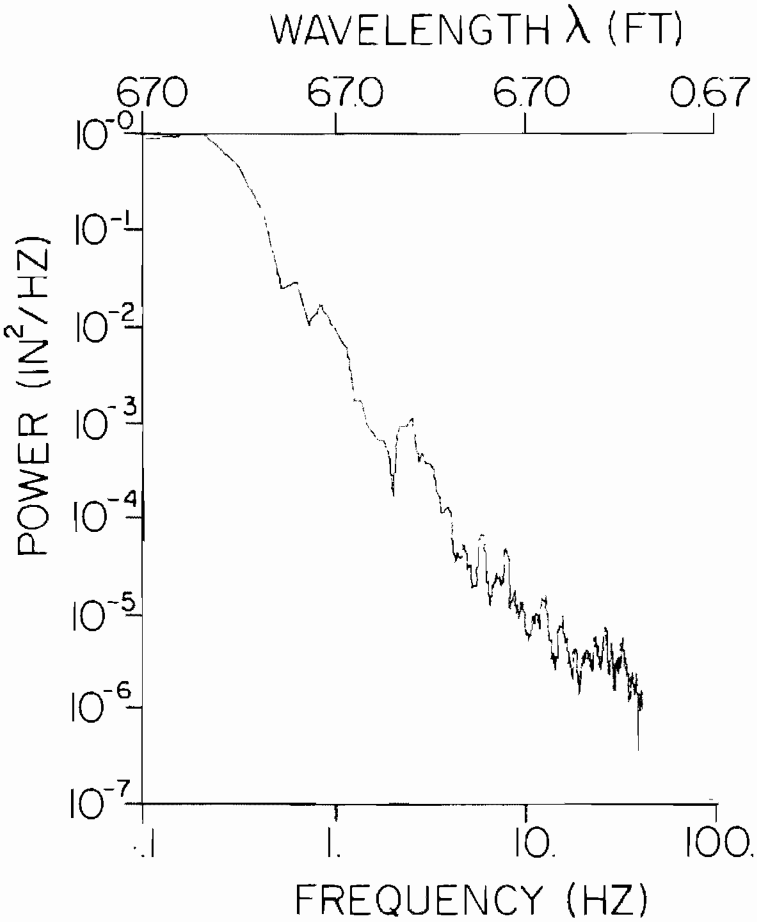

Section 8 Left

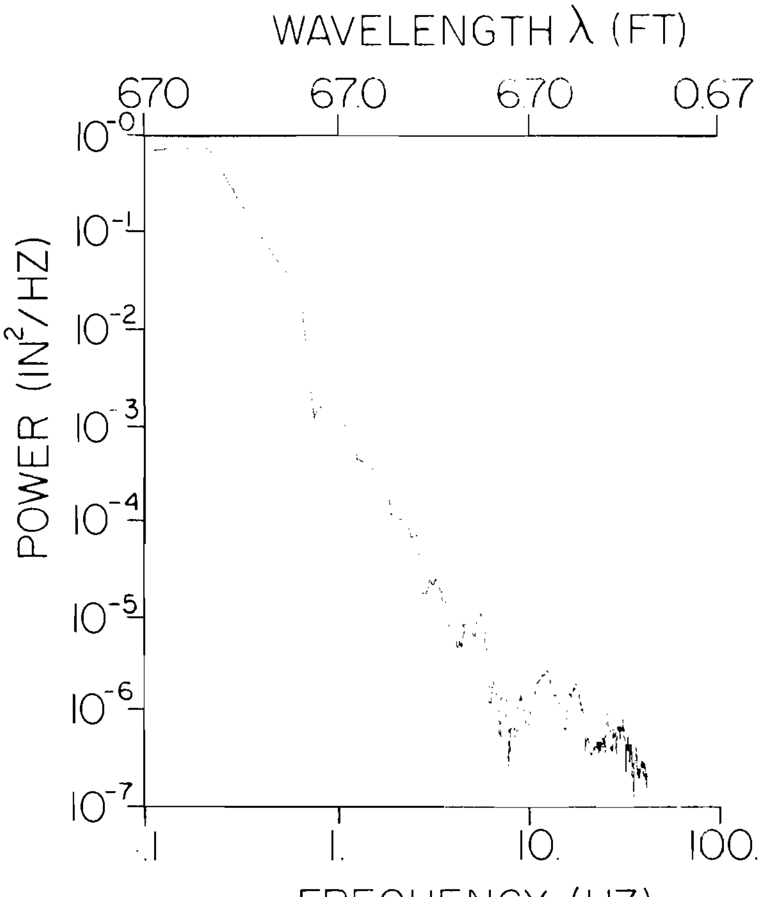

Section 9 Right

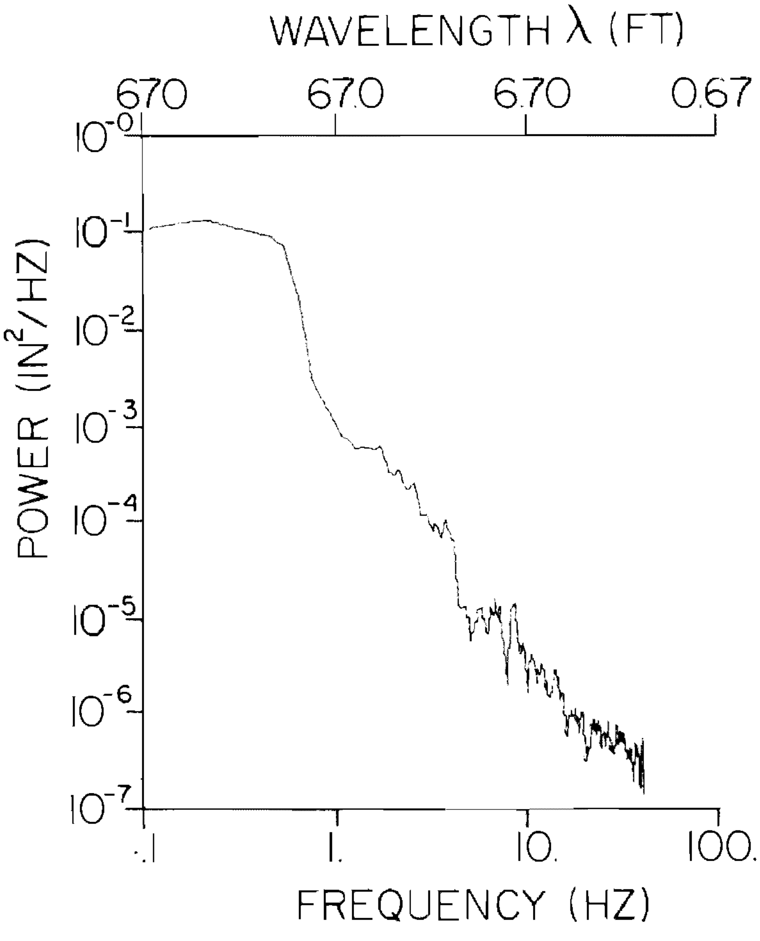

Section 9 Left

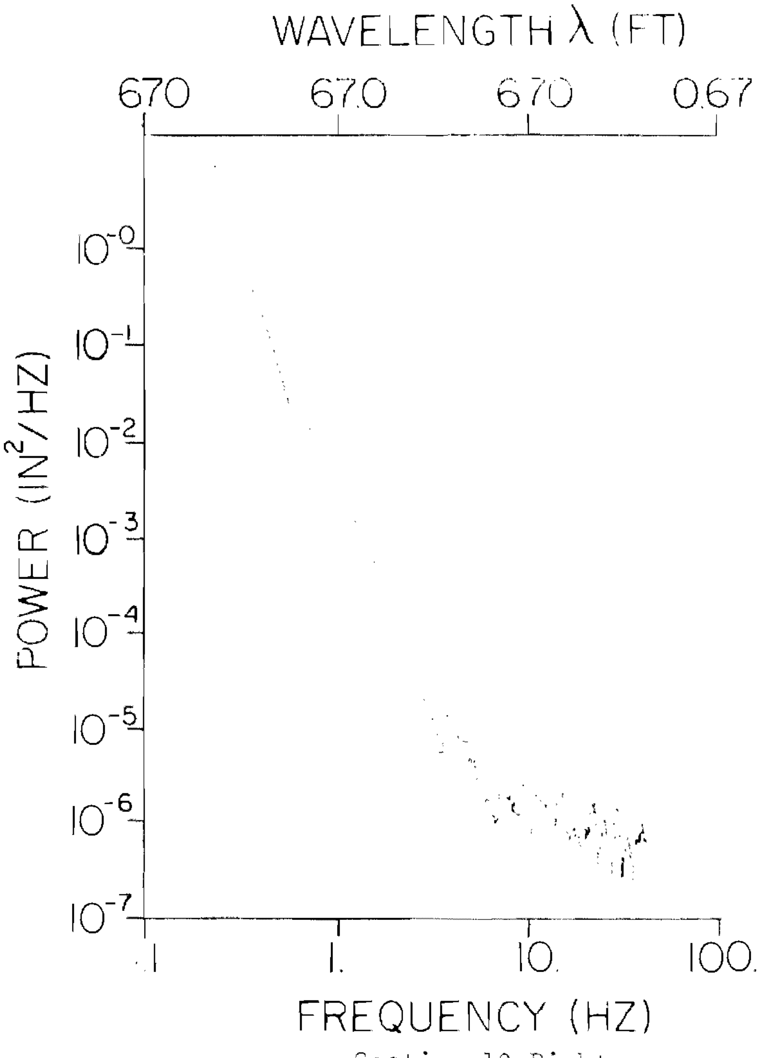

Section 10 Right

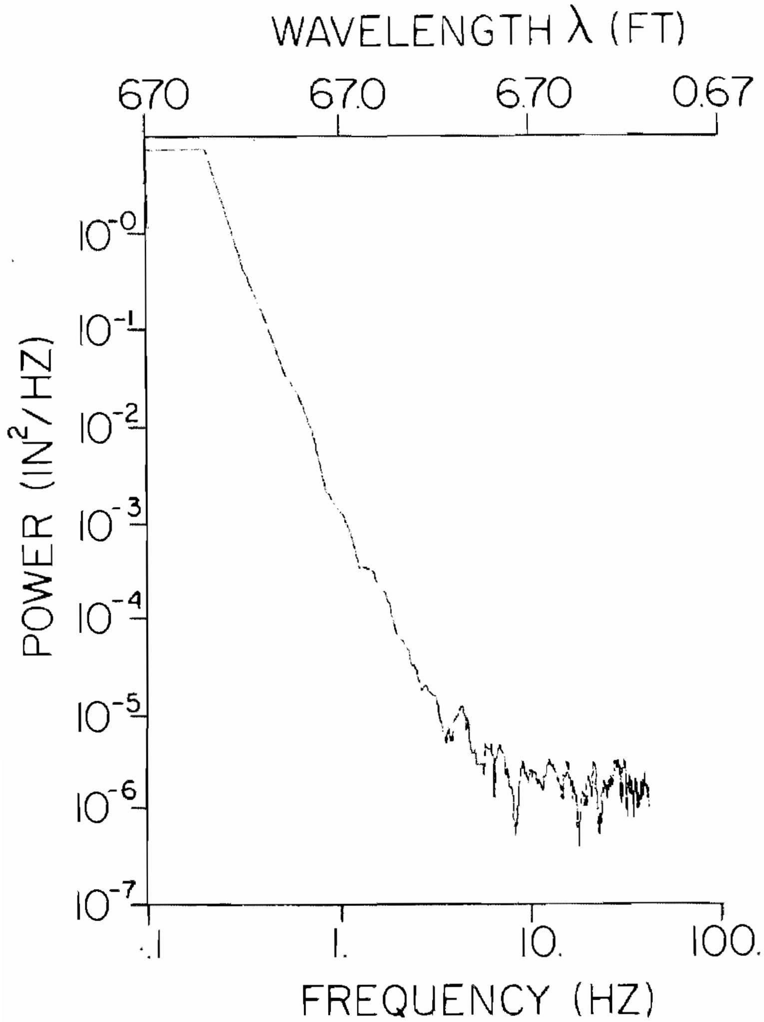

Section 10 Left

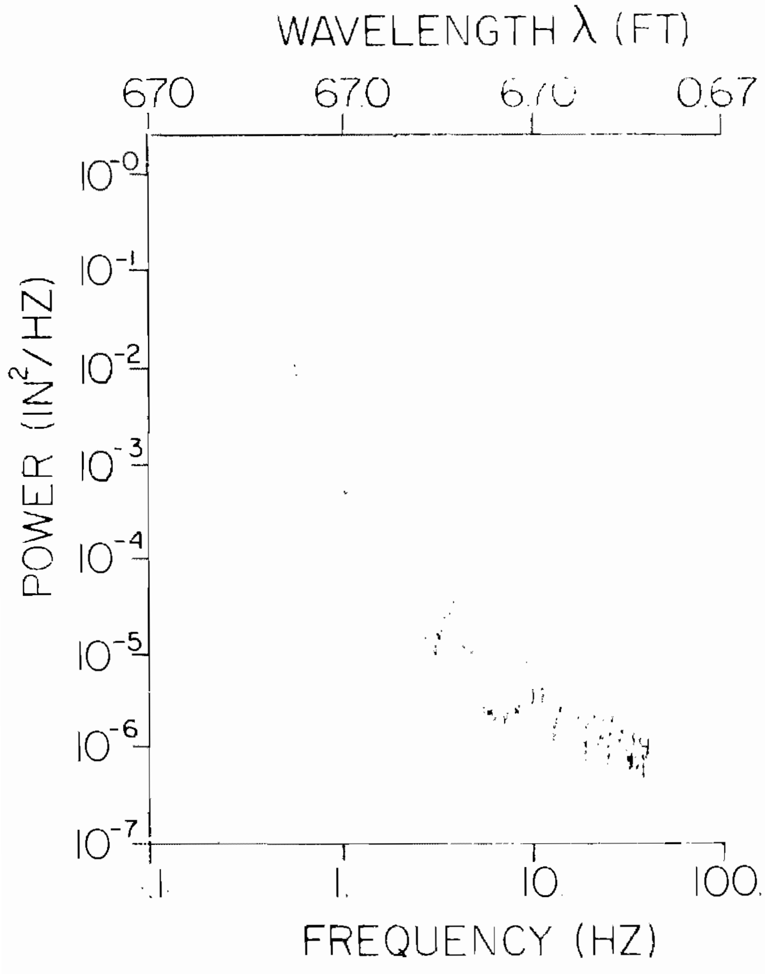

Section 11 Left

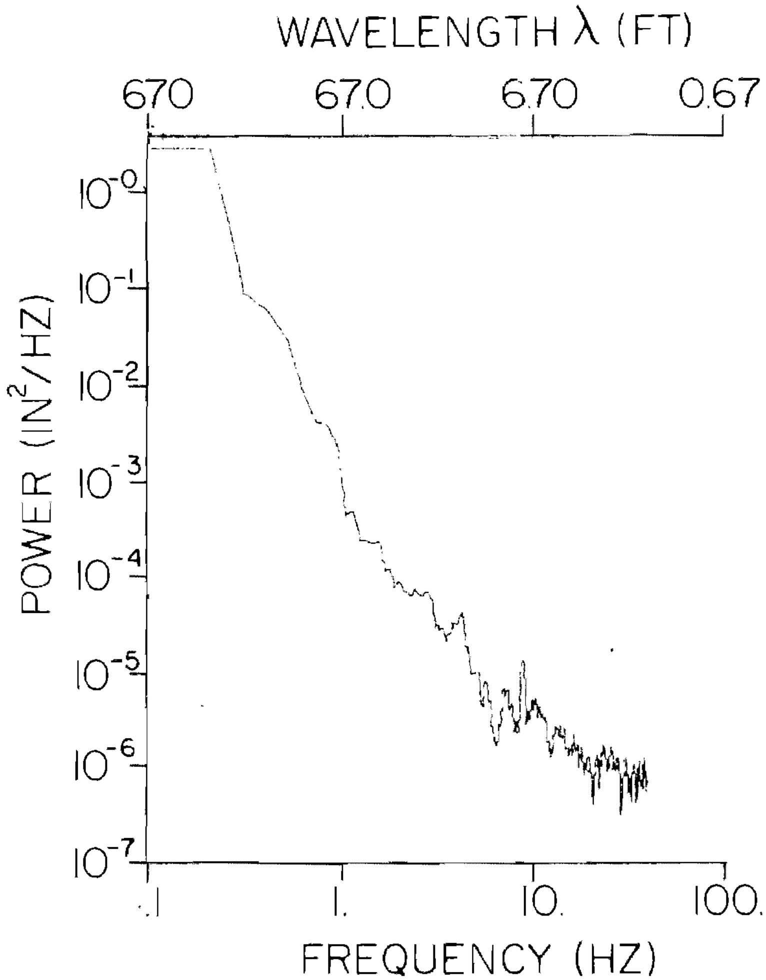

Section 11 Right

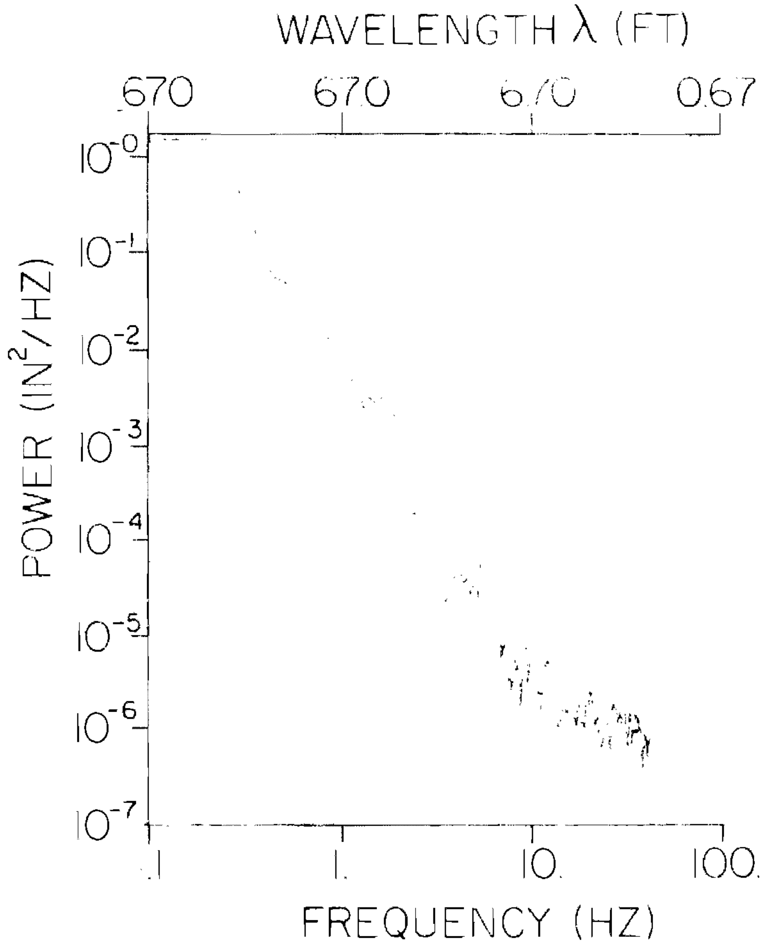

Section 12 Right

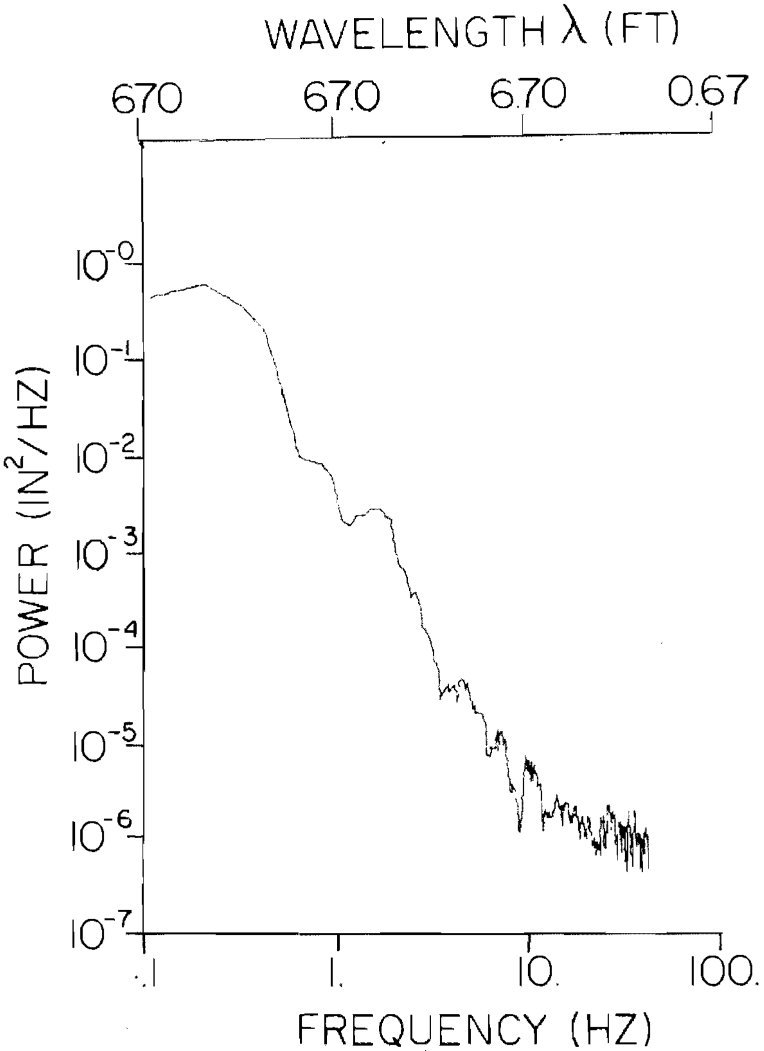

Section 12 Left

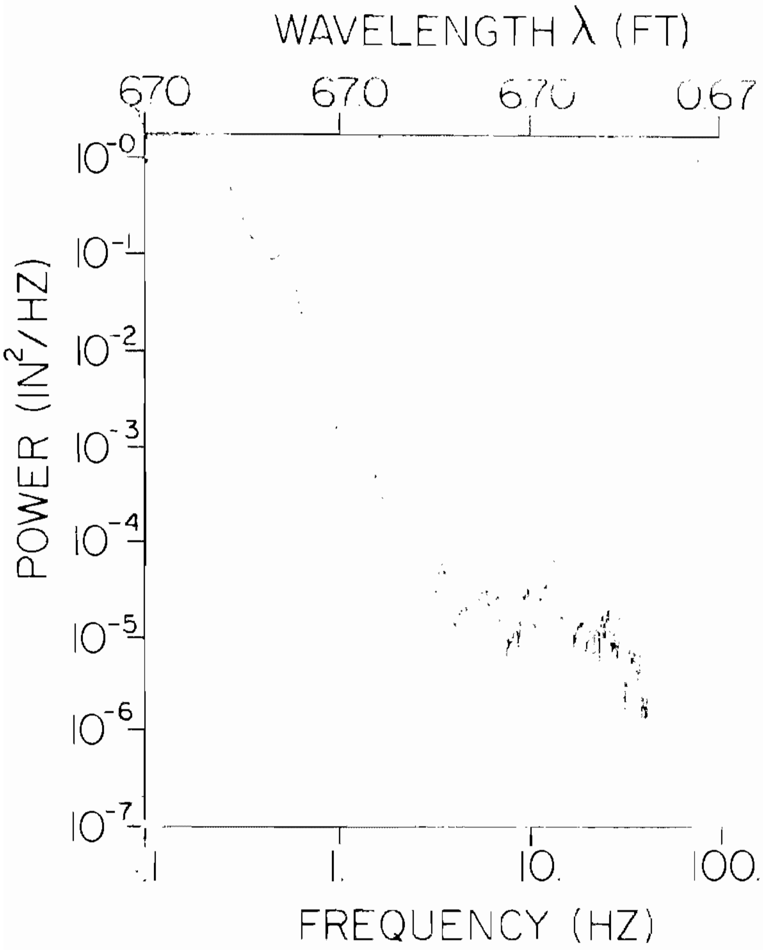

Section 13 Right

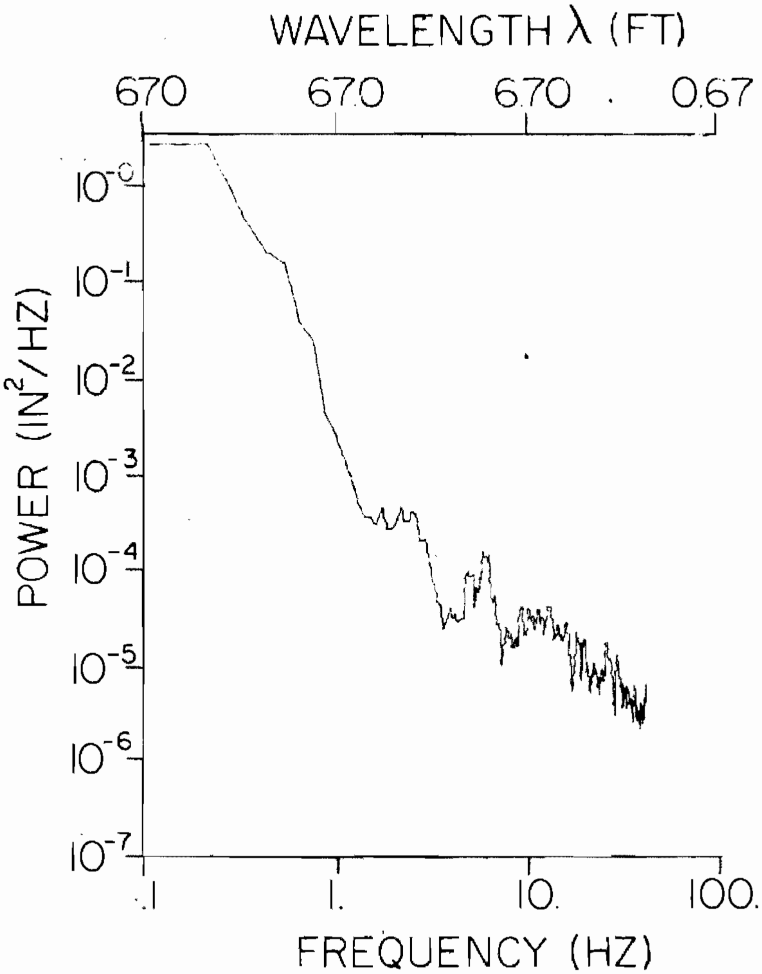

Section 13 Left

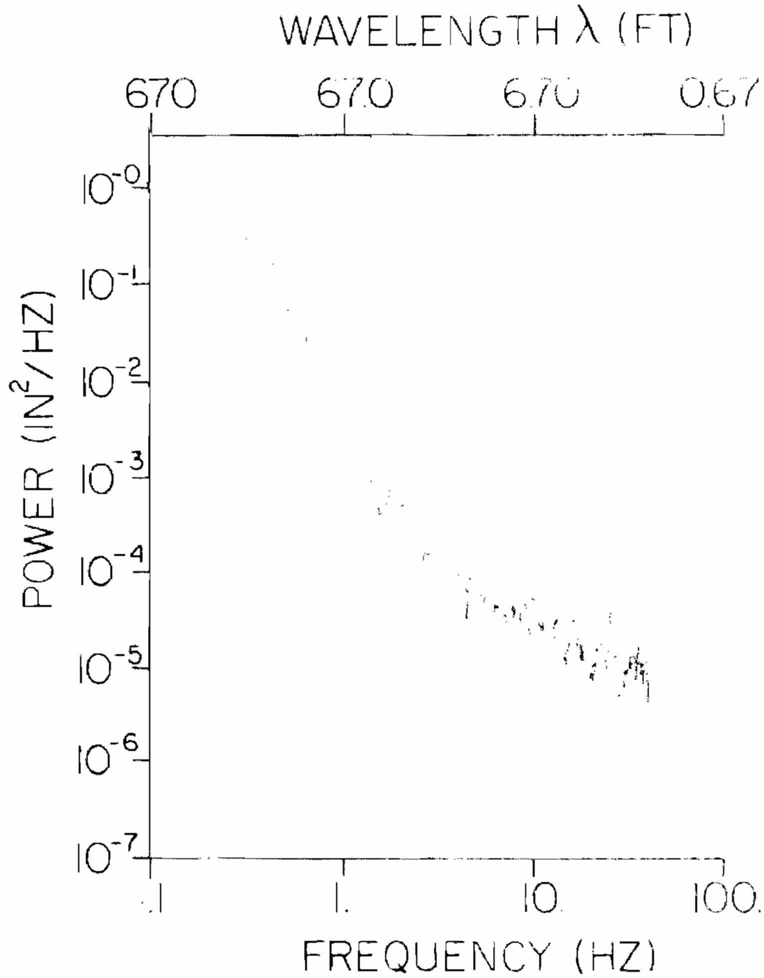

Section 15 Right

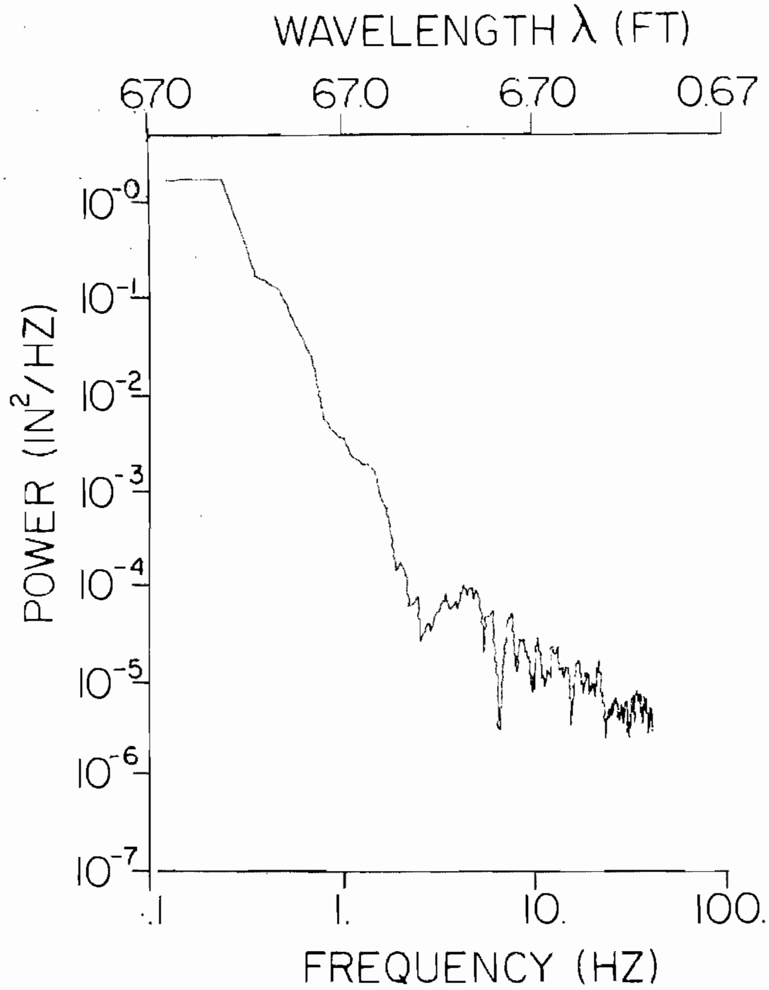

Section 15 Left

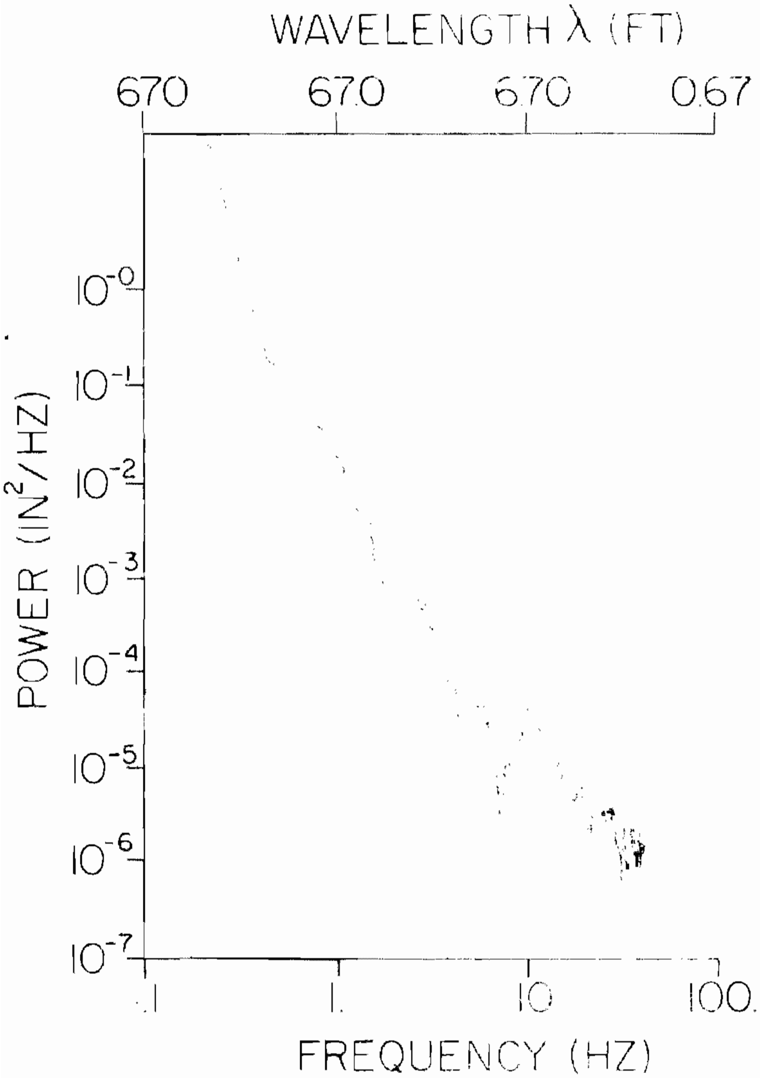

Section 35 Right

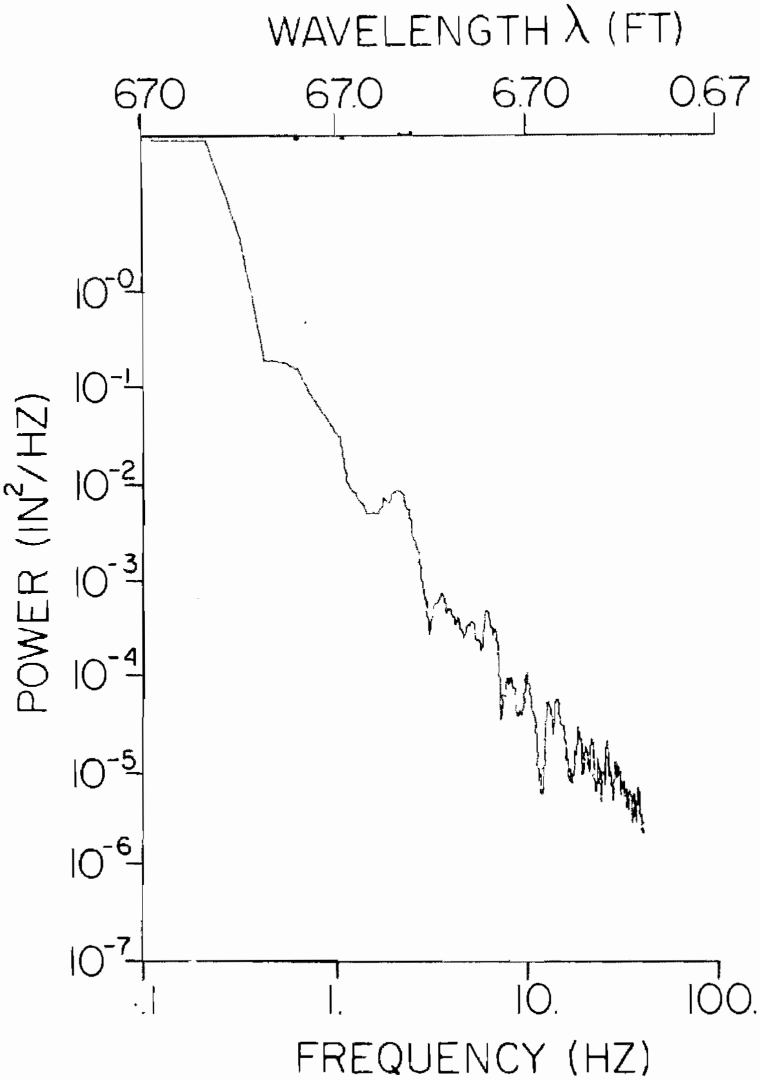

Section 35 Left

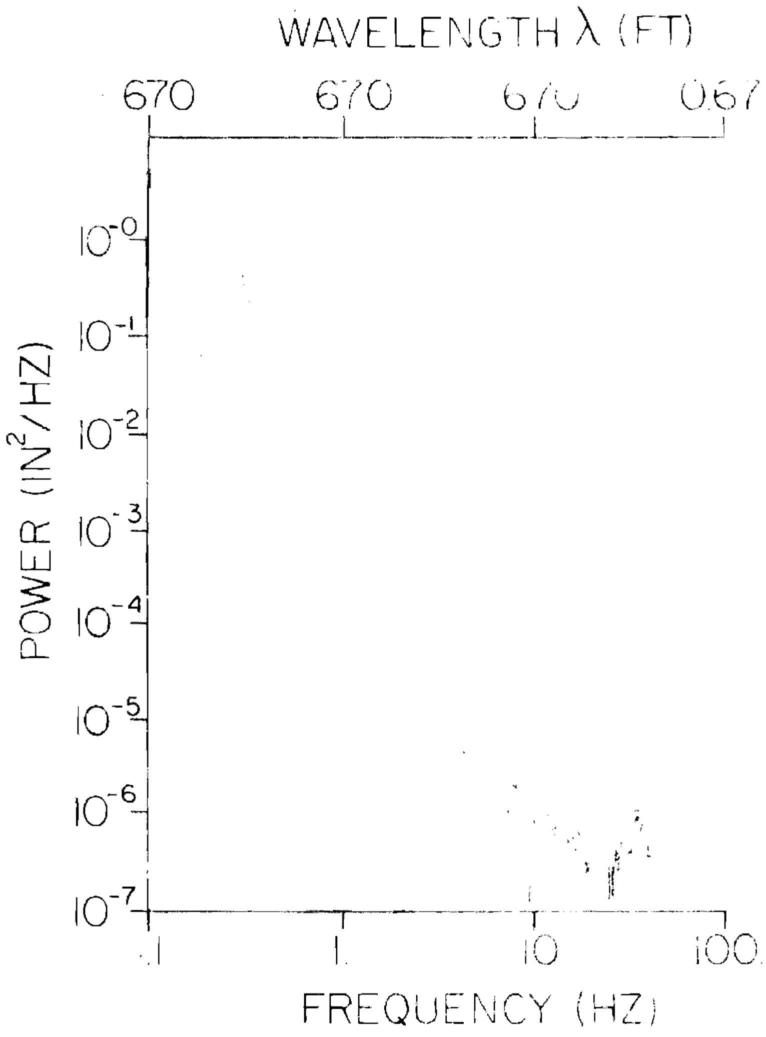

Section 36 Right

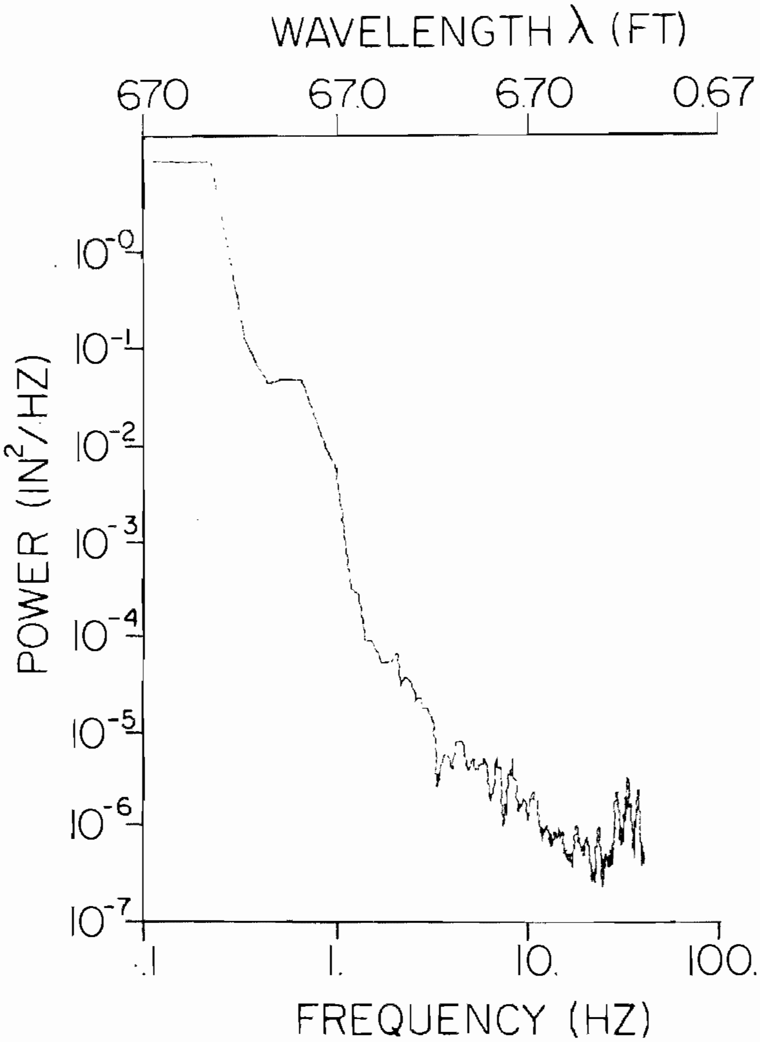

Section 36 Left

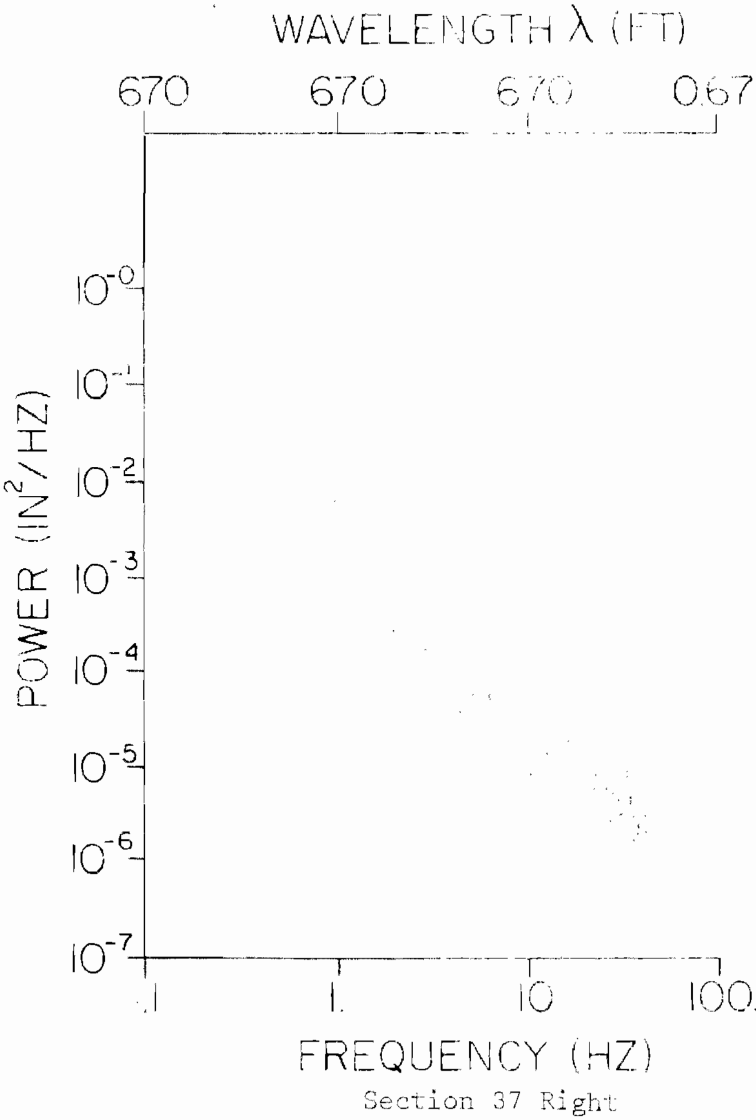

Section 37 Right

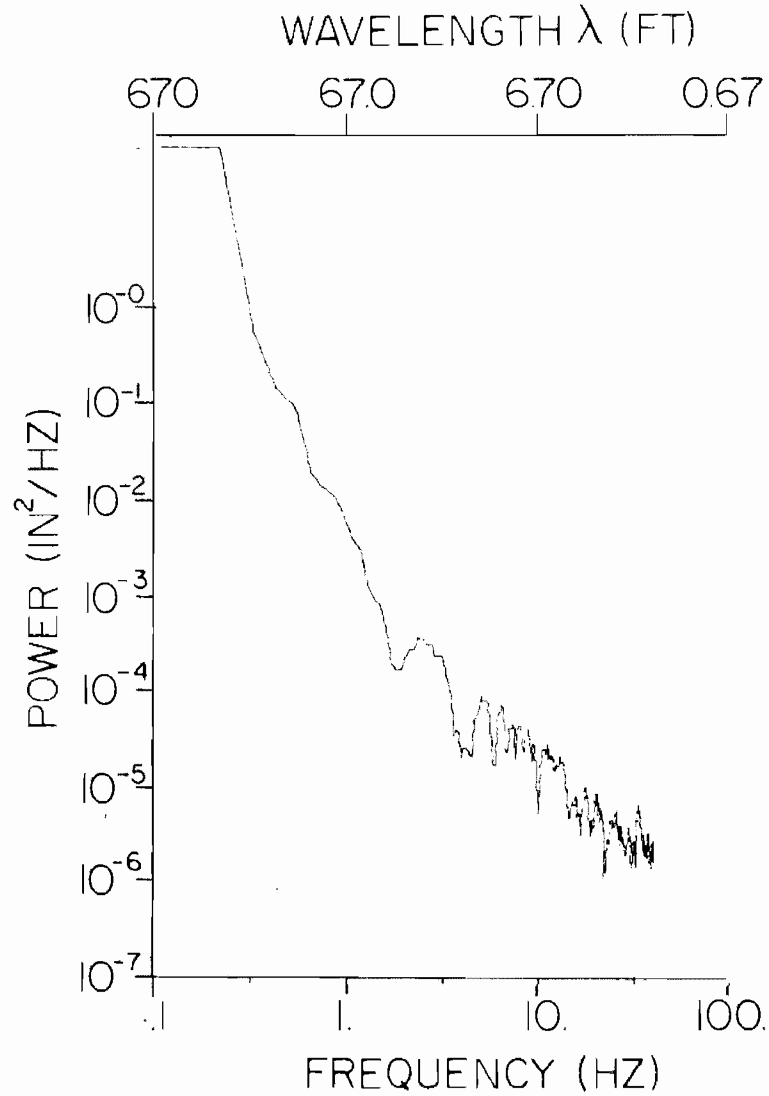

Section 37 Left

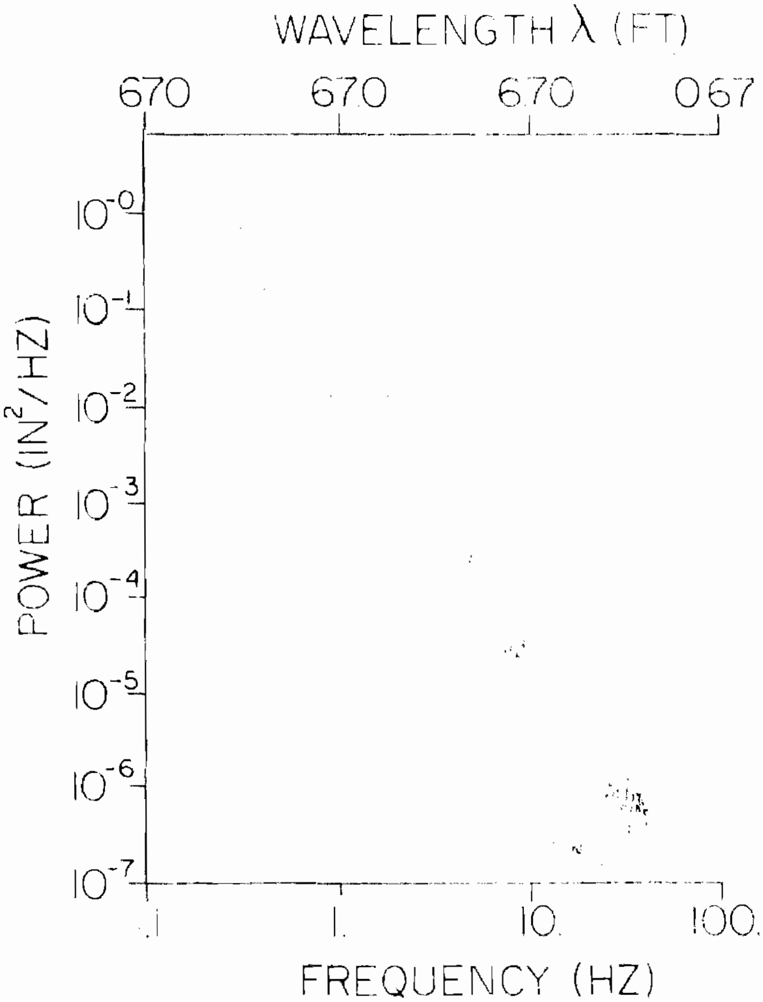

Section 38 Left

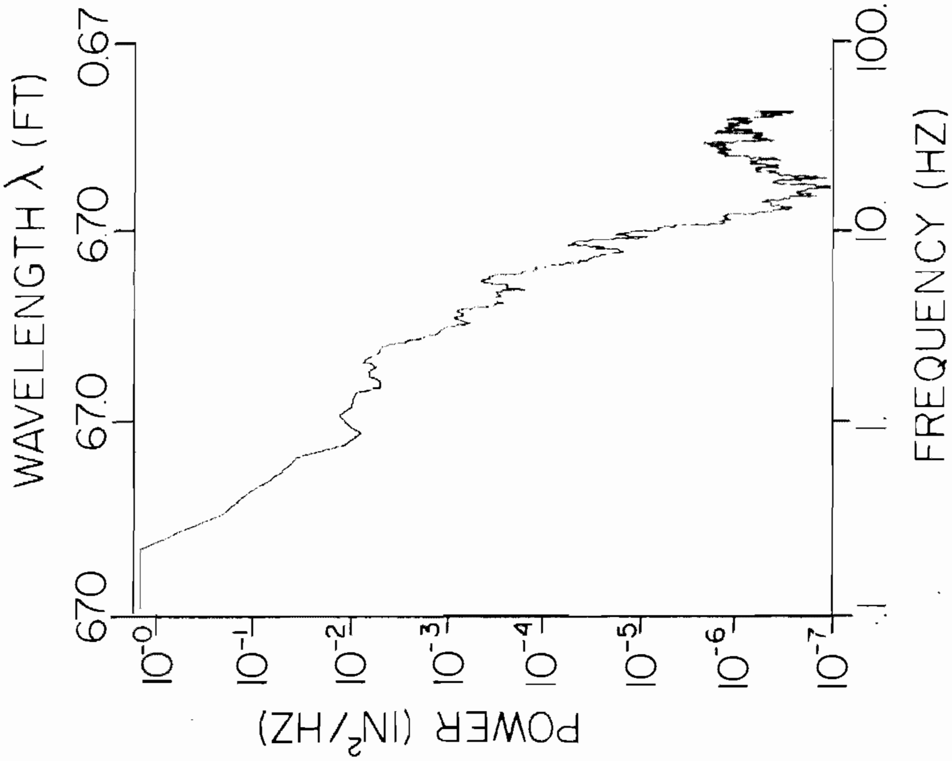

Section 38 Right

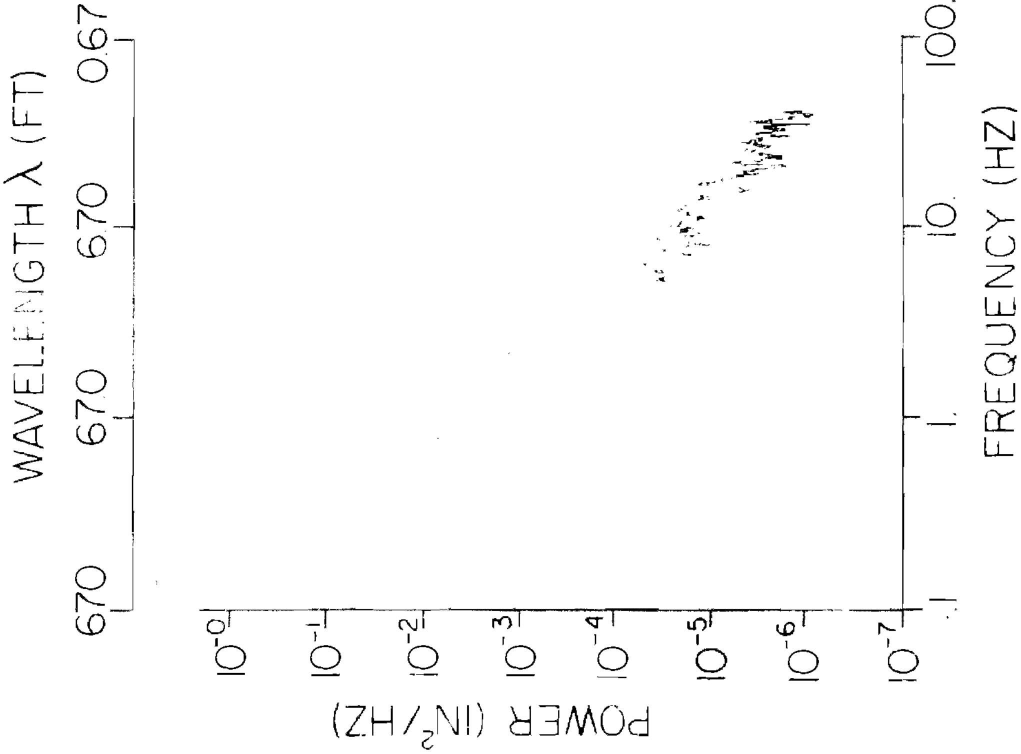

Section 39 Right

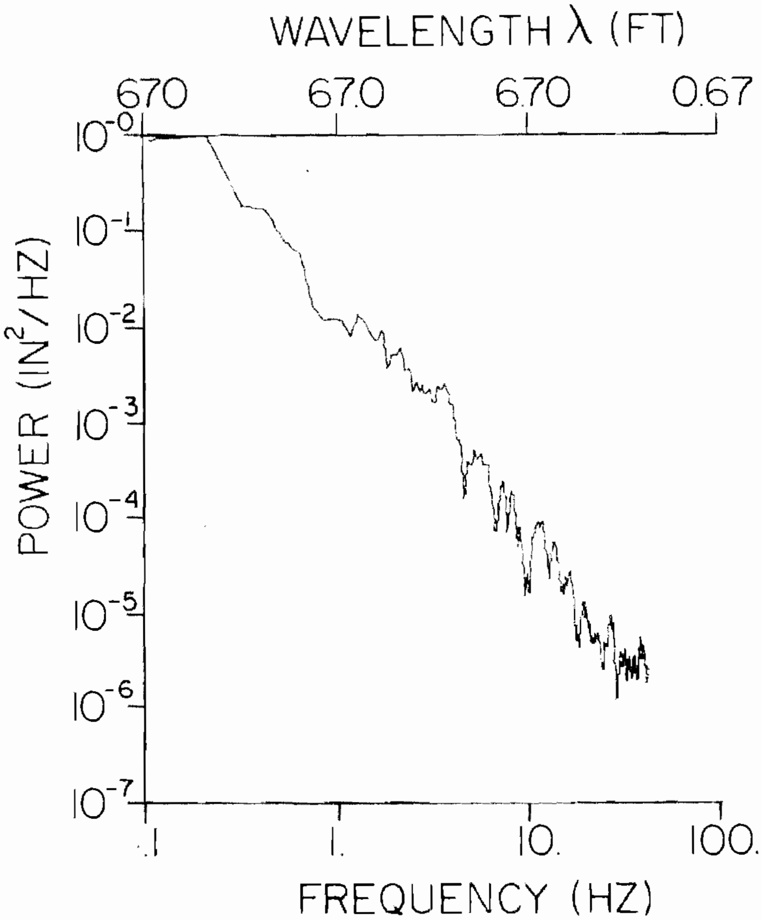

Section 39 Left

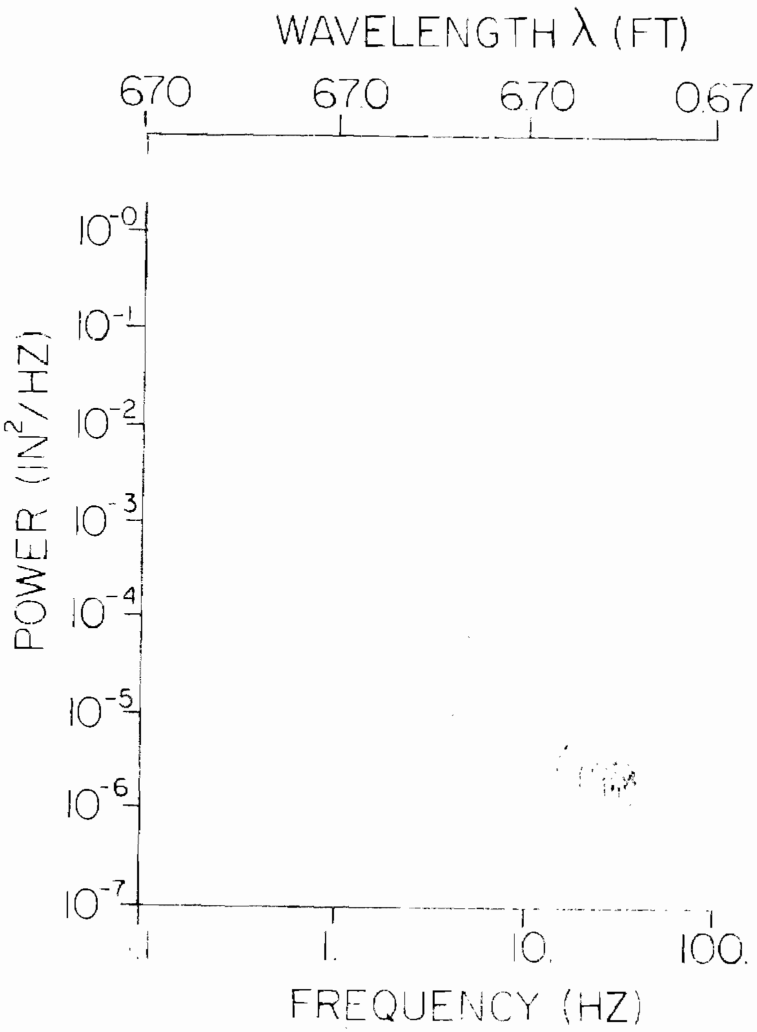

Section 40 Left

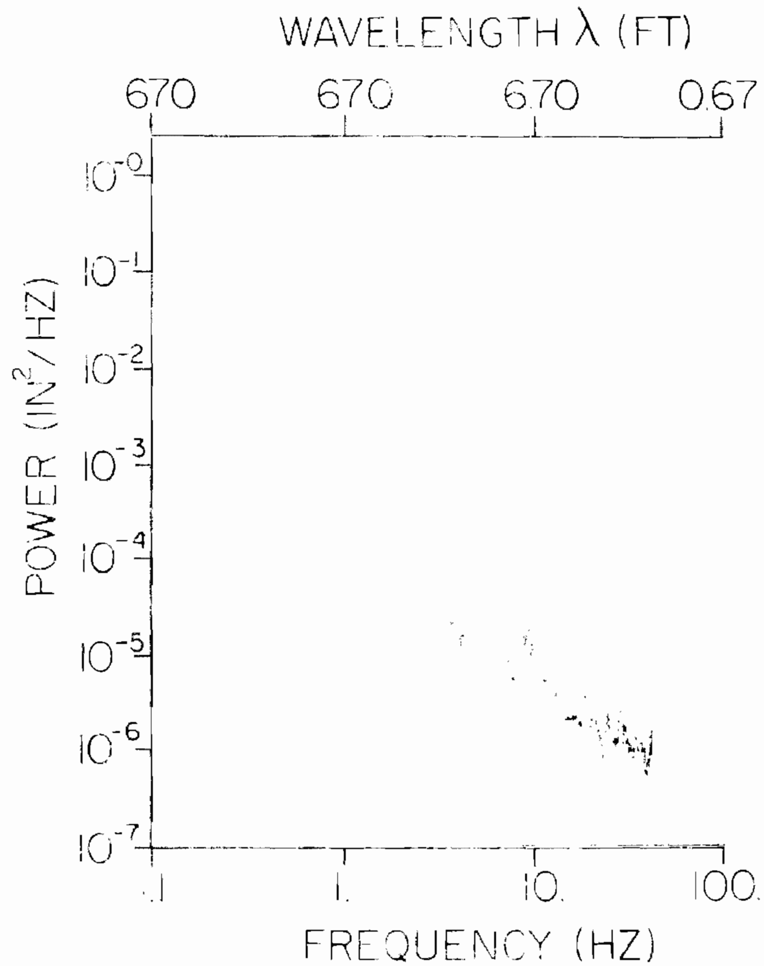

Section 40 Right

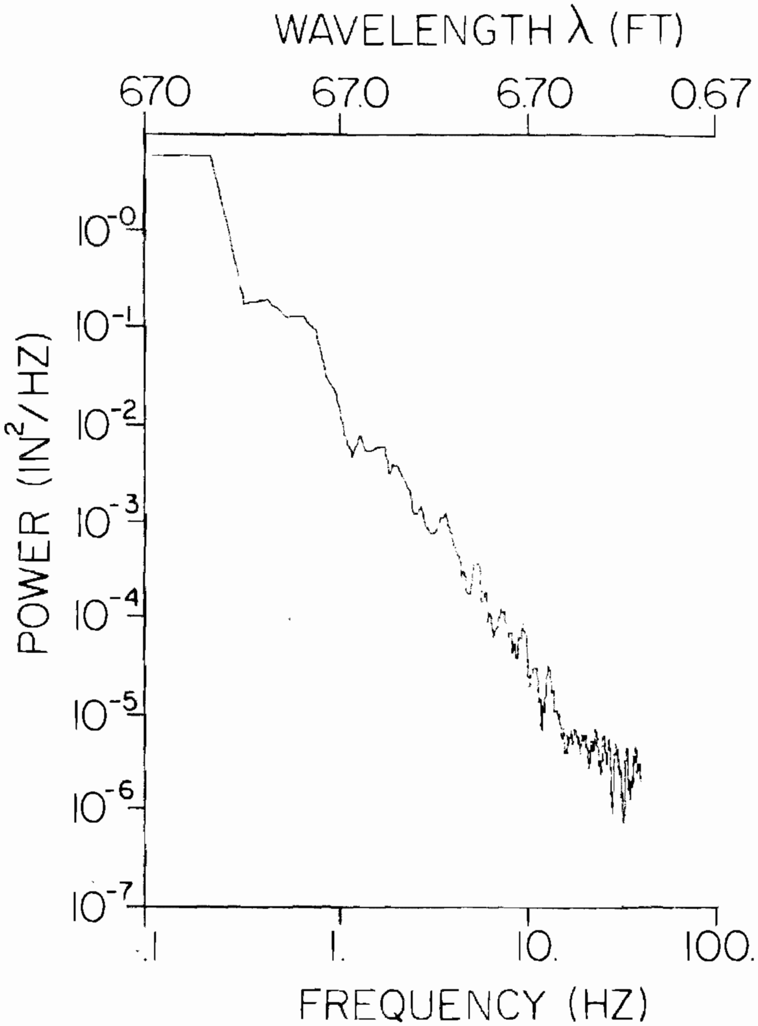

Section 41 Left

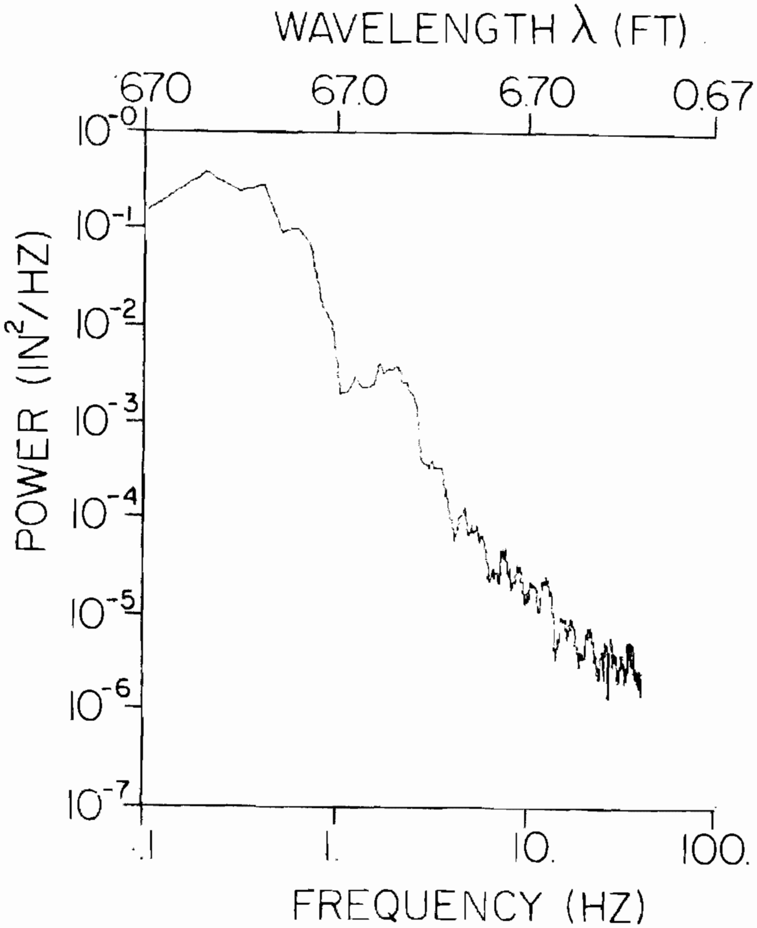

Section 41 Right

RESEARCH MEMORANDA PUBLISHED BY THE COUNCIL FOR ADVANCED TRANSPORTATION STUDIES

1 *Human Response in the Evaluation of Modal Choice Decisions.* C. Shane Davies, Mark Alpert, and W. Ronald Hudson, April 1973.

2 *Access to Essential Services.* Ronald Briggs, Charlotte Clark, James Fitzsimmons, and Paul Jensen, April 1973.

3 *Psychological and Physiological Responses to Stimulation.* D. W. Wooldridge, A. J. Healey, and R. O. Stearman, August 1973.

4 *An Intermodal Transportation System for the Southwest: A Preliminary Proposal.* Charles P. Zlatkovich, September 1973.

5 *Passenger Travel Patterns and Mode Selection.* Shane Davies, Mark Alpert, Harry Wolfe, and Rebecca Gonzalez, October 1973.

6 *Segmenting a Transportation Market by Determinant Attributes of Modal Choice.* Shane Davies and Mark Alpert, October 1973.

7 *The Interstate Rail System: A Proposal.* Charles P. Zlatkovich, December 1973.

8 *Literature Survey on Passenger and Seat Modeling for the Evaluation of Ride Quality.* Bruce Shanahan, Ronald Stearman, and Anthony Healey, November, 1973.

9 *The Definition of Essential Services and the Identification of Key Problem Areas.* Ronald Briggs and James Fitzsimmons, January, 1974.

10 *A Procedure for Calculating Great Circle Distances Between Geographic Locations.* J. Bryan Adair, March 1974.

11 *MAPRINT: A Computer Program for Analyzing Changing Locations of Non-Residential Activities.* Graham Hunter, Richard Dodge, and C. Michael Walton, March 1974.

12 *A Method for Assessing the Impact of the Energy Crisis on Highway Accidents in Texas.* E. L. Frome and C. Michael Walton, February 1975.

13 *State Regulation of Air Transportation in Texas.* Robert C. Means and Barry Chasnoff, April 1974.

14 *Transportation Atlas of the Southwest.* Charles P. Zlatkovich, S. Michael Dildine, Eugene Robinson, James W. Wilson, and J. Bryan Adair, June 1974.

15 *Local Government Decisions and Land-Use Change: An Introductory Bibliography.* W. D. Chipman, May 1974.

16 *An Analysis of the Truck Inventory and Use Survey Data for the West South Central States.* Michael Dildine, July 1974.

17 *Towards Estimating the Impact of the Dallas-Fort Worth Regional Airport on Ground Transportation.* William J. Dunlay and Lyndon Henry, September 1974.

18 *The Attainment of Riding Comfort for a Tracked Air-Cushion Vehicle Through the Use of an Active Aerodynamic Suspension.* Bruce Shanahan, Ronald Stearman, and Anthony Healey, September 1974.

19 *Legal Obstacles to the Use of Texas School Buses for Public Transportation.* Robert Means, Ronald Briggs, John E. Nelson, and Alan J. Thiemann, January 1975.

20 *Pupil Transportation: A Cost Analysis and Predictive Model.* Ronald Briggs and David Venhuizen, April 1975.

21 *Variables in Rural Plant Location: A Case Study of Sealy, Texas.* Ronald Linehan, C. Michael Walton, and Richard Dodge, February 1975.

22 *A Description of the Application of Factor Analysis to Land Use Change in Metropolitan Areas.* John Sparks, Carl Gregory, and Jose Montemayor, December 1974.

23 *A Forecast of Air Cargo Originations in Texas to 1990.* Mary Lee Metzger Gorse, November 1974.

24 *A Systems Analysis Procedure for Estimating the Capacity of an Airport: A Selected Bibliography.* Chang-Ho Park, Edward V. Chambers III, and William J. Dunlay, Jr., August 1975.

25 *System 2000—Data Management for Transportation Impact Studies.* Gordon Derr, Richard Dodge and C. Michael Walton, September 1975.

26 *Regional and Community Transportation Planning Issues—A Selected Bibliography.* John Huddleston, Ronald Linehan, Abdulla Sayyari, Richard Dodge, C. Michael Walton, and Marsha Hamby, September 1975.

27 *A Systems Analysis Procedure for Estimating the Capacity of an Airport: System Definition, Capacity Definition, and Review of Available Models.* Edward V. Chambers III, Tommy Chmores, William J. Dunlay, Jr., Nicolau D. F. Gualda, B. F. McCullough, Chang-Ho Park, and John Zaniewski, October 1975.

28 *The Application of Factor Analysis to Land Use Change in a Metropolitan Area.* John Sparks and Jose Montemayor, November 1975.

29 *Current Status of Motor Vehicle Inspection: A Survey of Available Literature and Information.* John Walter Ehrfurth and David A. Sands, December 1975.

30 *Executive Summary: Short Range Transit Improvement Study for The University of Texas at Austin.* C. Michael Walton (Supervising Professor), May 1976.

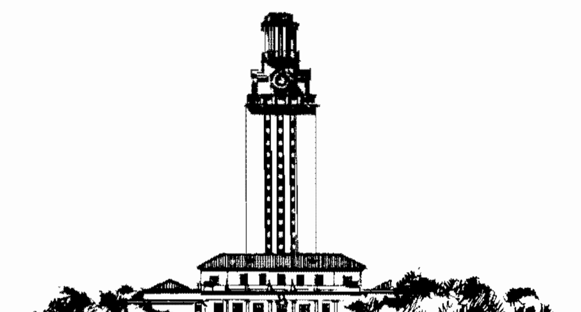

Council for Advanced Transportation Studies

THE UNIVERSITY OF TEXAS AT AUSTIN

CATS RR-13 MEASUREMENT OF ROADWAY ROUGHNESS AND AUTOMOBILE RIDE ACCELERATION SPECTRA A. HEALEY, R. STEARMAN